



PISA, ANNO 2020

PERFEZIONAMENTO IN NEUROBIOLOGIA

TESI:

Upon the way through which astrocytes sense and react to a reduction of extracellular Nerve Growth Factor level

NGF and Astrocytes in neurodegenerative disease models

PERFEZIONANDO:

Dr. Nicola Maria Carucci

RELATORI:

Prof. Antonino Cattaneo, PhD

Prof.ssa Simona Capsoni, MV, PhD

**ATTIVITÀ CONDOTTE PRESSO IL LABORATORIO DI
BIOLOGIA DELLA SCUOLA NORMALE SUPERIORE, PISA**



SCUOLA
NORMALE
SUPERIORE



“Siamo amanti e cultori di una sapienza umana che può considerarsi compiuta quando arriva a scorgere ciò che il senso rivela e ciò che si può desumere dalla similitudine, come i fenomeni percepiti per mezzo del senso. [...]

Noi non abbiamo seguito nient'altro che il senso e la natura, la quale, sempre in massimo accordo con se stessa, fa le stesse cose allo stesso modo e sempre produce i medesimi effetti.”

De rerum natura iuxta propria principia (1586),

Bernardino Telesio

Index

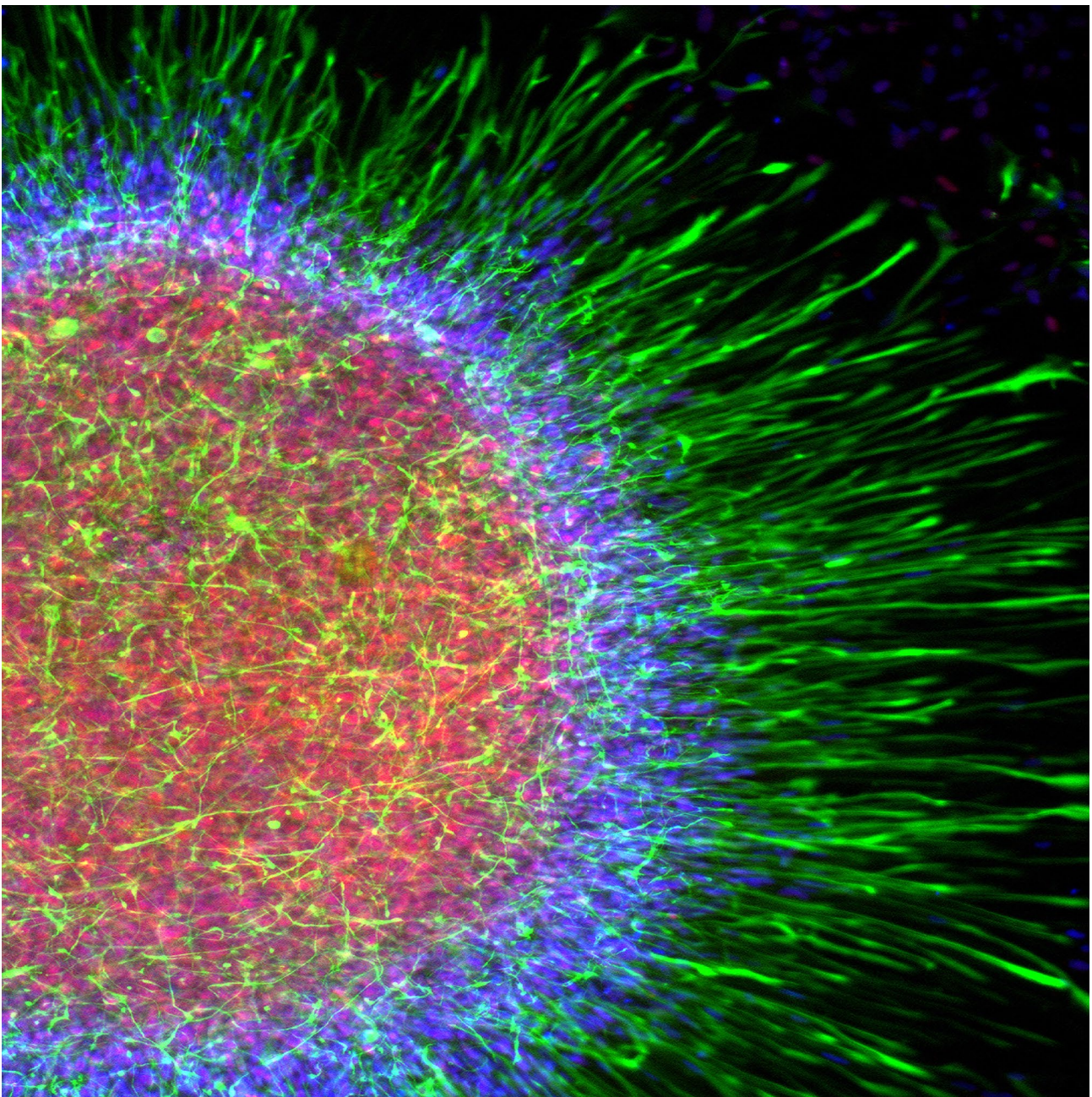
1. NEUROTROPHINS AND ASTROCYTES	11
1.1 Summary	11
1.2 More on NGF and AD	14
1.3 NGF and Alzheimer's Disease	15
1.4 The AD11 mouse	17
2. GENERAL BACKGROUND	23
2.1 The fall of idols	23
2.3 Astrocytes and Neurons, a well consolidated cooperation	29
3. NATURAL HISTORY OF NEUROGLIA	35
3.1 Neuroglia: from glue to glory	36
3.2 Classification of neuroglia	40
3.3 Phylogenetic importance of neuroglia	43
4. THE ASTROCYTE	49

4.1	Unsuspected heterogeneity	49
4.2	Defining an astrocyte: common properties	53
4.3	Morphology of the main type of astrocyte	58
4.4	Human astrocytes	60
5.	ASTROCYTES IN ACTION	65
5.1	The tripartite synapse	65
5.2	Ca ²⁺ -mediated cellular excitability of astrocytes	69
5.3	Astrocyte Ca ²⁺ is controlled by synaptic activity	70
5.4	Astrocyte Ca ²⁺ signal in vivo	72
5.5	Synaptic information processing by astrocytes	75
5.6	Astrocytes discriminate the activity of synaptic pathways	76
5.7	Astrocyte Ca ²⁺ signals show a nonlinear relationship with the synaptic activity	79
5.8	Gliotransmission and modulation of synaptic transmission	80
5.9	Astrocytes and synaptic plasticity	88
5.10	Are all synapses tripartite?	90
6.	RESULTS	93
6.1	NGF deprivation induces morphological alterations of astrocytes in vivo	100

6.2 Mechanism(s) at the basis of astrocytes altered morphology: role of proNGF	112
6.3 In vitro effects of NGF depletion	115
6.4 Astrocytes express NGF receptors in vitro	121
6.5 Atrophic astrocytes induced by anti NGF antibody treatment display a phenotype of reactive astrocytes	124
6.6 The NGF depletion increases astrocyte calcium oscillation	127
6.7 The Ca^{2+} involved in anti-NGF dependent calcium waves derives from ER-stores	131
6.8 Calcium oscillations induced by anti NGF antibodies are abolished if TrkA expression is chemogenetically inhibited in astrocytes	135
6.9 Transcriptomic changes at 8, 24 and 48 hours after anti-NGF antibody administration	138
6.10 In astrocyte-neuron co-cultures, the NGF starvation leads to neuronal impairment and death	142
6.11 The effects of NGF deprivation onto astrocytes might imply the production of β amyloid oligomers or glutamate excitotoxicity, impairing neurons	147
6.12 The astrocyte Ca^{2+} elevations induced by NGF starvation trigger Ca^{2+} hyper-activation in neurons	152
6.13 In vivo rescue of astrocytes atrophy by NGF in different AD models	158
6.14 NGF modulate astrocyte calcium activity in vivo	162

6.15 Reducing NGF levels increases astrocyte calcium in the awake behaving animal	167
6.16 Upregulation of NGF translation after 5 min of NGF deprivation	172
7. DISCUSSION	177
7.1 Astrocytes and NGF: secretion, signalling and mouse models	178
7.2 Pathological implications of atrophic astrocytes	180
7.3 Early events after NGF deprivation	182
7.4 Long term events after NGF deprivation	184
7.5 Adaptive homeostatic functions of astrocytes	185
7.6 A new mechanism of neuronal death mediated by NGF-deprived neurotoxic astrocytes	188
7.7. Widening the potential clinical application of NGF	191
8. METHODS	193
8.1 Animals	193
8.2 Intranasal Delivery	194
8.3 Cell cultures	195
8.4 Immunoblot analysis	197
8.5 Immunocytochemistry	199

8.6 Immunofluorescence on slice	200
8.7 Flow cytometry	201
8.8 Microarray transcriptome analysis	202
8.9 Neuron/astrocytes co-cultures	203
8.10 Confocal microscopy and image analysis	204
8.11 Data Analysis and statistics	205
8.12 Transgenic mice for in vivo Ca^{2+} experiments	206
8.13 In vivo imaging with two-photon microscopy in the anesthetized mouse	207
8.14 Surgical preparation for imaging awake, head-restrained mice	208
8.15 Drug through an open window in the skull	211
8.16 Statistical analyses for in vivo Ca^{2+} experiments	211
8.17 NGF immunoprecipitation and Western Blot	212
9. REFERENCES	215



Astrosphere: astrocytes grown from embryonic induced stem cells.

Credit: the laboratory of UW-Madison, Su-Chun Zhang, 2011.

1. Neurotrophins and Astrocytes

1.1 Summary

My starting observation was that that chronic exposure of hippocampal astrocytes to anti-nerve growth factor (NGF) antibodies is associated with early and progressive changes in astrocytic morphology reminiscent of reactive gliosis. Similar morphology changes are found in the hippocampal astrocytes from proNGF overexpressing

transgenic mice and from Alzheimer's 3XTg and 5xFAD mice at early stages of neurodegeneration. Interestingly, this phenotype can be rescued by intranasal NGF delivery to 3xTG and proNGF mice.

These findings prompted us to investigate the mechanisms whereby interfering with the signalling of NGF causes astrocytes to undergo these changes.

The astrocytic morphological alterations in mouse models of neurodegeneration were reproduced *in vitro* by culturing naïve hippocampal astrocytes with mAb α D11 anti-NGF antibodies. These dramatic changes of astrocyte morphology are accompanied by robust transcriptomic changes at 8, 24 and 48 hours after anti-NGF administration, which identify a transcriptional fingerprint typical of reactive type A1 neurotoxic astrocytes⁷⁰. Since cultured astrocytes express both TrkA and p75 NGF receptors and secrete NGF, I postulated that anti NGF antibodies disrupt a homeostatic autocrine or paracrine NGF signalling, inducing their transition to the A1 neurotoxic phenotype.

I went on to investigate intracellular Ca^{2+} transients in astrocyte cultures. While NGF failed to reveal any effect on Ca^{2+} , anti NGF potently induced within 5 minutes large intracellular Ca^{2+} transients, from ER intracellular stores.

Chemogenetic experiments indicate that the antiNGF-induced Calcium waves are TrkA-mediated.

The functional consequences of anti NGF treatment of astrocytes on neuronal physiology were studied in hippocampal astrocyte-neuronal co-cultures. In these conditions, anti NGF treated astrocytes induced a strong Ca^{2+} activity in hippocampal neurons, ultimately leading to massive neuronal death.

In conclusion, I have demonstrated that, in vitro and in vivo, astrocytes are sensors of ambient levels of NGF and respond to reduced levels of NGF by the activation of a strong and rapid Ca^{2+} response that eventually leads them to assume a A1 neurotoxic phenotype and negatively impact neuronal physiology and brain homeostasis.

1.2 More on NGF and AD

The role of NGF in neurodegeneration has an old root, linked to its pro-survival and phenotypic maintenance action on cholinergic neurons of the basal forebrain. The discovery that other cells in the brain, besides neurons, like glial cells, could respond to NGF and modulate the neuronal physiology broadened the possible NGF targets to potentially all the brain, boosting the comprehension of some pathologies - like Alzheimer disease - and supporting new therapeutic strategies.

Here I propose, based on my experiments, a new mechanism whereby astrocytes can sense locally the NGF level. They respond to a decrease in extracellular NGF, potentially triggering an activation loop sustained by an increase in calcium oscillations that can cause astrocytes to become active and change their morphology.

First experimental evidence reveals that in a short time these paradoxically active astrocytes, when co-cultured with neurons, determine an increase of calcium transients in neurons as well, leading them to death.

More experiments are necessary to unveil these proposed mechanisms and go deeper in the comprehension of astrocyte physiology, but the framework established by the

experiments presented in this PhD thesis allow future experiments to be grounded on a solid basis.

1.3 NGF and Alzheimer's Disease

NGF is not translated as such, but as a pre-pro-protein which is cleaved, typically by furin enzyme, in the trans-Golgi network to yield mature NGF⁷¹. ProNGF was initially thought to be simply a chaperone to allow NGF to be folded and mature NGF to be finally secreted. ProNGF can also be released as such and represents the major form of NGF in the brain⁷³ and can be cleaved extracellularly by plasmin and matrix metalloproteases⁷². ProNGF and NGF have distinct biological activities⁴³: proNGF has a higher affinity for p75NTR and a lower one for TrkA compared to mature NGF and induces p75NTR-dependent apoptosis.

ProNGF can also induce TrkA-dependent neuronal survival, although less effectively than NGF⁷³.

The pro-domain of NGF interacts with sortilin, a neuronal type-1 VPS10-domain receptor, a co-receptor with p75NTR for proNGF⁷⁴. Sortilin, together with the VPS10-containing protein sorLA, binds the retromer complex in neurons.

The levels of proNGF and of its coreceptor sortilin increase in mild cognitive impairment and early AD brains⁹⁰, paralleling the progressive decline in TrkA receptors. A diminished conversion of proNGF to mature NGF and an increased NGF degradation in AD brains was definitely reported⁷².

Thus, the biological effects of proNGF versus NGF influence the balance between cell death and cell survival^{74, 75} and an imbalance in this complex ligand/receptor system has been correlatively linked to AD neurodegeneration, although no causally direct proof in vivo is available.

1.4 The AD11 mouse

NGF (Levi-Montalcini, 1952) is required for the differentiation and the survival of specific neuronal populations during development, including sensory, and sympathetic neurons in the peripheral nervous system and basal forebrain cholinergic neurons in the central nervous system (Levi-Montalcini, 1987). NGF also exerts actions on non-neuronal cell populations (Levi-Montalcini, 1987).

After the early use of anti-NGF antibodies (Levi-Montalcini and Booker 1960), NGF functions in vivo have been investigated with different approaches, including the systemic (Levi-Montalcini and Angeletti, 1966; Gorin and Johnson, 1979, 1980) or local (Li et al., 1995; Van der Zee et al., 1995; Molnar et al., 1998) delivery of anti-NGF antibodies and the disruption of the NGF gene, by homologous recombination, in transgenic mice (Crowley et al., 1994).

The embryonic ablation of NGF function gives rise to a lethal phenotype in the early postnatal period, preventing the analysis of NGF function in adult animals. On the other hand, adult heterozygous NGF knockout mice show only a mild cholinergic phenotype and no other described deficits (Chen et al., 1997).

Given the potential clinical relevance of some of the described actions of NGF, the use of specific and not-lethal models represents a desirable tool.

After the demonstration that recombinant antibodies can be efficiently secreted by cells of the nervous system (Cattaneo and Neuberger, 1987), a novel approach for phenotypic knockout, the neuroantibody approach, has been proposed and validated (Piccioli et al., 1991, 1995).

With all these pivotal assumptions, a transgenic mouse that lacks enough mature nerve growth factor was generated, and, among the relevant outcomes, it suffers from a progressive AD-like syndrome. Moreover, the delivery of NGF or of a cholinergic agonist were able to reduce the pathology.

The mouse model, called AD11, was created to explore the possibility that the death of basal forebrain cholinergic neurons in Alzheimer's disease is related to reductions in nerve growth factor levels. AD11 was created by inserting a gene that expresses an anti-NGF antibody (formally, 2 genes for light and heavy chains), named α D11, that efficiently binds *only the mature form* of the neurotrophin (Ruberti et al. 2000, Paoletti et al., 2009) (fig 1.1).

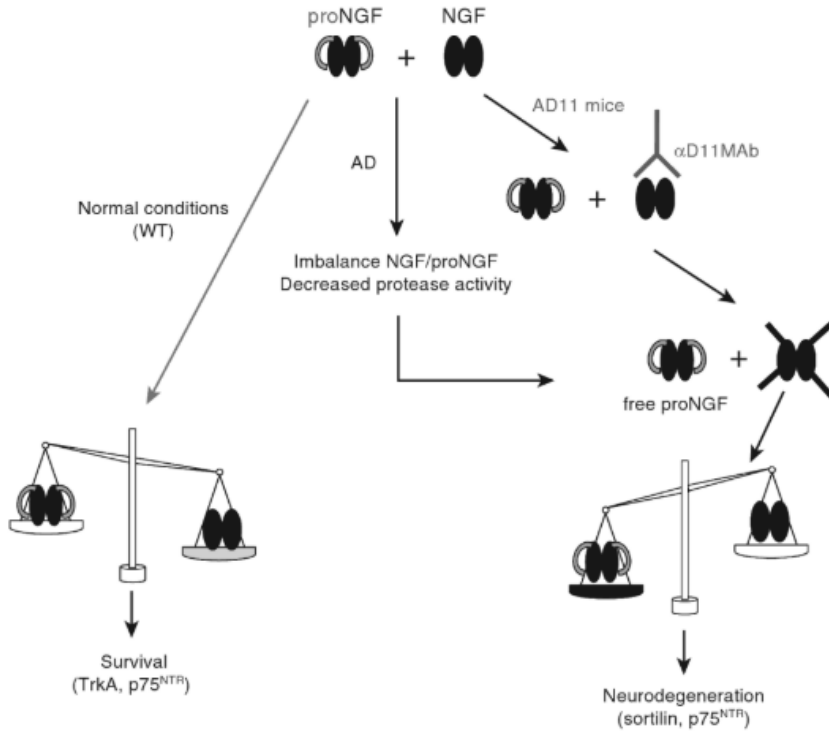


Fig 1.1 Schematic representation of the proNGF/NGF imbalance model

On the left side is the "normal" condition, when nerve growth factor (NGF) signaling is achieved mainly through the NGF/TrkA/p75^{NTR} system. In the middle-right part of the scheme is a representation of the pathological conditions (middle, AD conditions;

right, AD11 model): in both cases, an imbalance in the proNGF/NGF ratio takes place.

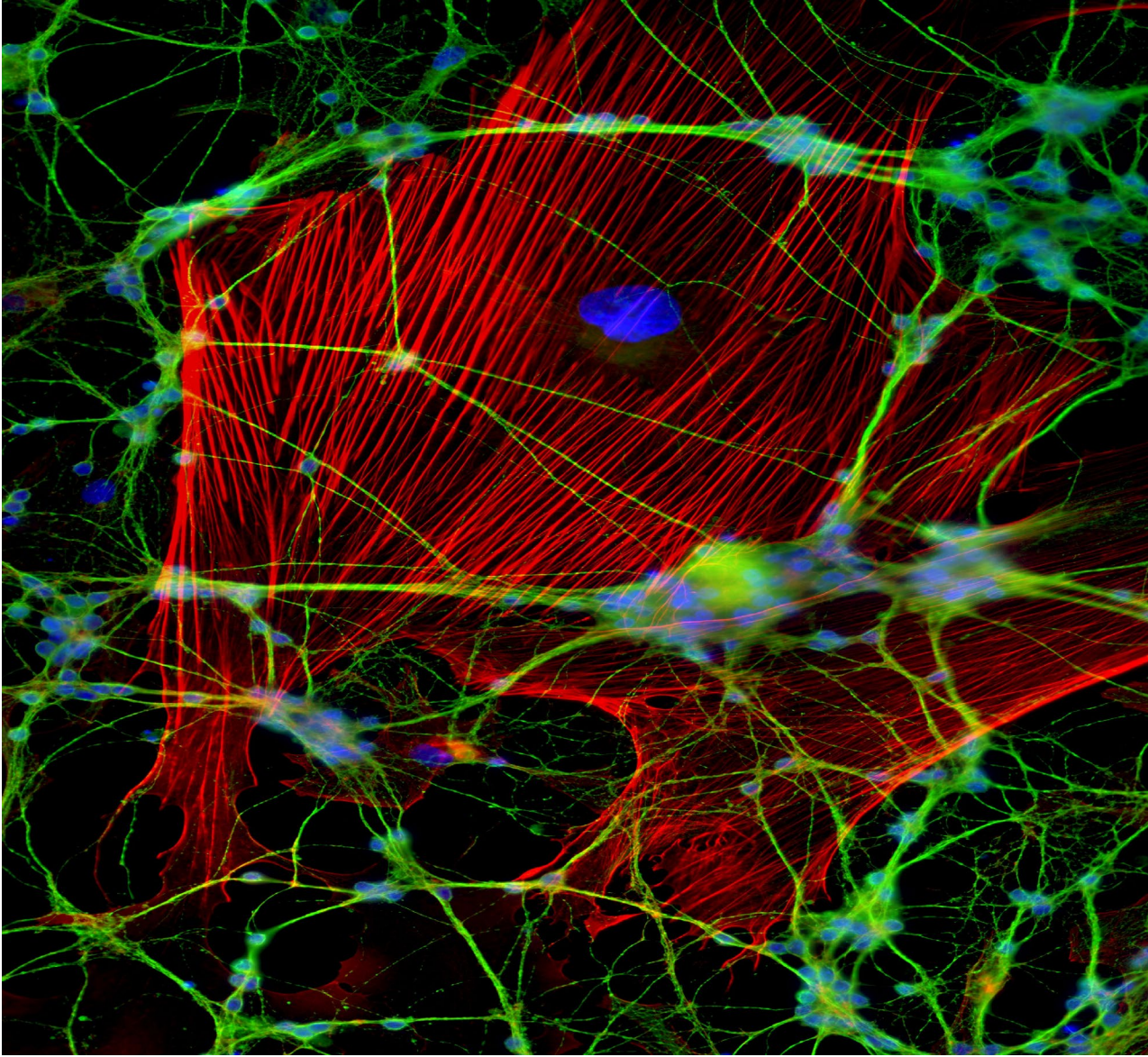
From Nerve Growth Factor and Alzheimer's Disease: New Twists to an Old Story, 2011, MIT Press, 26th chapter by Antonino Cattaneo.

Capsoni, Cattaneo and their colleagues have described how the depletion of extracellular mature NGF in this model progressively recapitulates features of Alzheimer's disease. The AD11 mouse shows neuronal loss, tau hyperphosphorylation and insolubility, neurofibrillary tangle-like abnormalities, and behavioral deficits linked to cholinergic atrophy (Capsoni et al., 2000).

It also exhibits amyloid plaques (from the endogenous mouse amyloid precursor protein) (Capsoni et al. 2002), and deficits in cortical synaptic plasticity (Pesavento et al. 2002), all of which led Cattaneo and associates to propose this mouse as a comprehensive model for sporadic AD and, among the other numerous outcomes, identifying a novel mechanism of neurodegeneration induced by proNGF/NGF imbalance.

In addition, in 2011 D'Onofrio et al. showed that, in these mice, the onset of neuroinflammation was preceding the appearance of tau hyperphosphorylation and amyloid plaques.

This prompted us to study the effects of NGF deprivation on one cell type involved in neuroinflammation: the astrocyte.



"It's a crowded party in the body, and biologists want to see what's going on"

From "A Brain in a Plate?"

Credit: Jan Schmoranzger.

2. General background

2.1 The fall of idols

The neuron-centred view of the past disregarded or downplayed the role of astroglia as a primary component in the pathogenesis of neurological diseases.

As this concept is changing, so is also the perceived role of astrocytes in the healthy and diseased brain and in the spinal cord. Researchers have started to unravel the different signalling mechanisms that trigger specific molecular, morphological and functional changes in astrocytes and that may be critical for repairing tissue and maintaining function in

CNS pathologies, such as neurotrauma, stroke, or neurodegenerative diseases. An increasing body of evidence shows that the effects of astrogliosis on the neural tissue and its functions are not uniform or stereotypic but vary in a context-specific manner. Indeed, astrogliosis can be an adaptive beneficial response under some circumstances but also a maladaptive and deleterious process in another context.

There is a growing support for the concept of *astrocytopathies* in which the disruption of normal astrocyte functions, *astrodegeneration* or dysfunctional/maladaptive *astrogliosis* are the primary cause or the main factor in neurological dysfunction and disease. For this reason, there is a big interest in the mechanism of dysfunctional/maladaptive astrogliosis and on the factors that execute the toxic actions of astrocytes in neurodegeneration conditions. This thesis proposes a new homeostatic mechanism of astrocytes in the healthy CNS describing how they could react to an unbalance of NGF/proNGF in the microenvironment around them.

This finding increases the diversity of astrocytes responses in neurological disorders and argues that targeting astrocytes may represent an effective therapeutic strategy for Alzheimer Disease (AD) as well as other neurodegenerative diseases.

2.2 Astrocytes in the brain: beyond scaffold cells

It is nowadays well understood that astrocytes cannot be just be considered as scaffold cells deputed to feed and preserve neuronal activity but, since they are involved in a large number of functions, they are critical to the performance of the Central Nervous System (Verkhratsky et al., 2014; Gallo et al., 2014).

It is more and more evident that the peculiar properties of these cells can actively contribute to the extraordinary complexity of the brain and, on the other hand, to the dysfunctions and diseases classically related to other cell types, especially neurons (Allen et al., 2009; Lin et al., 2012).

New evidence indicates that astrocytes could really make the difference in mammalian brain evolution (Molofsk et al., 2012), corroborated by the impressive discovery that mice enhance some behavioural aspects if expressing human astrocytes (Zang et al., 2013; He et al., 2015).

The essential and various functions astrocytes provide include i) homeostasis of extracellular ions, pH, idratation (Simard et al., 2004); ii) uptake and clearance of neurotransmitters (Schousboe et al., 2004; Yi et al., 2006); iii) energy and metabolism (Allaman et al., 2011); iv) blood flow regulation(Attwell et al., 2010); v) neuronal activity

coordination and synaptic functions (Clarke et al., 2013; Halassa et al., 2010; Bergami et al., 2008; Bazargani et al., 2016).

If a large number of evidences are now reported regarding how these functions might involve astrocyte specialization and heterogeneity, the degree to how astrocytes maintain or modulate their participation in these functions, or adopt new functions, is not well understood (Anderson et al., 2014; Colangelo et al., 2014; Trias et al., 2013; Wyss-Coray et al., 2002).

As mentioned before, some aspects traditionally related to neuronal degenerative pathologies, together with some well described neuronal physiological properties, could be reasonably re-interpreted keeping in mind that astrocytes, and their contribution, might have been underestimated

A large number of *in vitro* studies on *bona fide* neuronal preparations include *de facto* astrocytes, due to the difficulties to obtain really pure neuronal cultures. Obviously, astrocytes are also present in the majority of the *in vivo* and *ex vivo* experimental preparations.

With the aim of addressing this need, and of turning these limitations into new perspectives,

to explore if and how astrocytes could react to proNGF/NGF imbalance and, eventually, influencing the neuron homeostasis,

I took advantage from our AD11 mouse model, in which the expression of the recombinant α D11 anti Nerve Growth Factor (NGF) antibody causes an imbalance between the mature and immature form of NGF.

This lead, progressively, to a generalized Alzheimer-like phenotype (Ruberti et al. 2000; Capsoni et al., 2000 and 2002) overcoming the concept that the “classical” neuronal target cells for NGF could appear a limiting factor for the model acceptancy (Cattaneo et al., 2008).

The glia cells (microglia and astrocytes) could be the target cells contributing to explain this widespread effect.

The link between Alzheimer's disease and astrocytes is well described and is based on several components: they can take up A β , they are involved in plaque progression with death of A β loaded astrocytes giving rise to secondary plaques (Nagele et al., 2004); astrocytes have a modulatory effect on neuroinflammation²⁷, on neuron-neuron communication¹⁶ and

on tripartite (more recently, quadripartite) synapses^{28,29}. In this study, I describe a new way by which astrocytes can respond to a change in brain homeostasis such as NGF local acute deprivation.

In presence of a decrease in the level of NGF astrocytes become active and modify their morphology. I propose also a new way they could influence neuronal activity and cause neuronal death.

2.3 Astrocytes and Neurons, a well consolidated cooperation

The multi-partite synapse of the CNS represents a striking example of such a specialization (fig 2.1) with pre- and post-synaptic membranes being packed with exocytotic machinery, neurotransmitter receptors and proteins responsible for plasticity, whereas all “homeostatic” molecules (i.e. transporters and enzymes responsible for ion and transmitter homeostasis in the synaptic cleft, for transmitter catabolism, for metabolic support, etc.) being localized in the perisynaptic astrocytic processes .

The synaptic assembly also includes a microglial cell process that frequently senses the synapse status. Already at this elementary level of CNS organization, the cellular functions are divided. Neuronal compartment assures fast information flow whereas glial elements ascertain functional isolation and support of synapses, maintain synaptic operation through regulation of homeostasis and control synaptic survival or elimination depending on the network demands.

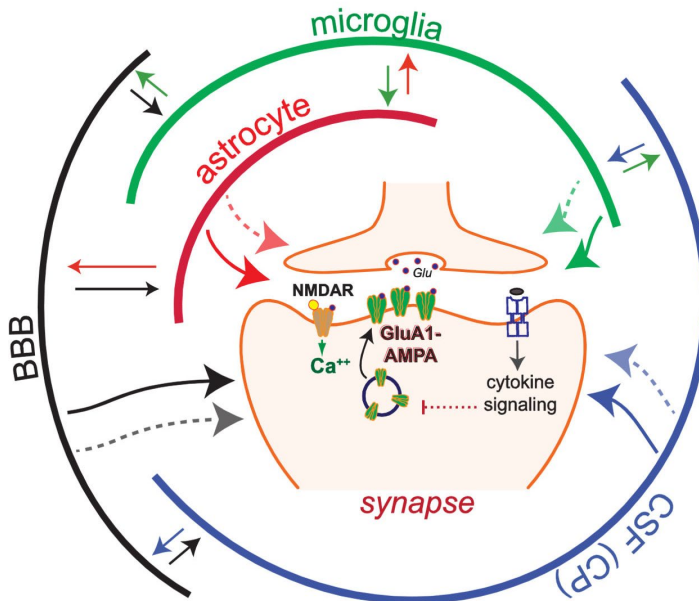


Fig 2.1 Multiparty synapse involving several CNS players.

This simplified model illustrates LTP, which relies on the NMDAR-dependent insertion of GluA1-containing AMPA receptors at the postsynaptic surface. In this model communication via cytokines is depicted by arrows, which can bi-directionally connect multiple cell populations.

Cytokine networks enable local interactions between neuronal and non-neuronal cells (e.g., astrocytes, microglia, vascular endothelial cells) in the brain, as well as brain-periphery communication via the brain-blood barrier (BBB) and the choroid plexus (CP).

The BBB releases cytokines and regulates the flux of cytokines from the blood; the CP produces cerebrospinal fluid (CSF) and cytokines and regulates the transport of cytokines and immune cells from blood

vessels. LTP modulation by cytokines has been widely studied, however, for most cytokines, is unclear if they modulate LTP by directly targeting synapses (one-direction arrows) or by indirect mechanisms relying on cytokine networks maintained by non-neuronal cells interactions.

Cytokines can induce the expression and release of multiple cytokines in their target cells, thus activating cytokine networks, which could modulate synaptic transmission by targeting synapses via both cytokine-dependent and -independent mechanisms (dotted arrows) From Prieto and Cotman 2017.

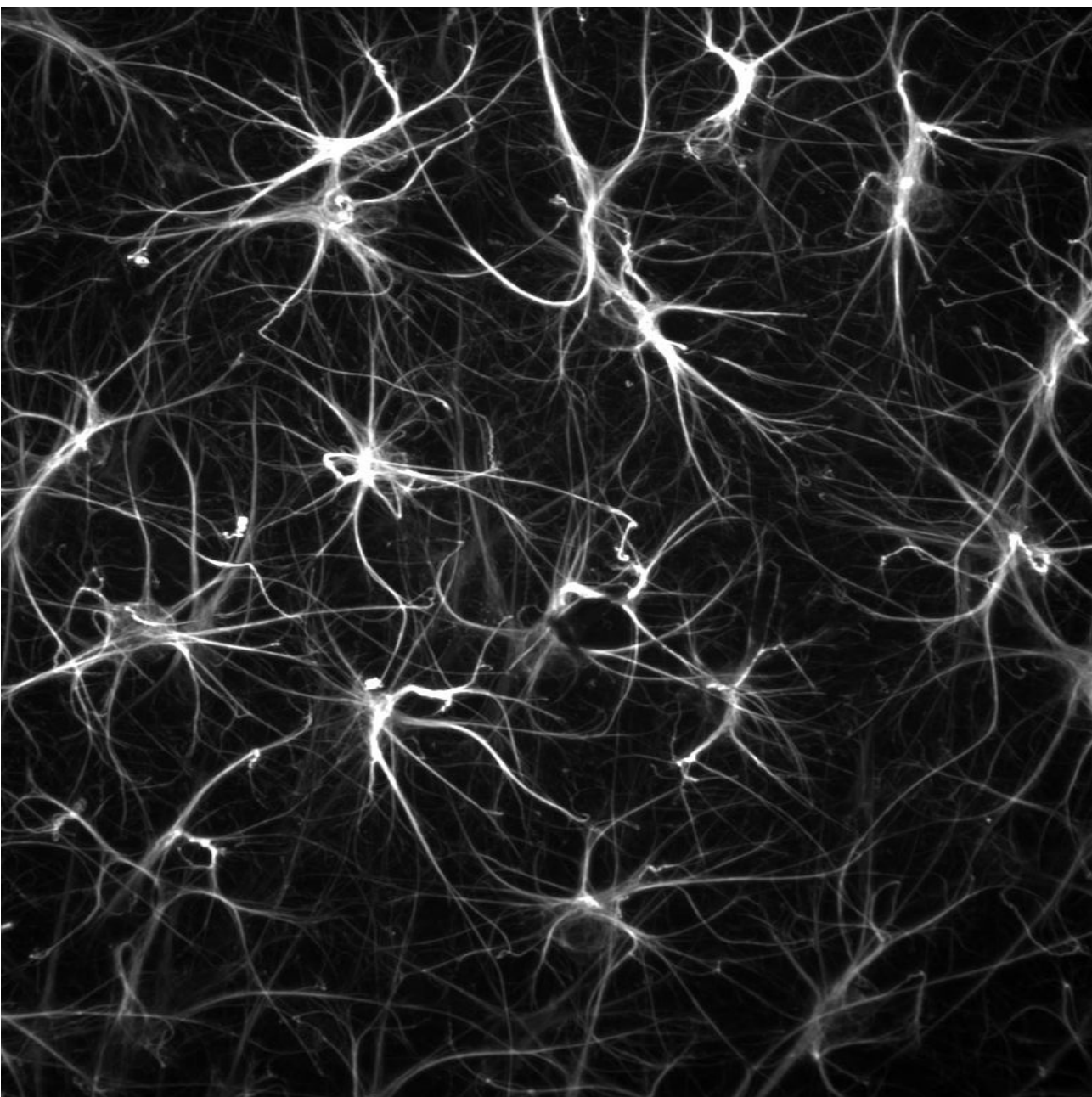
The very same specialization is observed at all levels of CNS organization. Neurons fire and establish multiple contacts whereas neuroglia control local micro-environment and protect neural tissue. In the grey matter, astrocytes divide (through the process known as tiling that starts in late embryogenesis) the parenchyma into relatively independent units traditionally known as neurovascular units, and recently often called astrogliovascular units, that integrate, within an individual astroglial territorial domain, neural and vascular elements. By employing a wide array of molecular mechanisms such as exocytosis, diffusion through plasmalemmal channels or membrane transporters, astrocytes secrete numerous neurotransmitters, neurohormones and trophic factors that regulate synaptic fields, neuronal groups and signal to other cellular elements (e.g. microglia, oligodendroglia, pericytes, endothelial cells).

At the level of the whole brain, astrocytes form *glia limitans* regulate emergence and function of brain–blood and brain–cerebrospinal fluid barriers and contribute to overall brain metabolism being the sole producers and repository of glycogen

The homeostatic function of astroglia is linked to their neuroprotective capabilities, as indeed astrocytes are principal

elements of CNS defence. Insults to the CNS, regardless of their aetiology, strain the organ homeostasis and in this case astrocytes, through dedicated molecular cascades, protect neurons against glutamate excitotoxicity, extracellular K⁺ overload, reactive oxygen species, and these are also astrocytes that supply stressed neurons with energy substrates.

The loss of these critical astroglial functions permits and exacerbates progression of various diseases, of which amyotrophic lateral sclerosis, toxic encephalopathies or Alzheimer's disease (AD) are prominent examples. Defensive function of astrocytes is manifested as reactive astrogliosis, a multi- component and complex remodelling of astroglia triggered by lesions to the CNS. Astrogliosis is an important component of cellular pathophysiology and its suppression often aggravates neuropathology.



Mouse Astrocytes, cortex.

Credit: Dr. Nybertuc.

3. Natural history of neuroglia

“THE NEUROGLIA is the delicate connective tissue which supports and binds together the nervous elements of the central nervous system. One part of it, which lines the central canal of the cord and ventricles of the brain, is formed from columnar cells, and is called ependyma, while the rest consists of small cells with numerous processes which sometimes branch and sometimes do not.”

Encyclopaedia Britannica, 1910, 11th Ed., v. 19, p. 401

“As the Greek name implies, glia are commonly known as the glue of the nervous system; however, this is not fully accurate. Neuroscience currently identifies four main functions of glial cells: to surround neurons and hold them in place, to supply nutrients and oxygen to neurons, to insulate one neuron from another, and to destroy pathogens and remove dead neurons. For over a century, it was believed that they did not play any role in neurotransmission. That idea is now discredited; they do modulate neurotransmission, although the mechanisms are not yet well understood.”

Glial Physiology and Pathophysiology, First Edition.

2013

3.1 Neuroglia: from glue to glory

To the continual surprise of everybody working in neuroglial research, the proper characteristics and capabilities of *neuroglia* are still a matter of debate. Many existing definitions highlight the supportive role of these cells, and some are based on the process branching and delicate morphology of these cells, but the most common definition assigned to neuroglia is “cells residing in the brain that are not electrically excitable neurons or vascular cells”.

As a result, neuroglia has become a generalised term that covers cells with different origins (ectodermal for macroglia and mesodermal for microglia), morphology, physiological properties and functional specialisation. Indeed, in the Central Nervous System (CNS), neuroglia include the cells of the choroid plexus, the oligodendrocytes, the ependymal cells, the radial glia of the retina, the immunocompetent microglia/innate macrophages and the hugely diverse astrocytes; whereas, in the peripheral nervous system (PNS), they include the diverse kinds of Schwann cells, satellite glia, olfactory ensheathing cells and the highly numerous enteric glia.

There is, however, one unifying fundamental property common for all these cell types and this is their ultimate function: *homeostasis of the nervous system*.

The evolution of the nervous system led to a specialisation of neurons, which become perfect elements for signalling and information processing. This came at the price of losing essential housekeeping functions, as neurons are generally incapable of regulating their own immediate environment and are vulnerable to many kinds of environmental insults. These main housekeeping functions went to the neuroglia, which have specialised themselves into

many types of cells to perform specific aspects of nervous system homeostasis.

This homeostatic function of neuroglia is executed at many levels, and includes: whole body and organ homeostasis (e.g. astrocytes control the emergence and maintenance of the CNS, peripheral glia are essential for communication between the CNS and the body, and enteric glia are essential for every aspect of gastrointestinal function);

- i) cellular homeostasis (e.g. astroglia and microglia);
- ii) morphological homeostasis (glia define the migratory pathways for neural cells during development, shape the nervous system cyto-architecture and control synaptogenesis/synaptic pruning, whereas myelinating glia maintain the structural integrity of nerves);
- iii) molecular homeostasis (which is represented by neuroglial regulation, of ion, neurotransmitter neurohormone, and neurotrophic factor concentrations in the extracellular spaces around neurons);
- iv) metabolic homeostasis (e.g. neuroglial cells store energy substrates in a form of glycogen and supply neurons with lactate);
- v) long-range signalling homeostasis (by myelination provided by oligodendroglia and Schwann cells);

vi) defensive homeostasis (represented by astrogliosis and activation of microglia in the CNS, immune reactions of enteric glia; all these reactions provide fundamental defence for neural tissue).

Moreover, some neuroglial cells act as chemosensitive elements of the brain that perceive systemic fluctuations in CO_2 , pH and Na^+ and thus regulate behavioural and systemic homeostatic physiological responses.

Therefore, the neuroglia can be broadly defined as homeostatic cells of the nervous system, represented by highly heterogeneous cellular populations of different origin, structure and function.

3.2 Classification of neuroglia

Generally, see the scheme below, the neuroglia in the mammalian nervous systems are sub classified into peripheral nervous system (PNS) glia and central nervous system (CNS) glia.

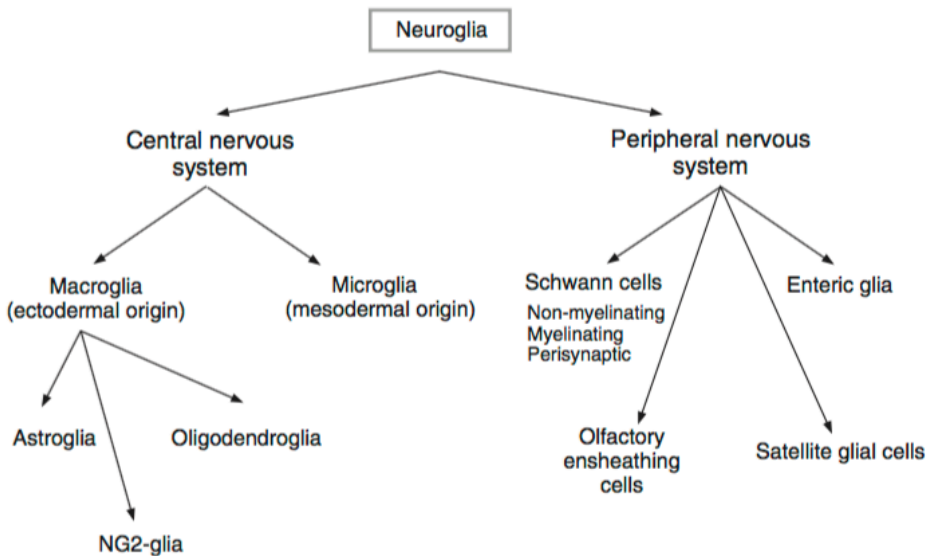


Fig 3.1 The neuroglia in the mammalian nervous system

From Verkhratsky 2013.

The PNS glial cells which surround neurons in peripheral ganglia are known as satellite glial cells, and those in

the olfactory system are known as olfactory ensheathing cells. Finally, the PNS includes enteric glia, which reside in the enteric nervous system.

CNS glia are generally subdivided into astrocytes, oligodendrocytes, NG2-glia and microglia. Astrocytes are the main homeostatic cells of the gray matter. Oligodendrocytes are the myelinating cells in the CNS and NG2-glia act as oligodendroglial precursors.

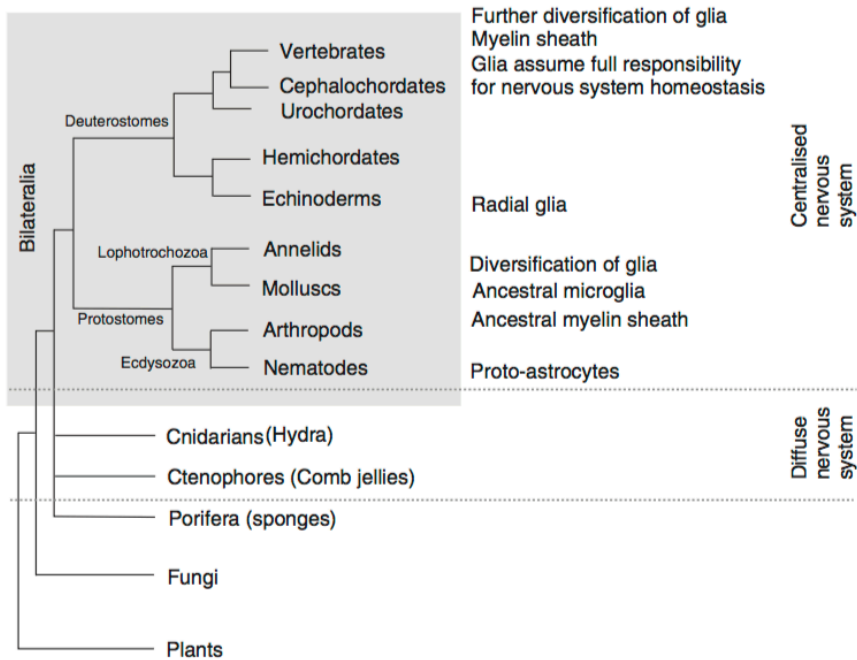


Fig 3.2 The evolutionary origins of glial cells

From Verkhratsky 2013.

The early evolution of the nervous system can only be speculated upon, because fossils do not provide much material for analysis, and it is likely that many early life forms have not survived to our time. Nonetheless, certain generalisations can be drawn and overall, we are in possession of a rather logical system of views on the milestones of nervous system phylogeny.

There are some indications that glia have appeared in phylogeny on several occasions, and parallel evolution is likely. There is no evidence for the existence of glial cells in diffuse nervous systems and no cells associated with neurons or their processes have been detected in the comb jellies. Similarly, no glial cells were found in Cnidaria polyps, with the exception of scyphomedusae, in which some glia-like cells were apparently reported from Hartline in 2011, but neither their function nor their glial identity, has been analysed in detail.

3.3 Phylogenetic importance of neuroglia

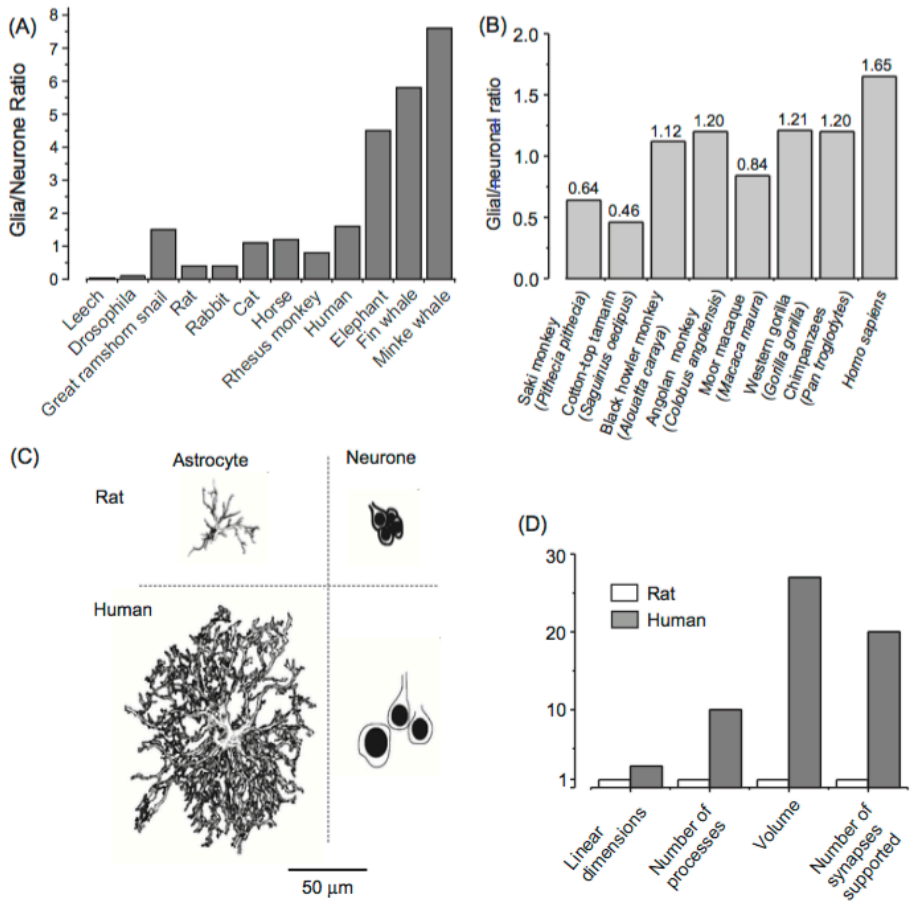


Fig 3.3 Glia/neurons ratio: a panoramic view

(a) *Glia-to-neuron ratio in the nervous system of invertebrates and in the cortex of vertebrates. Glia-to-neuron ratio is generally increased in phylogeny; this ratio more or less linearly follows an increase in the size of the brain.*

(b) *The glia/neuron ratio in the cortex of higher primates; this ratio is highest in humans (From Sherwood et al., 2006).*

(c) *Graphic representation of neurons and astroglia in mouse and in human cortex. Evolution has resulted in remarkable changes in astrocytic dimensions and complexity.*

(d) *Relative increase in glial dimensions and complexity during evolution. Linear dimensions of human astrocytes, when compared with mice, are .ca 2.75 times larger, and their volume is 27 times larger; human astrocytes have .ca 10 times more processes and every astrocyte in human cortex wraps .ca 20 times more synapses.*

(c) *From Oberheim et al., 2006.*

Most probably, neuroglia appeared with the emergence of a centralised nervous system, when neurons acquired specialisation and subsequently began to amass into sensory organs and ganglia. The very first glial cells are associated with sensory organs and have the same epithelial origin as neurons. More advanced and much more characterised are glial cells in nematodes, as extensively studied in *Caenorhabditis elegans*.

The brains of primates contain specific astroglial cells which are absent in other vertebrates. Most notable of these are the interlaminar astrocytes, which reside in layer I of the cortex; this layer is densely populated by synapses but almost completely devoid of neuronal cell bodies. These interlaminar astrocytes have a small cell body (10 μm), several short and one or two very long processes. The latter penetrate through the cortex and end in layers III and IV; these processes can be up to 1 mm long. The endings of the long processes create a rather unusual terminal structure, known as the ‘terminal mass’ or ‘end bulb’, which is composed of multilaminar structures containing mitochondria.

Incidentally, the processes of interlaminar astrocytes and size of “terminal masses” were particularly large in the brain of Albert Einstein (Colombo et al., 2006).

The function of these interlaminar astrocytes remains completely unknown, although it has been speculated that they

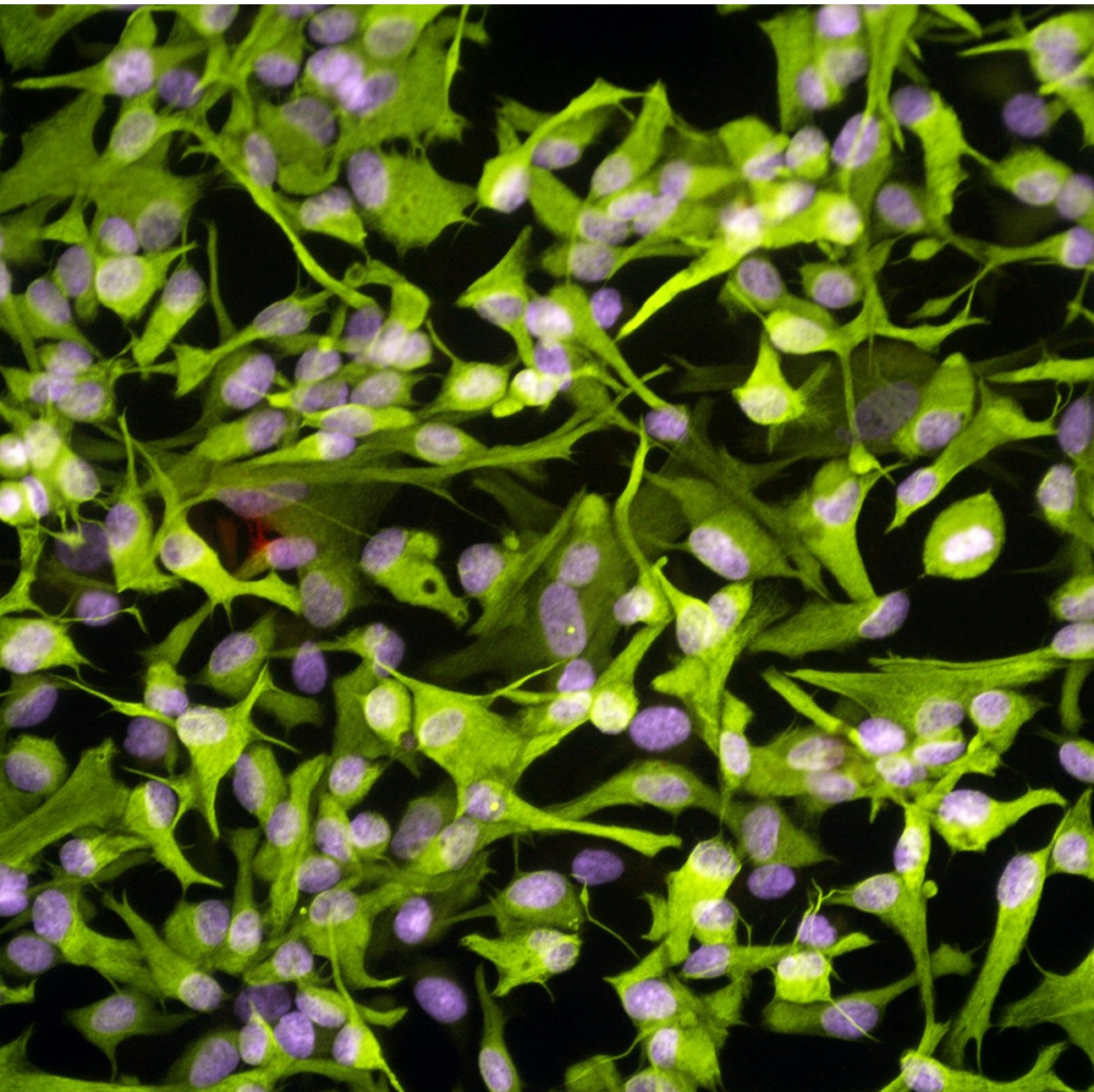
are the astroglial counterpart of neuronal columns, which are the functional units of the cortex, and that they may be responsible for a long-distance signalling and integration within cortical columns. Interestingly, inter-laminar astrocytes are altered in Down syndrome and Alzheimer's disease.

Human brains also contain polarized astrocytes, which are uni- or bipolar cells that dwell in layers V and VI of the cortex, quite near to the white matter; they have one or two very long (up to 1 mm) processes that terminate in the neuropil. The processes of these cells are thin (2–3 mm in diameter) and straight, and they also have numerous varicosities. Once more, the function of polarized astrocytes remains enigmatic, although they might be involved in para-neuronal long-distance signalling.

The evolution of neurons produced fewer changes in their appearance – that is, the density of synaptic contacts in rodents and primates is very similar (in the rodent brain, the mean density of synaptic contacts is about 1397 millions/mm³, which is not much different from humans, where synaptic density in the cortex is about 1100 millions/mm³). Similarly, the number of synapses per neuron does not differ significantly between primates and rodents.

The shape and dimensions of neurons also have not changed dramatically over the phylogenetic ladder. Human

neurons are certainly larger, yet their linear dimensions are only about 1.5 times greater than in rodents. Thus, at least morphologically, evolution resulted in far greater changes in glia than in neurons. Most likely this fact has important, although yet undetermined, significance.



Astrocyte cells in the brain of a human fetus.

Credit: Dr Amjad.

4. The Astrocyte

4.1 Unsuspected heterogeneity

Generally, astrocytes arguably are the most diverse glial cells in the CNS. They are variable among different areas and also within the same region. The classic most generally acknowledged definition of astrocyte is based on the morphology and on the expression of specific astroglial markers. Indeed, it is commonly believed that an archetypal

feature of astrocytes is their expression of intermediate filaments, which form the cytoskeleton. The main types of astroglial intermediate filament proteins are Glial Fibrillary Acidic Protein (GFAP) and vimentin; expression of GFAP is commonly used as a specific marker for identification of astrocytes.

The astrocyte is therefore generally defined as a cell with star-like appearance expressing GFAP. In reality, most of the astrocytes do not have a star-like morphology and many astrocytes do not express GFAP. Indeed, the normal levels of GFAP expression vary quite considerably between brain regions. For example, GFAP is expressed by virtually every Bergmann glial cell in the cerebellum and by fibrous astrocytes in white matter, whereas only about 15–20 percent of protoplasmic astrocytes express GFAP in the cortex of mature animals. In general, the name ‘astroglia’ is an umbrella term that covers many types of glial cells.

Some astrocytes do, indeed, have a star-like appearance, with several primary (also called stem) processes originating from the soma, although most of them have more complex morphology.

i) Possibly the largest groups of astrocytes are represented by the *protoplasmic astrocytes* and fibrous astrocytes of the grey and white matter, respectively.

ii) The second big group of astroglial cells is the *radial glia*. These are bipolar cells with an ovoid cell body and elongated processes. Radial glia usually produce two main processes, one of them forming endfeet on the ventricular wall and the other at the pial surface. They are a common feature of the developing brain, as they are the first cells to develop from neural progenitors. From very early embryonic stages, radial glia also form a scaffold which assists neuronal migration. After maturation, radial glia disappear from many brain regions and transform into stellate astrocytes, although radial glia-like cells remain in the retina (Müller glia) and the cerebellum (Bergmann glia).

iii) In addition to the two major groups of astroglial cells, there are smaller populations of specialised astroglia localised to specific regions of the CNS, namely the *velate astrocytes* of the cerebellum, *the interlaminar and polarised astrocytes* of the primate cortex, *tanycytes* (found in the periventricular organs, the hypophysis and the raphe part of the spinal cord), *pituicytes* in the neuro-hypophysis, and *perivascular and marginal astrocytes*.

iv) Astroglia also include several types of cells that line the ventricles or the subretinal space, namely *ependymocytes*, *choroid plexus cells* and *retinal pigment epithelial cells*.

All these diverse cell types differ in their morphology and gene expression, in physiological properties, sensitivity to various neurotransmitters and finally in functional features. Studies over recent decades have found that astrocytes from different brain regions differ substantially in expression of genes for the most fundamental proteins responsible for glial function, including genes encoding ion channels and neurotransmitter receptors, glutamate, GABA and glycine transporters, for nitric oxide synthase and for enzymes metabolising dopamine and serotonin (monoamine oxidase) and GABA (GABA transaminase).

Physiological experiments *in vitro*, *in situ* and *in vivo* have revealed similar regional differences throughout the brain for the functional expression of ion channels and neurotransmitter receptors, the latter most likely being regulated by the local neurotransmitter environment (Verkhratsky et al., 1998, 2011).

Identification of astrocytes, therefore, requires a rather complex set of criteria, which is difficult not only because of the huge astroglial heterogeneity, but also due to developmental changes in astroglial phenotype and because of the wide presence of NG2-glia, which in some past studies were considered a subtype of astrocyte.

4.2 Defining an astrocyte: common properties

In some systematic studies, Harald Kimelberg (Kimelberg, 2009, 2010) has elaborated eight criteria for identifying astrocytes, as follows:

- i) Absence of electrical excitability (i.e. astrocytes cannot generate action potential).
- ii) A very negative membrane potential (-80 to -90 mV) because of a prevalence of K^+ permeability of the plasmalemma; the membrane of astrocyte behaves as an almost ideal K^+ electrode.
- iii) Functional expression of transporters for GABA and glutamate that permits the astroglial role in neurotransmitter homeostasis.
- iv) A large number of intermediate filament bundles, which are the sites of the astrocyte specific protein GFAP.
- v) Glycogen granules.
- vi) Processes from each cell contacting and surrounding blood vessels.
- vii) Elaborated perisynaptic processes.
- viii) Linkage to other astrocytes by gap junctions formed by connexin 43 and/or 30.

This classification, although being straightforward and conceptually simple, omits too many classes of cells that share functional properties considered fundamental and defining for astrocytes. This fundamental property of astrocytes is the maintenance of CNS homeostasis. In this respect, the family of astrocytes can be functionally defined as the homeostatic cells of the CNS that provide for molecular, cellular and organ homeostasis.

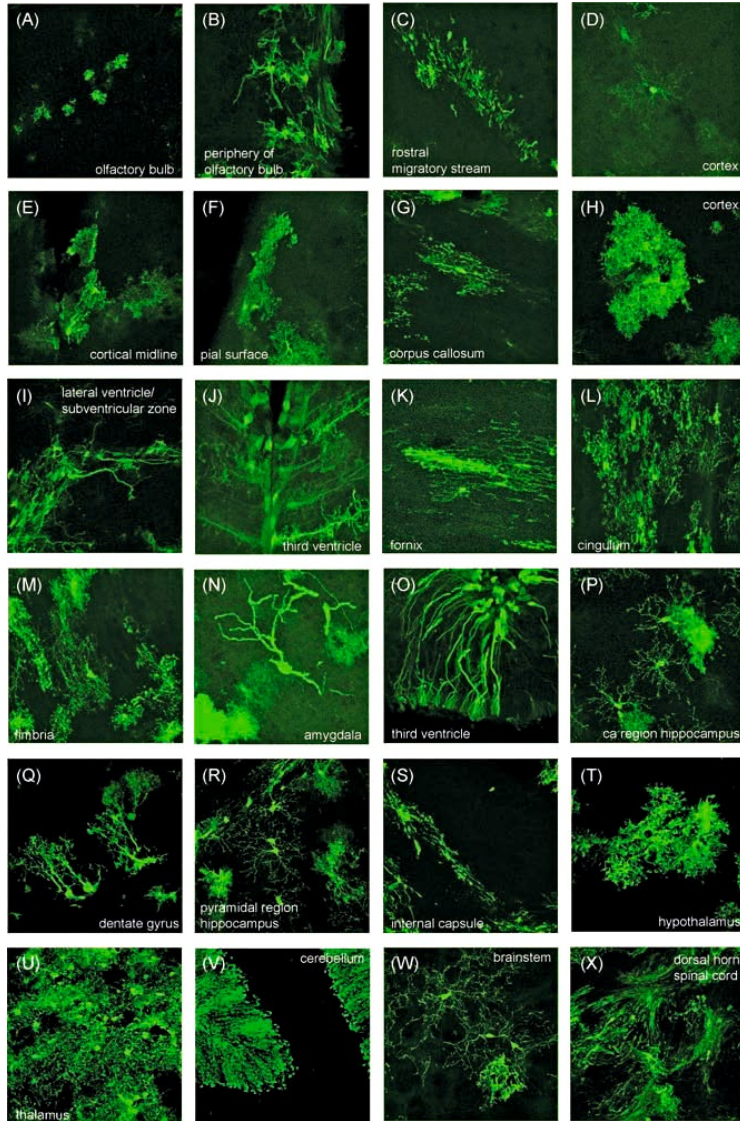


Fig 4.1 Morphological diversity of astrocytes throughout the brain.

Reconstructions from confocal images stacks of astrocytes taken from different regions of the brain and the spinal cord of the adult transgenic mouse expressing enhanced green fluorescence protein under control of glia-specific promoter.

From Emsley and Macklis, 2006.

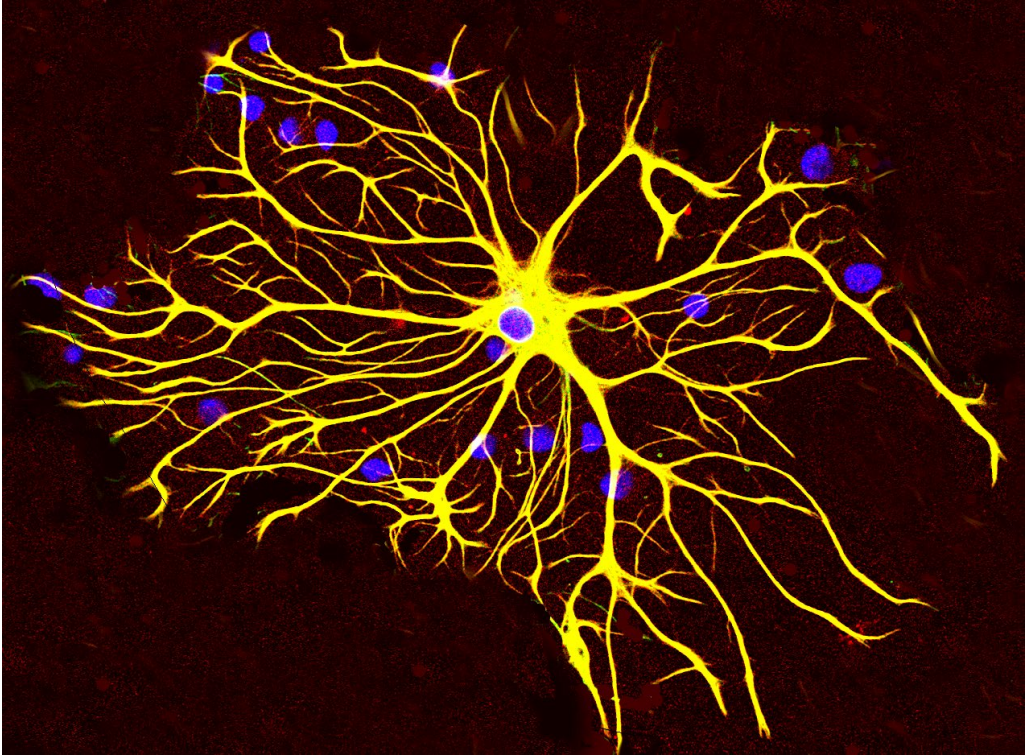


Fig 4.2 An astrocyte in culture

An astrocyte cell grown in tissue culture stained with antibodies to GFAP and vimentin. The GFAP is coupled to a red fluorescent dye and the vimentin is coupled to a green fluorescent dye. Both proteins are present in large amounts in the intermediate filaments of this cell, so the cell appears yellow, the result of combining strong red and green signals. The blue signal is DNA revealed with DAPI and shows the nucleus of the astrocyte and of other cells in this image. Image was captured on a confocal microscope in the EnCor Biotechnology laboratory.

4.3 Morphology of the main type of astrocyte

Some classical staining techniques, such as Golgi impregnation or gold chloride sublimate staining method of Cajal, as well as immunohistochemical staining with GFAP antibodies (fig 4.1) have provided oversimplified images of protoplasmic astrocytes. These techniques mostly revealed the main astroglial processes, which contributed to our image of astroglia as star-like cells. The introduction of staining techniques that utilised either filling astrocytes with fluorescent dyes, staining with rhodamine 101 (which preferably accumulates in the astrocyte cytosol), or using targeted expression of cytoplasmic fluorescent proteins, have revolutionised morphological studies of astroglia. Indeed, protoplasmic astrocytes have an incredibly complex arborisation of processes that cannot be seen so deeply by GFAP immunolabeling.

The bulk of this arborisation is made of short, feather-like, ultra-fine and extensively ramified processes, 2–10 μm long, extending from principal processes to endow protoplasmic astrocytes with a spongiform appearance.

These fine processes also exhibit rapid structural plasticity, especially at the sites contacting to synapses, where

astrocytes extend lamellipodia-like membrane protrusions along neuronal surfaces, or filopodia-like extensions, which protrude and retract within tens of seconds (Hirrlinger et al., 2004). The arborisation of protoplasmic astrocytes delineates discrete territorial domains, and there is little overlap (<10 %) between neighbouring cells. On average, protoplasmic astrocytes in rodent hippocampus of rats occupy the volume of $\approx 43,000\text{--}66,000 \text{ mm}^3$ (Bushong et al., 2002; Wilhelmsson et al., 2006). The process surface area of protoplasmic astrocytes may reach up to $80,000 \text{ mm}^2$ and cover most of neuronal membranes within their domain. Some processes of protoplasmic astrocytes contact blood vessels, forming so-called perivascular endfeet, and some protoplasmic astrocytes also send processes to the pial surface, where they form subpial endfeet, which contribute to *glia limitans*.

The density of protoplasmic astrocytes is different in various brain regions. A single protoplasmic astrocyte in rodent cortex contacts 4–8 neurons, surrounds $\approx 300\text{--}600$ neuronal dendrites and provides cover for up to 20,000–120,000 synapses residing within its domain (Bushong et al., 2002; Halassa et al., 2007b).

4.4 Human astrocytes

Human protoplasmic astrocytes are 2–3 times larger and exceedingly more complex; the processes of a single human protoplasmic astrocyte cover approximately 2 million synapses. The morphology of protoplasmic astrocytes across the brain is highly heterogeneous. Even within the same CA1 hippocampal area, protoplasmic astrocytes have different shapes, with sub-populations of fusiform cells, spherical or markedly elongated astrocytes (Bushong et al., 2002). Protoplasmic astrocytes in the entorhinal cortex are elongated cells with several main processes, whereas astrocytes in other brain regions have distinctly different morphology.

These differences are clearly revealed by both immunocytochemistry with GFAP (which visualises cytoskeleton) and with genetically targeted green fluorescent protein (that is distributed within the cytosol and therefore also shows fine processes).

Polarised astrocytes are a class of cells possibly confined to the brains of primates, which are positioned in the deep cortical layers very near to the white matter. These cells have one or two long (up to 1mm in length) processes that penetrate into superficial cortical layers.

Also the *varicose projection* astrocytes appear to exist only in the brains of humans. These cells are characterised by several (up to 5) long (up to 1 mm) unbranched processes that extend in all directions through the deep cortical layers. These processes are endowed with evenly spaced varicosities. Once more, the role of these types of cells remains unknown.

In addition to these *classical* astrocytes, more types of astroglia, represented by radial-like glia and glia in specific organs, are distinguished in the brains of humans and, more in general, of mammals.

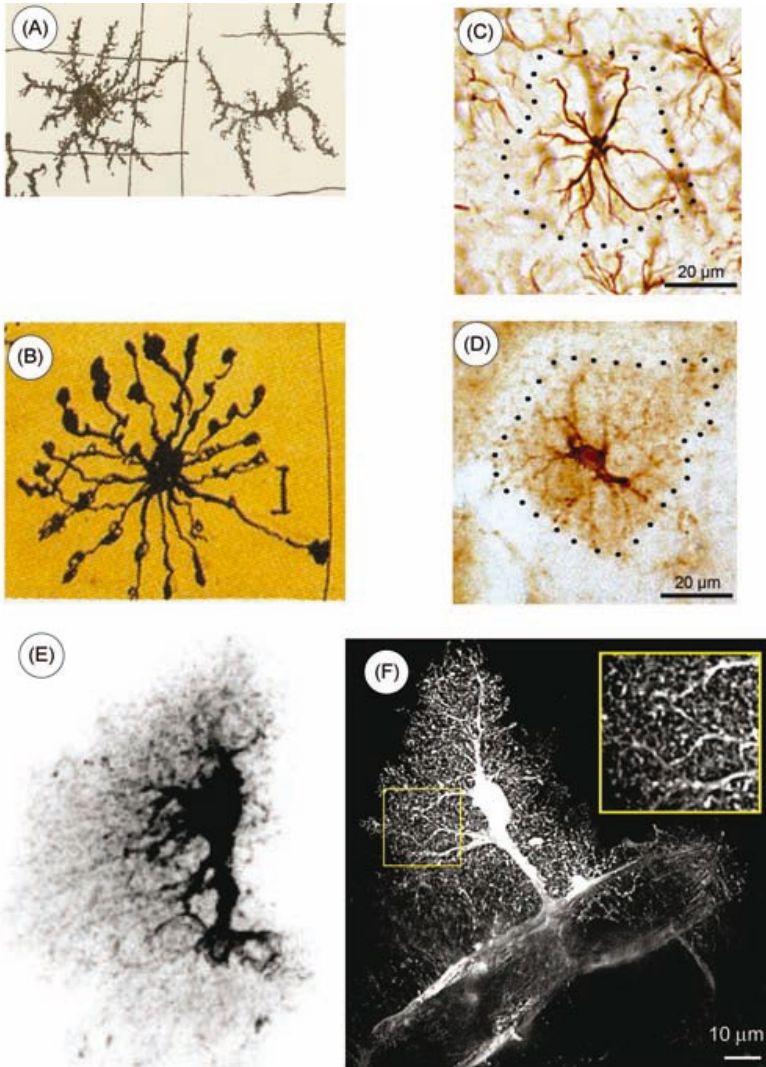


Fig 4.3 Visualisation of astrocytes with different techniques

*A,B. Human astrocytes stained by Golgi method
(A: reproduced from Retzius, 1894; B: drawing of Cajal).*

C. Hippocampal mouse astrocyte stained with antibody against GFAP.

D. Similar mouse hippocampal astrocyte stained with antibody against astroglia-specific enzyme, glutamine synthetase.

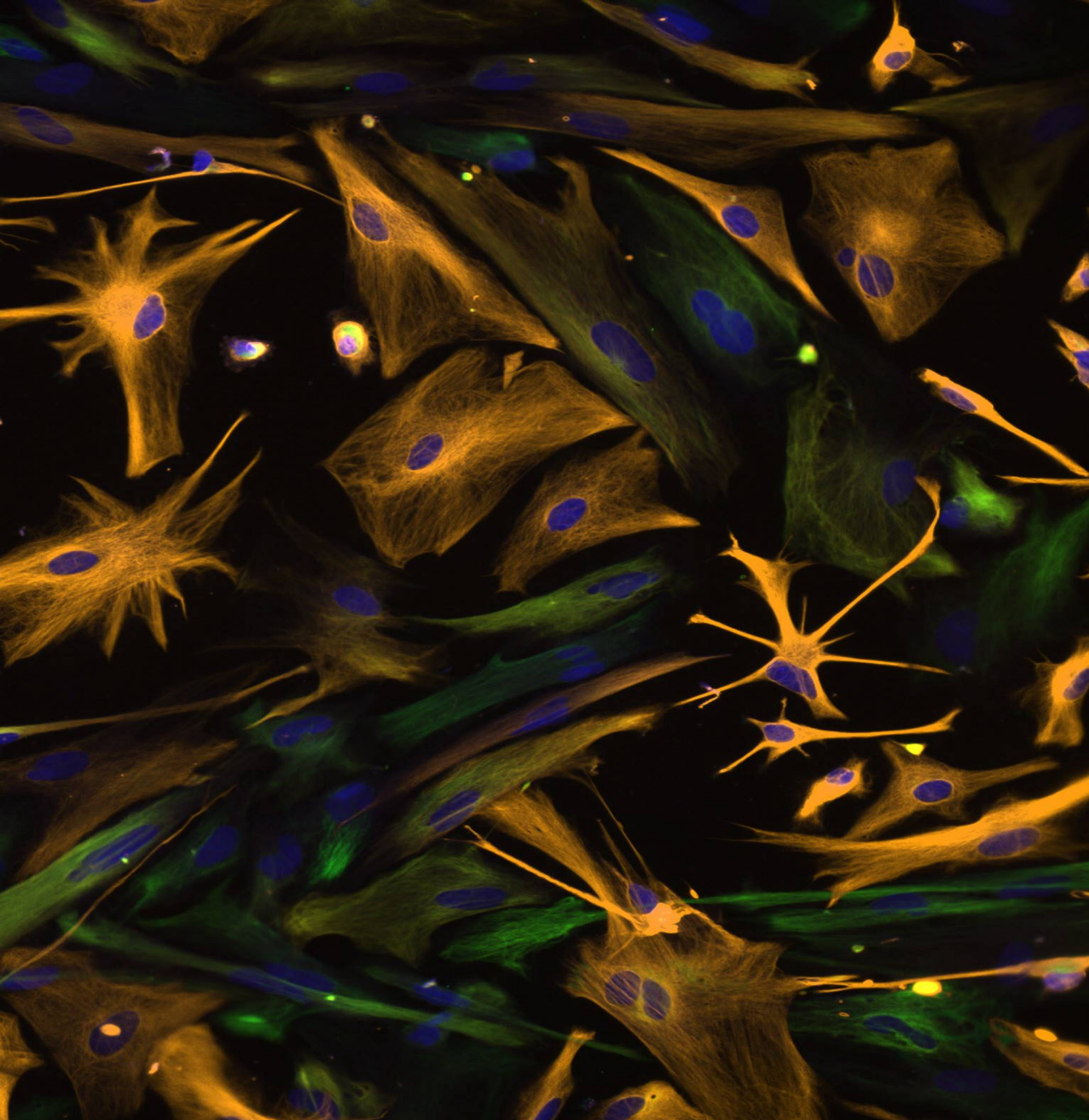
(C & D both from Olabarria et al., 2011).

E. A single astrocyte labelled with enhanced green fluorescent protein (eGFP). The fine intricate processes of protoplasmic astrocytes are visualised by eGFP fluorescence. Insert shows the eGFP labelled astrocytic processes in higher magnification. The astrocytes were transfected in situ by an intracortical injection of adenoviral eGFP. The brains were processed for histology 2–4 days later.

(From Wilhelmsson et al., 2006).

F. Image of hippocampal astrocyte injected with fluorescent dye Alexa Fluor 568; dye filling reveals a cloud of fine spongiform processes.

(From Nedergaard, et al., 2010).



Differentiation of multipotent human neural progenitor cells into astrocytes.

Credit: NIH.

5. Astrocytes in Action

5.1 The tripartite synapse

Twenty-five years ago, the term *tripartite synapse* was proposed to conceptualize the evidence obtained by many laboratories during the 1990s that revealed the existence of bidirectional communication between neurons and astrocytes.

It represents a concept in synaptic physiology wherein, in addition to the information flow between the pre- and postsynaptic neurons, astrocytes exchange information with the synaptic neuronal elements, responding to synaptic activity and regulating synaptic transmission.

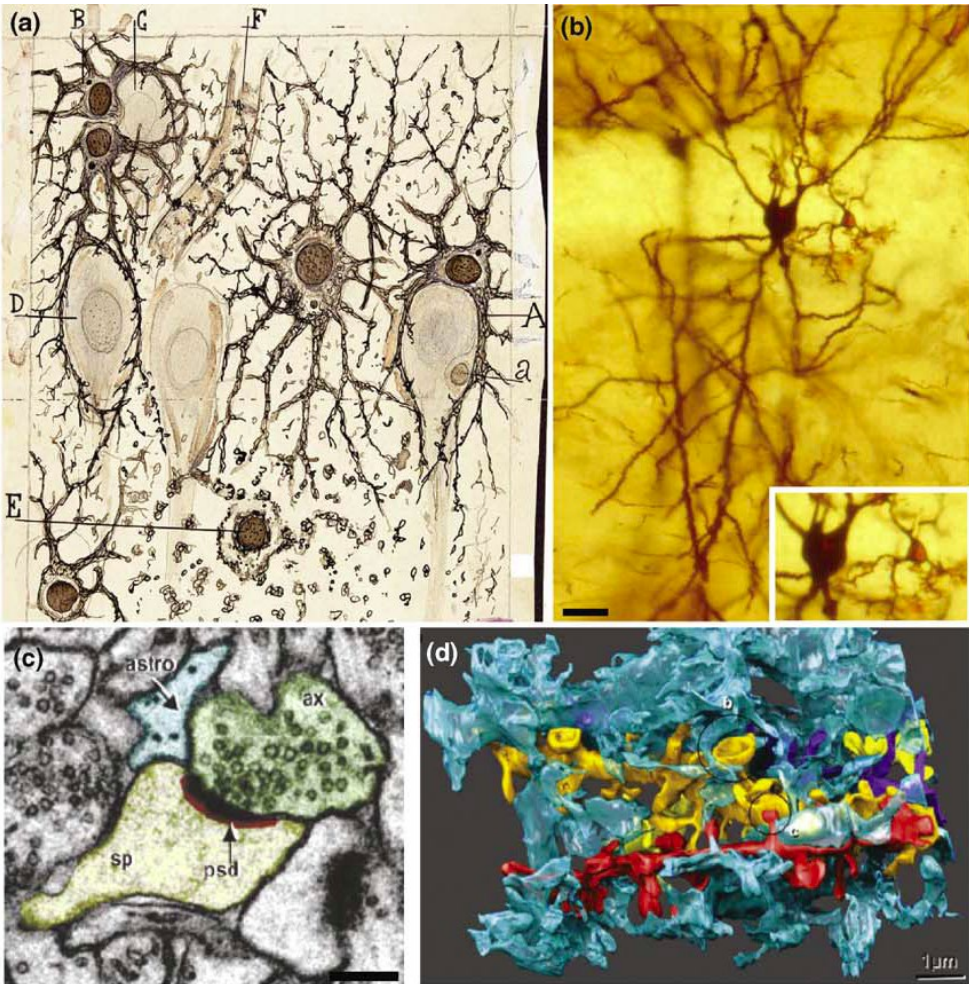


Fig 5.1 Views of the neuron–astrocyte interaction at the tripartite synapse level.

(a) *Cajal's drawing showing 'neuroglia' of the pyramidal layer and stratum radiatum of the Ammon horn (from an adult man autopsied three hours after death).*

Original labels: A, large astrocyte embracing a pyramidal neuron; B, twin astrocytes forming a nest around a cell, C, while one of them sends two branches forming another nest, D; E, cell with signs of 'autolysis'; F, capillary vessel.

(b) *Neuron and astrocyte stained with the Golgi method from a rat hippocampus. Inset: astrocyte and neuronal somas.*

(c) *Electron microscopy image of astrocyte process at the axon–spine interface:*

astrocyte process (astro, blue); postsynaptic density (psd, red); dendritic spine head (sp, yellow); axonal bouton (ax, green).

(d) *3D reconstruction of a single astrocyte process (blue) interdigitating among four dendrites (gold, yellow, red and purple). From Perera et al., 2009.*

The biology of astrocyte–neuron interaction has emerged as a rapidly expanding field and has become one of the most exciting topics in current neuroscience that is changing our vision of the physiology of the nervous system.

The classically accepted paradigm that brain function results exclusively from neuronal activity is being challenged by accumulating evidence suggesting that brain function might actually arise from the concerted activity of a neuron–glia network.

5.2 Ca²⁺-mediated cellular excitability of astrocytes

The astrocytic revolution in current neuroscience began in the early 1990s when pioneering studies used the fluorescence imaging techniques to monitor intracellular Ca²⁺ levels in living astrocytes. Those first studies^{30,31} revealed that cultured astrocytes display a form of excitability based on variations of the intracellular Ca²⁺ concentration. Until then, astrocytes had been considered as non-excitabile cells because, unlike neurons, they do not show electrical excitability. Since these pioneering findings, subsequent studies performed in cultured cells, brain slices and, more recently, in vivo have firmly established the astrocyte excitability, which is manifested as elevations of cytosolic Ca²⁺ mainly as a result of the mobilization of Ca²⁺ stored in the endoplasmic reticulum.

The elevated Ca²⁺ then acts as a cellular signal³². Whereas neurons base their cellular excitability on electrical signals generated across the plasma membrane, astrocytes base their cellular excitability on variations of Ca²⁺ concentration in the cytoplasm.

5.3 Astrocyte Ca^{2+} is controlled by synaptic activity

Astrocyte Ca^{2+} elevations can occur spontaneously as intrinsic oscillations in the absence of neuronal activity and they can also be triggered by neurotransmitters released during synaptic activity, which is of crucial importance because it indicates the existence of neuron-to-astrocyte communication.

The synaptic control of the astrocyte Ca^{2+} signal is based on the fact that astrocytes express a wide variety of functional neurotransmitter receptors. Many of these receptors are of metabotropic type, being associated with G proteins that, upon activation, stimulate phospholipase C and formation of inositol (1,4,5)-triphosphate (Ins(1,4,5)P3), which increases the intracellular Ca^{2+} concentration through the release of Ca^{2+} from intracellular Ins(1,4,5)P3-sensitive Ca^{2+} stores¹⁶⁻²¹.

Early studies using cultured cells showed that the astrocyte Ca^{2+} signal could propagate to neighbouring astrocytes as an intercellular Ca^{2+} wave involving dozens of cells^{4,5,22}. The synaptically evoked as well as the spontaneous Ca^{2+} signal originates in spatially restricted areas called *microdomains* of the astrocyte processes,^{24,25} from where it can eventually propagate intracellularly to other regions of the cell^{20,25,26}. As a single astrocyte might contact up to 10^5 synapses: the control of the spatial extension of the Ca^{2+} signal

could have relevant functional consequences for the physiology of the nervous system, because not all synapses covered by a single astrocyte are necessarily functionally locked to be similarly and simultaneously modulated.

Therefore, differential neuromodulation of specific synapses would provide an extraordinary increase of the degrees of freedom to the system.

5.4 Astrocyte Ca^{2+} signal *in vivo*

For many years, technical constraints limited astrocyte Ca^{2+} signal studies to cultured cells and brain slices. The recent use of novel imaging techniques, that is, two-photon microscopy and specific fluorescent dyes that selectively label astrocytes *in vivo*, enabled the study of astrocyte Ca^{2+} signals in the whole animal and has revealed important findings.

First, reports from studies of rat, mouse and ferret have demonstrated that astrocytes *in vivo* exhibit intracellular Ca^{2+} variations, indicating that astrocyte Ca^{2+} excitability is not a peculiarity of slice preparations. Second, like in brain slices, astrocyte Ca^{2+} variations occur spontaneously³⁰⁻³³ and are also evoked by neurotransmitters released during synaptic activity^{31,33-37}, indicating that neuron-to-astrocyte communication is present *in vivo*.

Finally, and of special relevance, astrocyte Ca^{2+} elevations might be triggered by physiological sensory stimuli. Indeed, stimulation of whiskers increased the astrocyte Ca^{2+} in the mouse barrel cortex³³ (fig 5.2).

Astrocytes of the sensory cortex also elevate their Ca^{2+} in response to a robust peripheral stimulation that is known to activate the locus coeruleus or to direct electrical stimulation

of this nucleus³⁴, as well as during running behaviour in alert mice³⁵. Astrocytes from other brain regions also respond to stimuli of corresponding sensory modalities. Astrocytes in the visual cortex not only show Ca^{2+} elevations in response to visual stimuli but also the properties of these responses indicate the existence of distinct spatial receptive fields and reveal an even sharper tuning than neurons to visual stimuli³⁷.

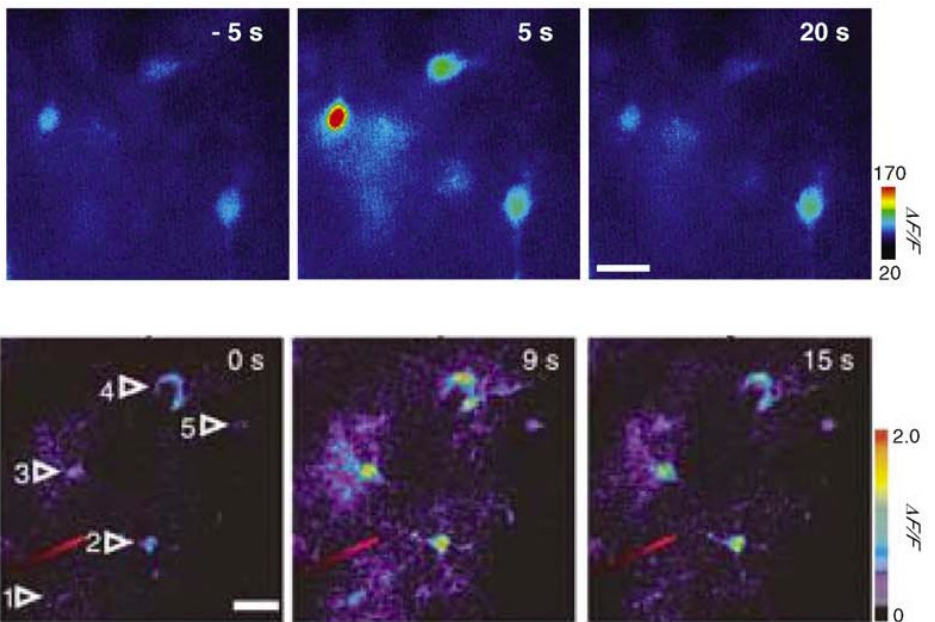


Fig 5.2 Astrocyte Ca^{2+} signalling in brain slices and in vivo.

Upper line: Pseudocolor images from rat hippocampal slices representing fluorescence intensities indicative of astrocyte Ca^{2+} levels before

(-5 s) and after (5 s, 20 s) electrical stimulation of Schaffer collaterals. Scale bar, 10 μ m.

Lower line: Two-photon microscopy images of the in vivo astrocyte Ca^{2+} signal in the barrel cortex. Pseudocolor images represent fluorescence intensities indicative of astrocyte Ca^{2+} levels before (0 s) and after (9 s, 15 s) evoked by whisker stimulation. Scale bar, 20 μ m. From Wang, X. et al., 2006.

In summary, astrocytes in vivo display Ca^{2+} excitability and respond to neuronal activity. Furthermore, because astrocytes in specific sensory areas respond to a variety of sensory stimuli, it is feasible that astrocytes participate in the brain representation of the external world.

5.5 Synaptic information processing by astrocytes

In contrast to the view of astrocytes as passive elements that provide the adequate environmental conditions for appropriate neuronal function and that respond to neurotransmitters, simply performing a linear readout of the synaptic activity, experimental evidence supports the idea that astrocytes integrate and process synaptic information elaborating a complex nonlinear response to the incoming information from adjacent synapses.

As previously affirmed, it is firmly established that astrocytes respond with Ca^{2+} elevations to synaptic activity. However, to understand the actual role of astrocytes in brain information processing, it is necessary to define whether the astrocyte Ca^{2+} signal passively results from different neurotransmitter concentrations attained during synaptic activity or, alternatively, whether neuron-to-astrocyte communication presents properties of complex information processing that are classically considered to be exclusive to neuron-to-neuron communication.

5.6 Astrocytes discriminate the activity of synaptic pathways

The astrocyte Ca^{2+} signal does not result from a nonspecific spillover of neurotransmitters. Instead, it is selectively mediated by the activity of specific synaptic terminals (fig 5.3). Astrocytes located in the *stratum oriens* of the CA1 area of the hippocampus respond to the stimulation of the alveus (which contains glutamatergic and cholinergic axons) with Ca^{2+} elevations that are specifically mediated by acetylcholine (ACh) but not by glutamate¹⁶.

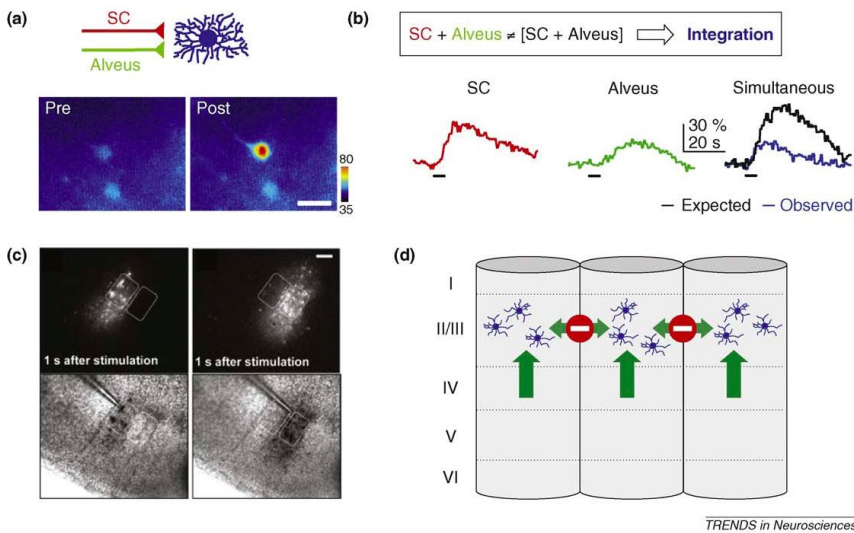


Fig 5.3 Astrocytes integrate synaptic information.

(a) Schematic drawing and pseudocolor images of astrocyte Ca^{2+} elevations evoked by stimulation of Schaffer collaterals (SC, red) or alveus (green). Astrocytes integrate synaptic information from different synaptic inputs. Scale bar: 15 μ m.

(b) Hypothesis of astrocyte integration of synaptic information induced by SC and alveus activity (top) and astrocyte Ca^{2+} signals evoked by independent and simultaneous stimulation of SC and alveus (bottom). Blue and black traces correspond to the observed and expected responses (i.e. the linear summation of the responses evoked by independent stimulation of both pathways), respectively. Horizontal lines at the bottom of each trace represent the stimuli. Note the lack of correspondence between observed and expected responses, that is, the relative reduction of the observed response versus the linear summation of the responses evoked independently, which is indicative of synaptic integration.

(c) Top, fluorescence images showing astrocytic Ca^{2+} signals evoked after electrical stimulation (responding cells are displayed in white) of two contiguous barrel cortex. Bottom, images showing an overlay of the bright-field image with the location of the stimulating pipette and the responding astrocytes (shown in black). Dotted white lines outline the barrels in layer 4. Scale bar: 100 μ m. Note that astrocytes that respond to the stimulation of the barrel column are located within the stimulated barrel column, and no astrocytes respond to the stimulation of the adjacent barrel column, which indicates the selectivity of astrocyte responses.

(d) Schematic drawing illustrating the discrimination and response selectivity of barrel cortex astrocytes to neuronal activity from layer IV but not from layer II/III of neighbouring barrels. From Schipke, C.G. et al., 2008.

By contrast, these astrocytes do respond to glutamate when it is released by different glutamatergic synapses, that is, the Schaffer collateral (SC) synaptic terminals²⁵. Hence, astrocytes selectively respond to different synapses that use different neurotransmitters (i.e. glutamate and ACh), and they discriminate between the activity of different pathways that use the same neurotransmitter (i.e. glutamatergic axons of SC and alveus)²⁵. Likewise, astrocytes in the ventrobasal thalamus respond to the stimulation of either sensory or corticothalamic pathways, but very few respond to the activity of both³⁸. Furthermore, astrocytes in the barrel cortex also respond selectively to the activity of different neuronal inputs, because astrocytes in layer 2/3 respond to glutamatergic inputs from layer 4 in the same column but not to glutamatergic projections from layer 2/3 of adjacent columns³⁹ (fig 5.3). Therefore, astrocytes show selective responses that discriminate the activity of specific synapses.

5.7 Astrocyte Ca^{2+} signals show a nonlinear relationship with the synaptic activity

The analysis of the astrocyte Ca^{2+} signal evoked by the activity of different synaptic terminals that release ACh and glutamate indicates that astrocytes integrate synaptic information²⁵. In hippocampal slices, the simultaneous stimulation of alveus and SC (that elicit Ca^{2+} elevations mediated by ACh and glutamate, respectively) evokes astrocytic responses that are inconsistent with a linear readout of the synaptic activity. The amplitude of the Ca^{2+} elevations elicited by simultaneous stimulation of both pathways is not equivalent to the linear summation of the Ca^{2+} signals evoked by independent stimulation²⁵ (fig 5.3). Therefore, the astrocyte Ca^{2+} signal is nonlinearly modulated by the simultaneous activity of cholinergic and glutamatergic synapses. Moreover, while the Ca^{2+} signal evoked by simultaneous stimulation at high frequencies (30 and 50 Hz) displays a sublinear summation of the responses evoked independently, it shows a supralinear summation after stimulation at relatively low frequencies (1 and 10 Hz); that is, the Ca^{2+} signal is relatively depressed or potentiated at relative high and low frequencies of neuronal activity, respectively. Therefore, the astrocyte Ca^{2+}

signal is nonlinearly modulated by the simultaneous activity of different synaptic inputs, and the sign of this modulation depends on the synaptic activity level²⁵.

5.8 Gliotransmission and modulation of synaptic transmission

One of the most stimulating topics in current neuroscience is the functional consequences of the astrocyte Ca^{2+} signal on neuronal physiology. Evidence obtained during the past 20 years has demonstrated that signalling between neurons and astrocytes is a reciprocal communication, where astrocytes not only respond to neuronal activity but also actively regulate neuronal and synaptic activity. Therefore, according to the concept of the tripartite synapse, to fully understand synaptic function, astrocytes must be considered as integral components of synapses where they have crucial roles in synaptic physiology.

Astrocytes release several neuroactive molecules, such as glutamate, D-serine, ATP, adenosine, GABA, tumor necrosis factor α (TNF α), prostaglandins, proteins and peptides, that can influence neuronal and synaptic physiology³. The

mechanisms and consequences of this process, called gliotransmission, have attracted considerable interest. Several mechanisms of transmitter release from astrocytes have been proposed.

Compelling evidence demonstrates that some transmitters are released in a Ca^{2+} -dependent manner^{10,43–48} through vesicle^{47–51} and lysosome^{52–54} exocytosis. Furthermore, ultrastructural studies have shown that astrocytic processes contain small synaptic-like vesicles, which are located in close proximity to synapses, apposed either to presynaptic and postsynaptic elements^{49,59}.

Alternative release mechanisms, including reversal of glutamate transporters, connexin/pannexin hemichannels, pore-forming P2X7 receptors and swelling-induced activation of volume-regulated anion channels, have also been proposed⁵⁵. Whether Ca^{2+} -dependent and -independent mechanisms coexist and under what physiological or pathological conditions they occur remain unclear.

The original demonstration of astrocyte-induced neuromodulation in cultured cells^{43,44,56} has been considerably expanded by later studies on acute brain slices.

Glutamate was one of the first gliotransmitters released from astrocytes to be identified and has been reported to exert many effects on neuronal excitability. Astrocytic glutamate evokes slow inward currents (SICs) through activation of postsynaptic N-methyl-D-aspartate (NMDA) receptors^{25,44,60–65} and synchronously excites clusters of hippocampal pyramidal neurons, indicating that gliotransmission increases neuronal excitability and operates as a nonsynaptic mechanism for neuronal synchronization^{60,62}. By contrast, astrocytic glutamate might also activate receptors localized at presynaptic terminals. Through activation of group I metabotropic glutamate receptors (mGluRs)^{46,26} or NMDA receptors⁵⁰, astrocytes enhance the frequency of spontaneous and evoked excitatory synaptic currents.

Alternatively, astrocytes induce the potentiation²⁰ or depression of inhibitory synaptic transmission by activation of presynaptic kainate⁶⁶ or II/III mGlu⁶⁷ receptors, respectively.

Therefore, a single gliotransmitter can exert multiple effects depending on the sites of action and the activated receptor subtypes, which provides a high degree of complexity to astrocyte–neuron communication. This complexity becomes even higher when considering that other gliotransmitters, such as GABA, ATP, adenosine (a metabolic product of ATP) or D-serine, could act on the same neuron or

act on different cell types, thus evoking distinctive responses^{63,68–72}. Moreover, in hippocampal astrocytes, Ca^{2+} elevations induced by activation of PAR-1 receptors, but not P2Y1 receptors, evoke NMDA receptor-mediated SICs in pyramidal neurons⁶⁵, indicating that the Ca^{2+} signal evoked by activation of different receptors might not be equally competent to stimulate gliotransmitter release.

A great effort has been made so far to identify different gliotransmitters and their potential modulatory actions, but it remains unknown whether different gliotransmitters are co-released or whether different gliotransmitters are released by different astrocytes or by different astrocytic processes or domains. It is also crucial to elucidate the specific incoming inputs, the molecular mechanisms and the physiological conditions that govern the precise release of each gliotransmitter.

Intracellular regulatory mechanisms of release and spatially defined specific intercellular signalling pathways seem to be present to grant a coherent astrocyte–neuron communication.

Besides glutamate, ATP and its product adenosine of astrocytic origin also control synaptic transmission^{68–71}.

Indeed, heterosynaptic depression of hippocampal synaptic transmission requires astrocyte release of

ATP/adenosine⁶⁹⁻⁷¹, which is stimulated by the GABAB mediated astrocyte Ca²⁺ signal elicited by interneuron activity evoked by SC⁷⁰.

This represents a paradigmatic example of the consequences of coordinated neuron–glia networks on synaptic function. Furthermore, it also shows that synaptically evoked astrocytic ATP might signal to other synapses, thus spreading neuronal information beyond activated synapses.

Likewise, glutamate from astrocytes stimulated by endocannabinoid released during neuronal activity could signal to adjacent unconnected neurons⁶⁴, suggesting that astrocytes serve as a bridge for non-synaptic communication between neurons.

In conclusion, astrocytes not only influence the active synapses through short-range signalling, but they might also have long-range effects on distant synapses.

Hippocampal slices are a useful experimental model to study synaptic transmission, and consequently they have been also widely used to analyse the astrocyte effects on synaptic transmission. Although a comprehensive characterization of the phenomenon in different brain areas is still lacking, glia-mediated synaptic transmission modulation has also been documented in retina, supraoptic nucleus and cerebellum, as

well as at the neuromuscular junction in the peripheral nervous system^{58,73}.

Finally, the effects of the activity of single astrocytes on single synapses have been investigated extensively in the hippocampus, also by performing paired recordings from pyramidal neurons and single astrocytes while stimulating SC single synapses, that is, by experimentally isolating the tripartite synapse⁴⁶.

Astrocyte Ca^{2+} elevations transiently increase the probability of neurotransmitter release from presynaptic terminals, thus enhancing the synaptic efficacy (fig 5.4).

This effect is mediated by Ca^{2+} and SNARE protein-dependent release of glutamate from astrocytes, which activates group I metabotropic glutamate receptors at the presynaptic terminal⁴⁶.

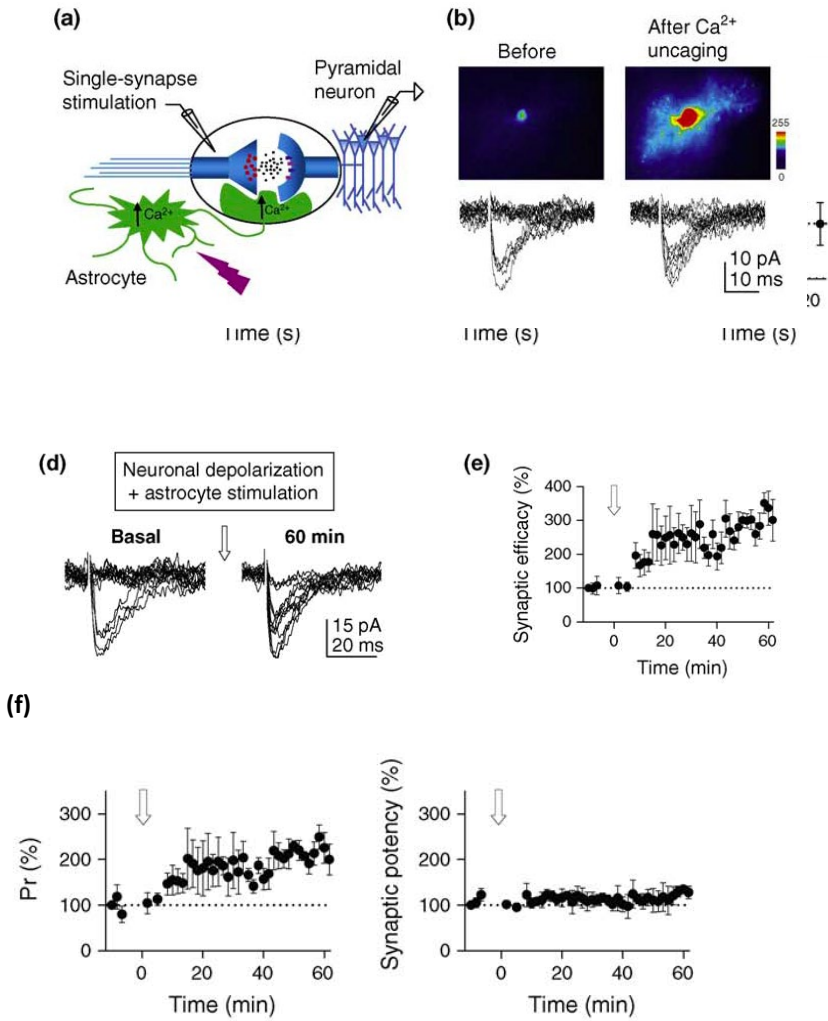


Fig 5.4 Astrocytes control synaptic transmission and plasticity at the tripartite synapse.

(a) *Schematic drawing showing recordings from one pyramidal neuron and one astrocyte, and the stimulation of a single synapse.*

(b) *Astrocyte Ca^{2+} levels (top) and synaptic responses (bottom) before and after Ca^{2+} uncaging at a single astrocyte. Note the increase in the proportion of successful synaptic responses after astrocyte Ca^{2+} elevation.*

(c) *Astrocytes potentiate synaptic efficacy (i.e. mean amplitude of all responses including failures), increasing the probability of transmitter release (Pr: ratio between the number of successes versus the total number of stimuli) without modulating the amplitude of synaptic responses (i.e. synaptic potency, defined as mean amplitude of the successful responses). Note the transient increase of synaptic efficacy and Pr after elevating astrocyte Ca^{2+} (at time zero).*

(d,e) *Temporal coincidence of astrocyte Ca^{2+} signal and postsynaptic neuronal depolarization induces long-term potentiation (LTP) of synaptic transmission. Excitatory synaptic currents before and 60 min after transiently pairing neuronal depolarization and astrocyte Ca^{2+} uncaging.*

(f) *Graphs showing relative change in synaptic efficacy, Pr and synaptic potency parameters over time. Arrows indicate pairing of astrocyte Ca^{2+} signal and mild neuronal depolarization. Note the persistent potentiation of synaptic efficacy and Pr induced by the transient pairing (for 5 min) of neuronal and astrocyte stimulation (at time zero).*

From Perea et al., 2007.

5.9 Astrocytes and synaptic plasticity

Astrocytes operate at lower time scales than synaptic neurotransmission. Whereas fast neurotransmission occurs in milliseconds, astrocytic effects on neuronal physiology last seconds or tens of seconds. In addition, astrocyte regulation of synaptic transmission runs on different time scales, because astrocytes can control transiently the synaptic strength (during seconds), and they can also contribute to long-term synaptic plasticity. Several mechanisms underlying the astrocyte effects on long-term potentiation (LTP) have been described.

Some studies indicate a passive or tonic mode of action, in which astrocytes tonically suppress or potentiate synaptic transmission^{69,72,74,75}. Astrocytes through ATP/adenosine release control the strength of the basal hippocampal synaptic activity by tonic suppression of neurotransmission, which results in an increase in the dynamic range for LTP⁶⁹. In the hypothalamic supraoptic nucleus, changes in the astrocytic coverage of synapses influence NMDA-receptor-mediated synaptic responses due to changes in the ambient levels of D-serine released by astrocytes⁷².

By contrast, astrocytes participate in the generation of LTP through a phasic signaling process, in which the temporal

coincidence of the astrocyte Ca^{2+} signal and the postsynaptic neuronal activity induces LTP through the activation of presynaptic type I mGluRs by Ca^{2+} -dependent glutamate release from astrocytes⁴⁶. These findings have expanded our traditional vision of the Hebbian LTP (a paradigm of synaptic plasticity based on the coincident activity of pre and postsynaptic neuronal elements) to include astrocytes as new sources of cellular signals involved in synaptic plasticity.

5.10 Are all synapses tripartite?

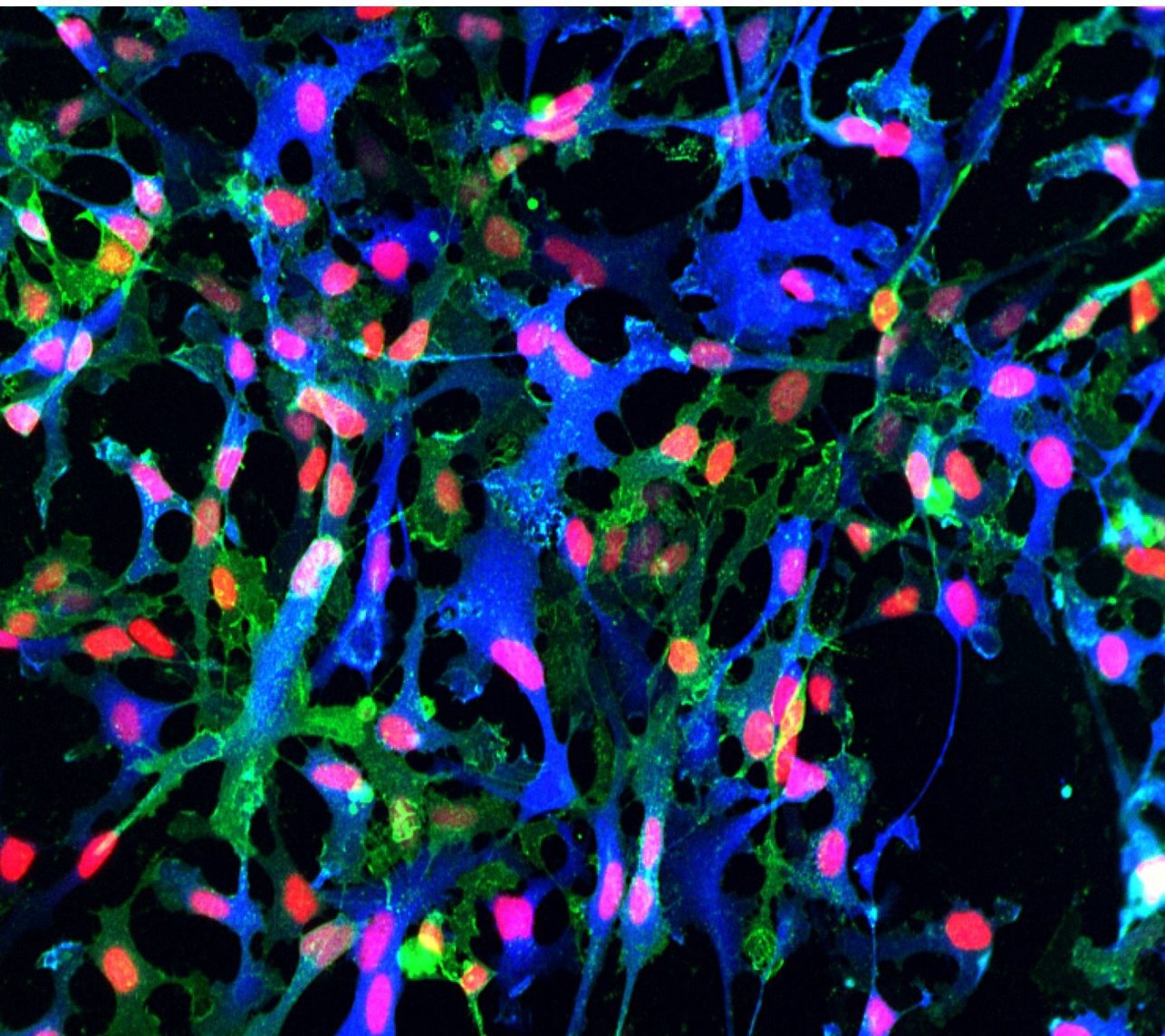
Experiments designed to observe the effects of the astrocyte Ca^{2+} signal on single hippocampal synapses showed that not all recorded synapses displayed modulation of the synaptic efficacy after astrocyte stimulation, but only a subset of synapses (around 40%) underwent astrocyte induced potentiation⁴⁶. Experimental conditions might account for some ineffective cases because, owing to the limits of optical resolution, it could not be excluded that the stimulated astrocyte was not in sufficient close proximity to the recorded synapse. Alternatively, it is feasible that, in some cases, the stimulated astrocyte and the recorded synapse were not functionally connected.

Whether this absence of connectivity is due to functional or structural bases is unknown, but it is interesting to note that ultrastructural data shows that only a subset of hippocampal excitatory synapses (again around 40%) are covered by astrocytic processes⁷⁸, which is consistent with the hypothesis that not all synapses are functionally tripartite.

The fact that Ca^{2+} elevations evoked in a large population of astrocytes by ATP application potentiated neurotransmission in around 40% of the recorded synapses

further supports this hypothesis⁴⁶. If this is the case, it would be interesting to test whether tripartite synapses are stable or dynamic functional units. The latter idea seems to be favoured by the observation that coordinated structural changes in astrocytic processes and synaptic spines occur in hippocampal synapses⁷⁹ and in the somatosensory cortex where whiskers stimulation evokes morphological changes on astrocytic processes that cover synapses⁸⁰.

The plasticity in the establishment of tripartite synapses might have a strong impact on the function of the neuron–glia network. In any case, the fact that only a subset of synapses were effectively modulated by single astrocytes indicates that neuromodulation does not result from a wide spillover of the gliotransmitter but, instead, suggests the existence of specific signalling pathways between astrocytes and neurons, probably as a point-to-point form of communication.



Pluripotent stem cells that the researchers used to produce astrocytic cells.

Credit: KTH, The Royal Institute of Technology.

6. Results

There are few and precise questions at the basis of my thesis. My experimental work started, at the beginning, from confocal morphological observations in AD11 mice (an AD-like mouse model characterized by a chronic deprivation of NGF, see introduction). Incredibly clear – and promising – alterations (shrinkage of spatial coverage and loss of cellular complexity) in morphology of astrocytes in AD11 mice at 2 month of age, i.e. still in a context of relatively healthy neurons, led to a complex journey through the glia-neuron relationship with the

aim of unveiling a new mechanism at the basis of neurodegeneration, and the consequence of wide the NGF therapeutic potential in neurodegeneration.

The questions that animated my work and that progressively led the journey are formulated below. I formulated the answer reported after each question, through the experimental work progressively described in the following paragraphs.

What happens to astrocytes morphology when NGF is starved?

The astrocytes in AD11 mice are clearly atrophic; they show a marked shrinkage at 2 months of age i.e. in an early pre-symptomatic phase of this mouse model when other Alzheimer's-like neurodegeneration or phenotypic hallmarks are not still presents in these animals.

What are the crucial events at the basis of these morphological alterations?

I suggest that the crucial event that determines these morphological alterations is the relative balance between the immature and mature form of NGF, not the absolute levels of each form of the neurotrophin.

Can we reproduce the changed astrocyte morphology in vitro?

I demonstrated that in vivo, as well as in vitro, there is a correlation between the morphological complexity of the astrocytes and the availability of mature NGF.

How do I explain the effect of the anti-NGF antibody? What about NGF receptors on astrocytes in vivo?

- i) Both NGF receptors are present in cultured astrocytes;*
- ii) the receptors are located on the membrane surface;*
- iii) they have the expected molecular weight and*
- iv) cultured astrocytes produce NGF and secrete it in the medium.*

What are the genes modulated in the early phases?

I found that specific genes identifying a reactive state of astrocytes were upregulated in α D11-treated astrocytes. Genes related to inflammation such as chemokines and receptors for immunoglobulins were individually upregulated up to 10-fold. In particular, kallikrein 6 (KLK6), a trypsin-like serine protease, has been found to be the top upregulated gene.

What are the short-term effects of anti NGF treatment?

I demonstrated that, in the astrocytes, NGF deprivation by anti NGF antibodies causes a fast and durable calcium response within 5 minutes. On the contrary, astrocytes are completely deaf to NGF, despite the fact that cultured astrocytes express both TrkA and p75NTR receptors.

This surprising striking result shows that cultured astrocytes can respond very rapidly to an acute reduction of the NGF levels, but not to an acute increase of NGF levels.

What is the source of the calcium ions involved in the oscillations induced by acute anti NGF treatment?

I demonstrated that the calcium ions involved in the oscillations induced by NGF deprivation derive from intracellular Calcium stores located in the ER.

What is the trigger of the calcium oscillations induced by acute anti NGF treatment?

I concluded that aD11 anti-NGF antibodies induce calcium oscillation via the activation of TrkA receptors.

What are the transcriptomic changes affecting the astrocytes at different times after anti-NGF antibody administration?

The RNA modulation occurring 24 hours after the exposure to the α D11 anti-NGF antibody was consistent with a pan-reactive phenotype and, in particular, with the acquisition of a full A1-like neurotoxic phenotype.

What happens to neurons, in astrocytes-neuron co-cultures, when astrocytes react to NGF starvation?

I demonstrated that the NGF neutralization leads to death hippocampal neurons, but only if the neurons are co-cultured with astrocytes.

What are the possible mechanisms that couple astrocytes and neuron impairment?

The neuronal impairment induced by anti NGF antibodies, is reduced by:

- i) the concomitant neutralization of the amyloid β oligomers with the specific anti- $A\beta$ -oligomer A13 antibody, or by*
- ii) the concomitant glutamate ionotropic receptors blockade.*

This indicates that the effects of deprivation of NGF might imply the production of β amyloid oligomers or

excitotoxicity.

Does the astrocyte Ca^{2+} elevations induced by NGF starvation might trigger Ca^{2+} hyper-activation in neurons?

I demonstrated that the fast increase in the astrocytes Ca^{2+} oscillations that follows the NGF neutralization is mediated by the TrkA and leads to an alteration in neuronal Ca^{2+} activity, leading neuron to death.

Can this atrophy in the brain of 3xTG-AD mice be reverted by the administration of NGF?

The results demonstrate that the astrocytes atrophy can be reverted by NGF nasally administered. I found the same results with both AD11 and 3xTg-AD mice.

Can NGF levels modulate astrocyte calcium activity also in vivo, in anesthetized animals? And in awake behaving animal?

We discovered that, also in vivo, while NGF exerted no effect on astrocytic Calcium activity, a lack of the neurotrophin by anti NGF induction increased astrocyte calcium activity in the anesthetized mouse as well as in the awake behaving animal.

What are the early events after an acute NGF starvation? Does the astrocyte react to acute NGF deprivation also translating new NGF protein?

An NGF pulse clearly appears after only 5 minutes from acute NGF starvation by α D11 antibody.

I demonstrated that the NGF pulse is new synthesized protein, i.e. not an amount previously stored in intracellular compartments.

6.1 NGF deprivation induces morphological alterations of astrocytes *in vivo*

What happens to astrocytes morphology when NGF is starved?

In order to investigate the relationship between NGF and the phenotype of astrocytes, I exploited the AD11 mouse model.

As described in the Introduction, the AD11 mice develop a progressive and comprehensive neurodegeneration, triggered by a proNGF/NGF imbalance caused by the expression of an antibody that blocks mature NGF but binds with 2000-fold less affinity to the proNGF precursor.

At the basis of my work, I started measuring the morphology of astrocytes from different mouse models in order to address the question if astrocytes could modify their morphology in reaction of NGF level modulation.

I analysed the astrocyte morphology in the hippocampus of AD11 or wild type (wt) mice of different ages, when the majority (ca. 80%) of astrocytes express GFAP. I evaluated four astrocyte morphological parameters: volume and area of the cells, the length of the processes and the number of branching points.

All measurements were performed on anti-GFAP labelled astrocytes in 40 μm hippocampal slices (fig 6.1 a).

I repeated the measures at 1, 2, 3, 6 and 12 months of age and found that in AD11 mice, compared to controls, there is a strong reduction of all the parameters at 2 months. These alterations persist (length, branching points), slightly reduce (area) or regress (volume) at 6 months. In between 6 and 12 months of age, an inversion of the trend was present. I found, definitely in 12 months old animals, that the wild type (wt) astrocytes show a reduction of all four morphological parameters values. This trend inversion is probably due to an astrogliosis caused by the aging and the concomitant Alzheimer-like phenotype in AD11 mice^{22,35,36}. Moreover, in every group of mice the complexity of the astrocytes morphology tends to reduce with the time.

Immunohistochemistry (IHC) was repeated also with anti-S100 β , to verify whether the actual structure of the astrocytes, and not only their GFAP amount, was really changed.

S100 calcium-binding protein β (S100 β) is a protein of the S-100 protein family. S100 proteins are localized in the cytoplasm and nucleus of a wide range of cells and involved in the regulation of several cellular processes such as cell cycle

progression and differentiation. S100 β is glial-specific and is expressed primarily by astrocytes.

With S100 β immunocytochemistry I found the same modifications observed with GFAP, with the only difference that the reduction of the area was not statistically significant. This is probably due to the fact that the anti-GFAP antibody does not label the cell body as the anti-S100B antibody does.

IHC against S100 β were performed in AD11 and wt animals of 2 months of age (fig 6.1 b).

The collected evidence leads to conclude that the morphological changes observed in astrocytes are really due to a structural change of these cells and could not be explained by a fluctuation of cell marker expression.

To further confirm the data, I used another staining technique: the silver impregnation according to Golgi-COX methods, that allows to visualize astrocytes independently from the use of antibodies against cytoskeletal proteins.

I found comparable results (fig 6.3) with what observed with IHC.

The astrocytes in AD11 mice are clearly atrophic; they show a marked shrinkage at 2 months of age i.e. in an early pre-symptomatic phase of this mouse model

when other Alzheimer's-like neurodegeneration or phenotypic hallmarks are not still presents in these animals.

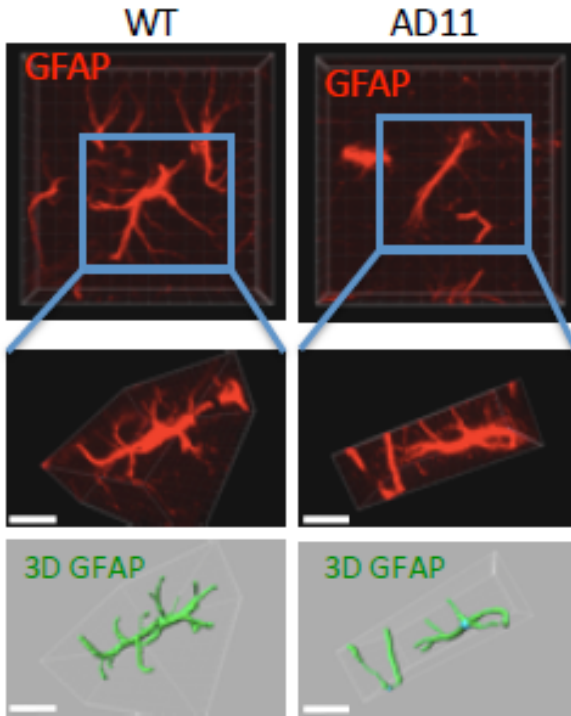


Fig 6.1- A1 - NGF deprivation induces morphological alterations of astrocytes in vivo.

AD11 are compared with WT, marked with GFAP antibody. All measurements were performed on anti-GFAP labelled astrocytes in 40 μm hippocampal slices. Here is reported the 2 months of a experiment.

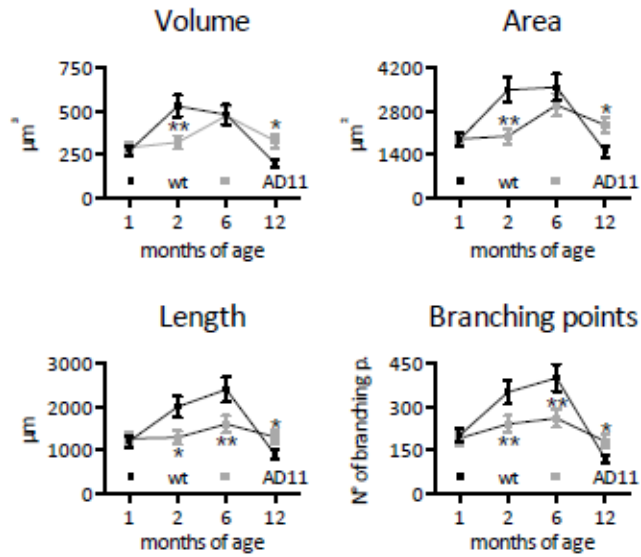


Fig 6.1- A2 - NGF deprivation induces morphological alterations of astrocytes in vivo.

AD11 are compared with WT, marked with GFAP antibody.

Quantification of the previous.

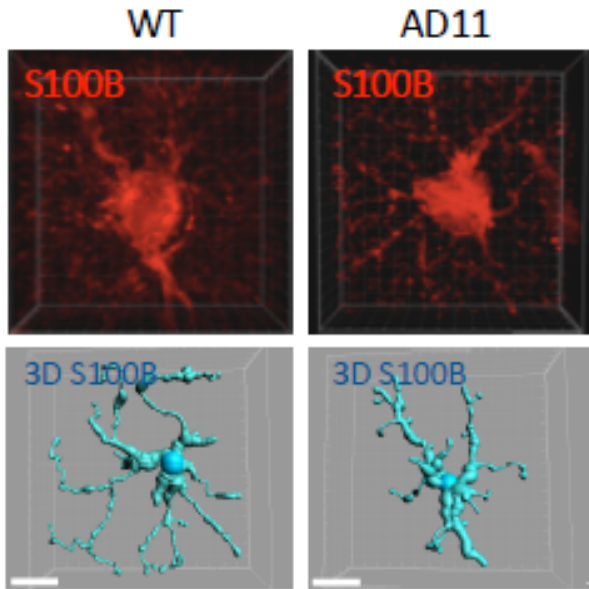


Fig 6.1- B1 - NGF deprivation induces morphological alterations of astrocytes in vivo.

*AD11 are compared with WT, marked with S100B antibody.
Mice: 2 m. of age.*

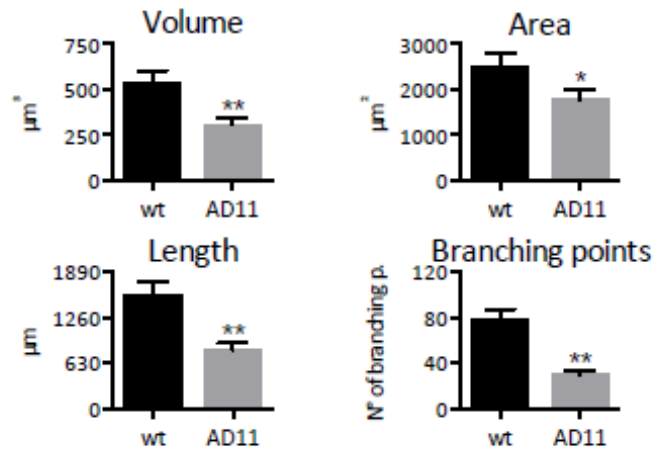


Fig 6.1- B2 - deprivation induces morphological alterations of astrocytes in vivo.

AD11 are compared with WT, marked with S100B antibody.

Quantification of the previous.

At this step it is clear that, in this anti-NGF mouse model, an astrocyte impairment is precociously present.

In this model, the neutralization of NGF by the transgenic antibody leads to variable amounts of captured NGF in different mice and, therefore, to variable amounts of free NGF. I measured the amounts of free NGF (see Methods) in the brains of individual mice and correlated this parameter with astrocyte morphology parameters.

The astrocyte atrophy well correlates with the free NGF levels (fig 6.2).

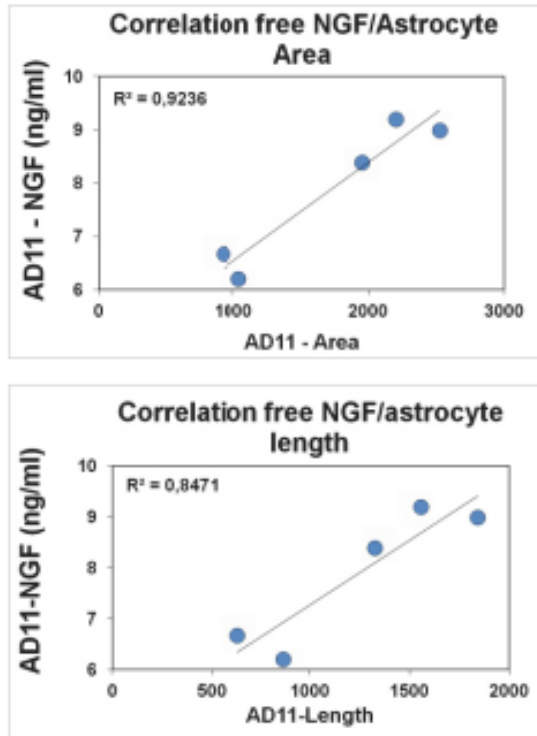


Fig 6.2 - part 1 of 2.

The atrophy well correlates with the free NGF level.

Here are reported the correlations with area and length of astrocytes. See M&M for details.

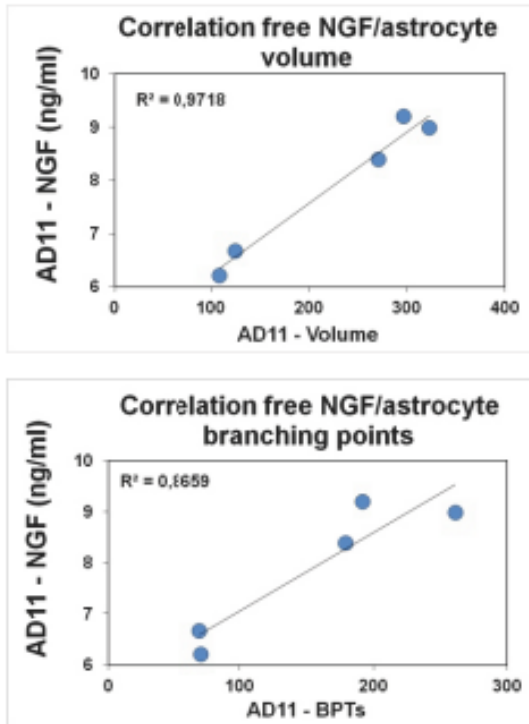
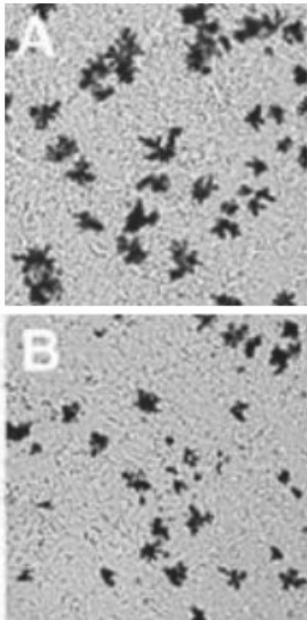


Fig 6.2 - part 2 of 2.

The atrophy well correlates with the free NGF level.

Here are reported the correlations with volume and number of branching points of astrocytes. See M&M for details.

Modified Golgi-COX staining



Wt mice,
2 months of age

AD11 mice,
2 months of age

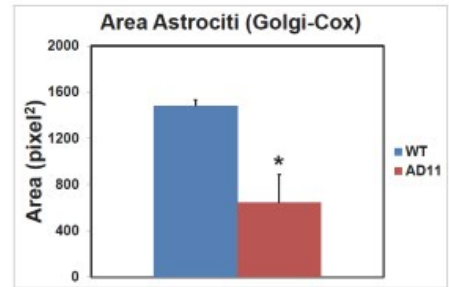


Fig 6.3 - The dysmorphic astrocyte morphology is measured also with Golgi-COX staining technique.

Pictures at left - A: Wt mice, B: AD11 mice, both of 2 months of age.

Histogram at right - quantification of astrocyte area: Wt vs AD11 mice.

6.2 Mechanism(s) at the basis of astrocytes altered morphology: role of proNGF

What are the crucial events at the basis of these morphological alterations?

In the introduction, I described the characteristics of the α D11 antibody and in particular the fact that at certain concentrations it recognizes and neutralizes in a specific manner the mature form of NGF, and not the pro-neurodegenerative precursor proNGF (Corvaglia et al., 2019).

Indeed, the affinity of α D11 anti NGF for mature NGF is 2000-fold higher than its binding affinity for proNGF (data from A. Cattaneo's lab).

This led to postulate that the experimental imbalance of proNGF versus NGF is responsible for the observed morphological change in AD11 mice.

In order to test this hypothesis with a different experimental manipulation, I postulated that also an over-expression of proNGF might contribute to the asthenic phenotype of astrocytes. To test this, I studied the morphology of astrocytes in mice over-expressing a proNGF

in a form which is uncleavable at the furin site (Tiveron et al., 2013).

These mice accumulate proNGF in the brain. In these animals I performed the same GFAP IHC previously described for AD11 mice, followed by image analysis of the cell phenotype for the 4 morphological parameters considered above.

In proNGF mice (formally TgproNGF#3 mice, see Tiveron et al., 2013) I found a more evident morphological alteration than that found in AD11 mice, described by the decrease of Area, Volume, number of Branching Points and Length of the astrocyte filaments in a statistically significant way, both with respect to AD11 and to control mice (see M&M for details, and fig 6.4).

We thus observed a similar change of astrocyte morphology by experimentally manipulating the proNGF and NGF levels in two different ways, either selectively interfering with mature NGF (in AD11 mice) or increasing the levels of proNGF (in the TgproNGF#3 mice).

For this reason, I suggest that the crucial event that determines these morphological alterations is the relative balance between the immature and mature form of NGF, not the absolute levels of each form of the neurotrophin.

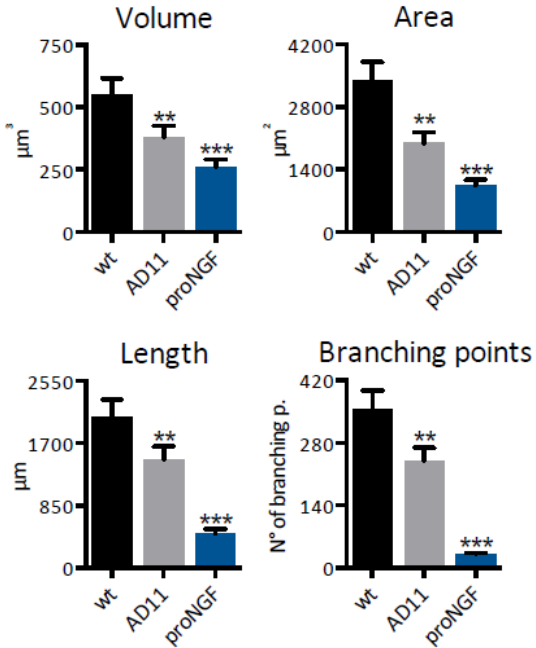


Fig 6.4 - proNGF (formally TgproNGF#3) mice shows a more evident morphological alteration than the one found in AD11 mice.

The age of both AD11 and proNGF mice was 2 months. See M&M for details.

6.3 *In vitro* effects of NGF depletion

Can we reproduce the changed astrocyte morphology in vitro?

To better understand the relationship between NGF and the changes in cellular morphology, I cultured astrocytes from P4 wild type mice, and I treated them *in vitro* with NGF or α D11 anti-NGF antibodies. The cells were evaluated at DIV28 after different treatments for 48 hours with or without NGF (100ng/ml) and, in sister cultures, with α D11 anti-NGF antibody or anti-V5 as a control-antibody at increasing concentrations. We previously developed a mathematical model that describes the interactions between NGF, proNGF and α D11 anti-NGF antibodies to choose 3 different α D11 concentrations in order to progressively neutralize NGF and not proNGF or both (Corvaglia et al., 2019).

I performed a Sholl test to evaluate the morphology. The results, quantified in fig 6.5 a, showed that the astrocytes complexity is unaltered with anti-V5 (see above, used as a control for antibody presence), NGF or low α D11 exposition (100 ng/ml). The number of filaments from the cell body to the periphery decreases if α D11 is added at a mild

concentration (200 ng/ml), and dramatically reduces with high concentrations (400 and 800 ng/ml).

The progressive and complete depletion of neurotrophin causes important changes in morphology in these cells and, on the other hand, no changes occur when NGF is added *in vitro* (fig 6.5 panel 1).

In conclusion, I demonstrated that, in vivo as well as in vitro, there are strong elements to assess a correlation between the morphological complexity of the astrocytes and the availability of mature NGF.

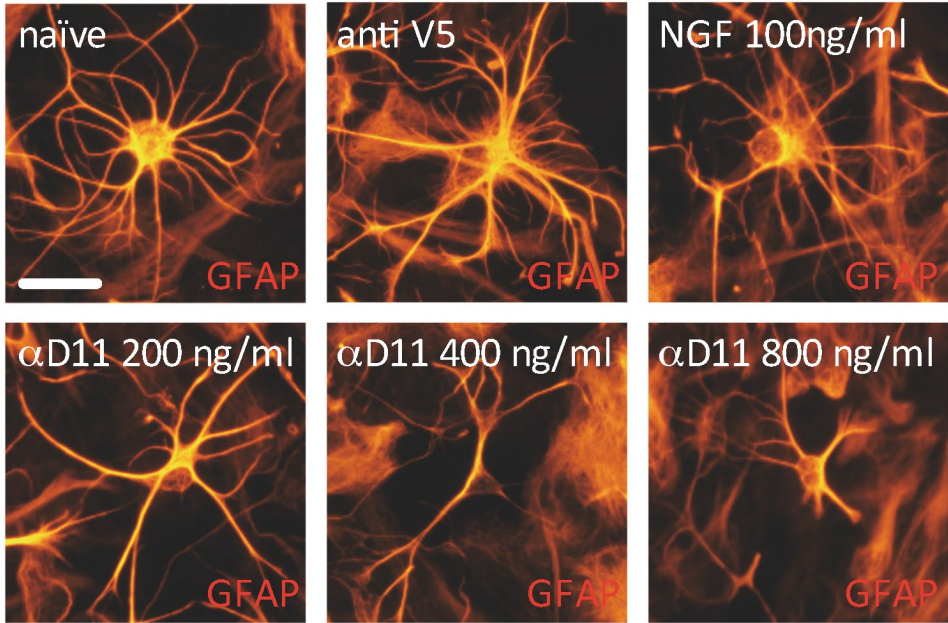


Fig 6.5 - panel 1 of 4. In vitro effects of NGF depletion.

The asthenic phenotype (i.e. reduction in morphological complexity) of astrocytes, observed in AD11 and TgproNGF#3 mice, can be reproduced in vitro, by incubation with anti NGF antibodies. Fluorescent microscope images of GFAP immunoreactive astrocytes after the treatment with NGF, anti-V5 or αD11 anti-NGF antibody.

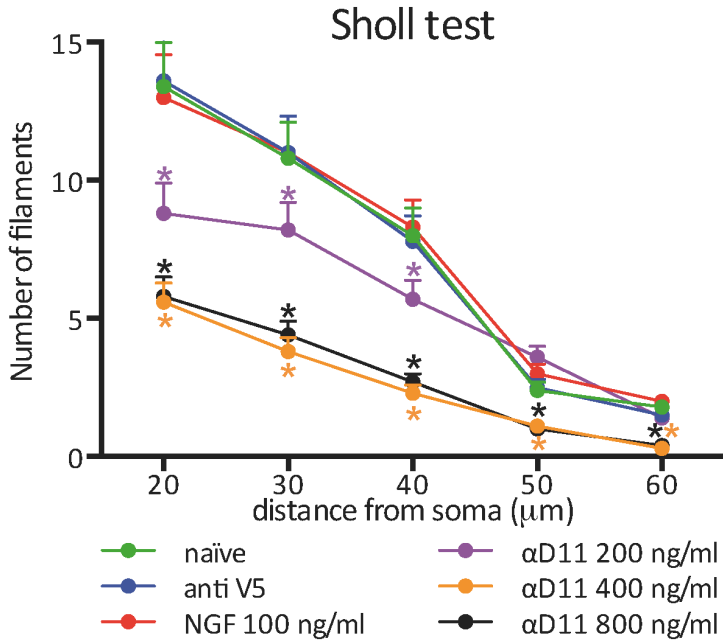


Fig 6.5 – panel 2 of 4. In vitro effects of NGF depletion.

Quantification of the previous.

Astrocyte labelled with GFAP antibody are treated with different αD11 anti-NGF antibodies and their morphology is measured with a Sholl test. The result is reported in the graph. See M&M for details.

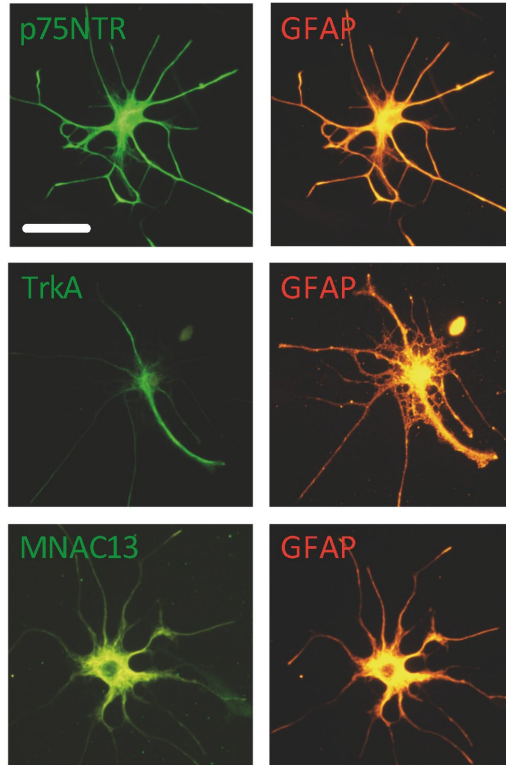


Fig 6.5 - panel 3 of 4. In vitro effects of NGF depletion

Expression of P75NTR and TrkA on cultured GFAP+ astrocytes. MNAC13: Astrocytes are labelled against TrkA using also the specific monoclonal antibody MNAC13.

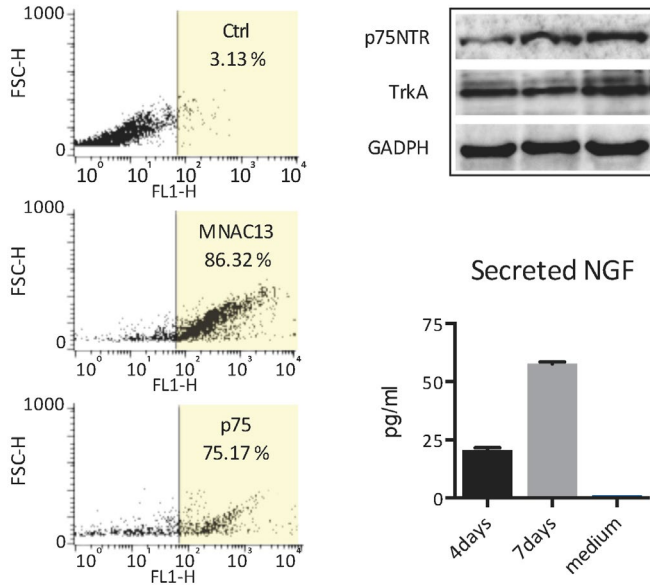


Fig 6.5 - panel 4 of 4. In vitro effects of NGF depletion

(a) FACS analysis to isolate cells expressing both GFAP and NGF receptors

(b) Western blot showing the expression of p75NTR and TrkA in three independent samples

(c) Quantification of the amount of NGF secreted in astrocytic medium.

6.4 Astrocytes express NGF receptors *in vitro*

How do I explain the effect of the anti-NGF antibody?

The presence of NGF high affinity (NTRK1) and low affinity (p75^{NTR}) receptors on the astrocytes *in vivo* and *in vitro* is still debated^{39,40}. Here I demonstrate that they are both expressed in cultured astrocytes using different techniques (fig 6.5).

First of all, I found that p75NTR and TrkA are both expressed on the membrane of cultured astrocytes, since the immunoreactivity was found by performing detergent-free IHC, i.e. without permeabilizing the membrane. In this experiment, to detect TrkA, I used a polyclonal commercial antibody and the monoclonal antibody MNAC13^{41,42} and I obtained the same result. The anti TrkA mAb MNAC13 has been produced in the lab and has been validated on sections from TrkA^{-/-} knockout mice.

To confirm these data, I was able to sort by FACS astrocytes labelled with anti-p75 and MNAC13 antibodies detecting, respectively, an enrichment of 75.17% and 86.32% in the GFAP+ fraction (fig 6.5 a). I also performed SDS-PAGE WB for the two receptors, in order to verify their correct molecular weight. As reported in the fig 6.5 b, I found

that both p75^{NTR} and TrkA are present at the expected molecular weight of, respectively, 75 KDa and 120 KDa.

In addition to the receptors, I demonstrated the capability of cultured astrocytes to produce NGF, by measuring the progressive NGF accumulation in the culture medium with an ELISA test (fig 6.5 c).

All these findings, taken together, demonstrates that:

- i) both NGF receptors are present in cultured astrocytes;*
- ii) the receptors are located on the membrane surface;*
- iii) they have the expected molecular weight and*
- iv) cultured astrocytes produce NGF and secrete it in the medium.*

Taken together, all these findings demonstrate that, at least *in vitro*, astrocytes have the capability to respond directly to NGF/proNGF levels (i.e. not obligatorily through the mediation of other cells) and, moreover, that they are capable

to deal and potentially interfere in an homeostatic way with the NGF levels.

What about NGF receptors on astrocytes in vivo?

Cortical astrocytes from wild-type mice do not express p75NTR and TrkA at detectable levels in vivo (Capsoni et al., 2017 and 2019), but do so in culture.

A significantly increased astrocytic p75NTR immunoreactivity was found in PBS-treated 5xFAD mice, which was decreased after human painless NGF (formally hNGFp; Capsoni et al., 2016 and 2017).

The hNGFp has identical neurotrophic potency as wild-type human nerve growth factor, but a 10-fold lower pain sensitizing activity treatment (Capsoni et al., 2016).

Most importantly, also in Alzheimer's disease brain sections, Capsoni and colleagues, in our lab, could detect an increased expression of both p75NTR and TrkA in astrocytes (Capsoni et al., 2017).

6.5 Atrophic astrocytes induced by anti NGF antibody treatment display a phenotype of reactive astrocytes

What are the genes modulated in the early phases?

To further characterize the phenotype of atrophic (called also *asthenic*) astrocytes triggered by anti NGF antibodies, a transcriptomic analysis was performed in cultured astrocytes after an incubation of 8 hours with the α D11 antibody (for experimental details see M&M).

I found that specific genes identifying a reactive state of astrocytes were upregulated in α D11-treated astrocytes (Table 1). Genes related to inflammation such as chemokines and receptors for immunoglobulins were individually upregulated up to 10-fold. In particular, kallikrein 6 (KLK6) (Table 1), a trypsin-like serine protease, has been found to be the top upregulated gene.

Interestingly, KLK6 has been reported to be upregulated in reactive astrocytes during injury and serve as a molecular trigger of select physiological processes involved in the development of astrogliosis (Scarlsbrick et al., 2012).

Indeed, KLK6 is involved in the transformation of astrocytes from an epithelioid to a stellate morphology which is characteristic of reactive astrocytes, via condensation of cortical actin (Yoon et al., 2018). Interestingly, KLK6 increases intracellular calcium. This correlates with the modulation of genes related to calcium movements in α D11 antibody-treated astrocytes.

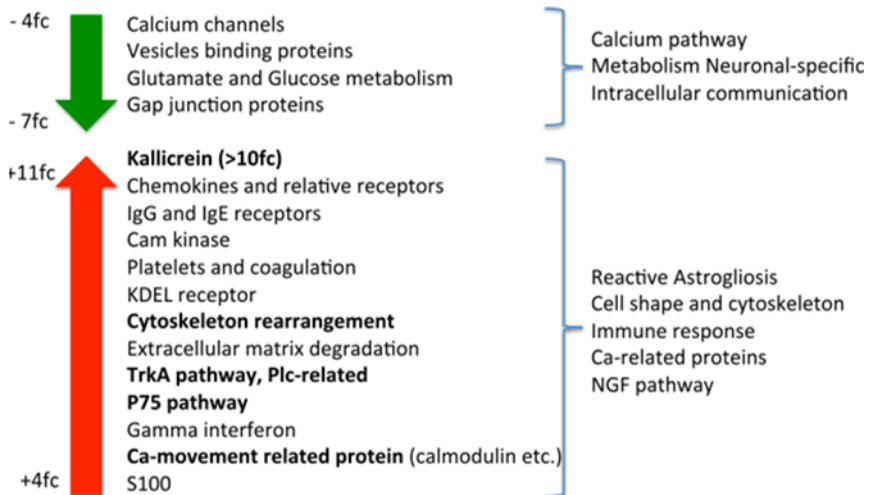


Table 1: gene modulation of astrocytes after 8 hours with the α D11 antibody. See above and M&M for details.

The upregulation of the expression of KLK6 has been confirmed by immunocytochemistry, in comparison to NGF and control antibody (V5 antibody) (Fig. 6.6).

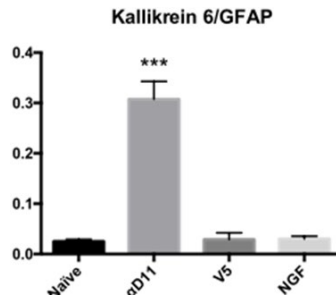
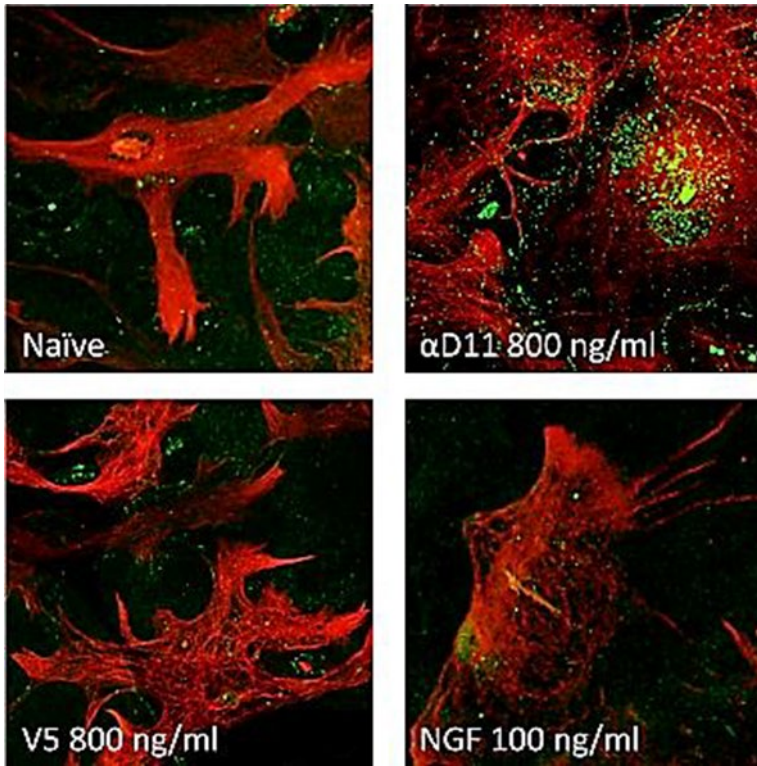


Fig. 6.6 (top) Immunofluorescence for Kallikrein 6 (green), a marker of astrocytic reactivity and (bottom) quantification. *** $P < 0.001$.

6.6 The NGF depletion increases astrocyte calcium oscillation

The results demonstrated above relate to a treatment of astrocytes with anti NGF of several hours (transcriptomic data) or days (morphological analysis).

What are the short-term effects of anti NGF treatment?

Prompted by the findings in the transcriptomic analysis, I set up to investigate the effects of NGF deprivation on the astrocytic calcium transients⁴⁴⁻⁴⁶.

Each registration session consists of 1000 single frames acquisition taken every 5 seconds, for a total duration of 1 hour after .ca 20 minutes of stabilization. The registration is conducted under still medium condition (no perfusion was running) due to the astrocytes mechanosensor that could modulate the calcium waves.

See fig 6.7 in order to appreciate a typical experimental output.

AD11_34_

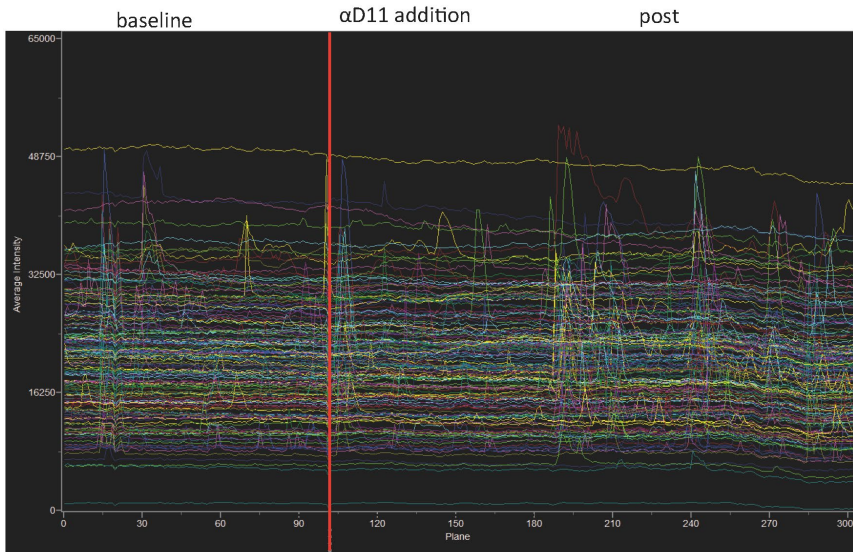
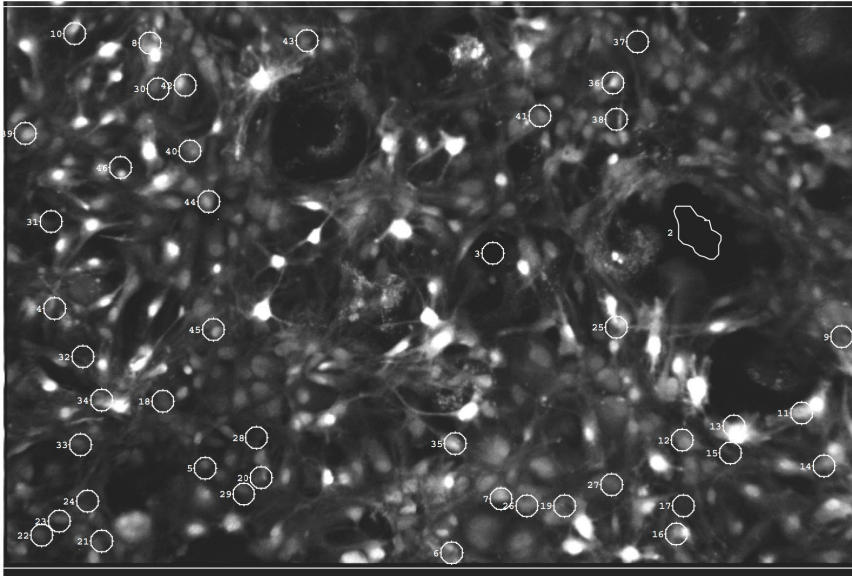


Fig 6.7 Calcium waves in astrocytes: my typical rough experimental output

After 250 frames (.ca 20 minutes) of baseline registration, I added anti-V5 antibody (800 ng/ml), α D11 (800 ng/ml) or murine NGF (100 ng/ml). The total volume in the registration chamber is 3 ml; the compounds were diluted in 20 μ l of KREBS (120 mM sodium chloride, 5 mM potassium chloride, 2 mM calcium chloride, 1 mM magnesium chloride, 25 mM sodium bicarbonate, and 5.5 mM D-glucose, pH 7.3, 0.22 micron filtered) solution and slowly added in the Petri dish with a small tip, far from the focused registration area.

I registered a very good and constant basal activity and expressed the results, due to the non-ratiometric intrinsic nature of the Oregon Green BAPTA-2, as the percentage of responding cells for each frame.

The experiment, summarized in fig 6.8, showed that there was no activity change whatsoever in presence with NGF 100 ng/ml. On the contrary, a strong and consistent increase in the number of responding cells was observed with a α D11 anti NGF 800ng/ml treatment, not occurring after incubation with the control antibody anti-V5.

I considered an active cell if the increase of the signal is 5% higher of the average brightness of the same cell calculated in the previous 15 and subsequent 15 frames.

The number of oscillating cells was about 30 cells per frame in the baseline, as well as in the control and NGF

experiments; 5 minutes after the administration of α D11 800ng/ml (or 400ng/ml but none 200ng/ml, see fig 6.8) the oscillation increase in number and amplitude.

A typical signal profile is shown in fig 6.8 a. More than 60 cells per frame were oscillating (fig 6.8).

Thus, in conclusion, I demonstrated that, in the astrocytes, NGF deprivation by anti NGF antibodies causes a fast and durable calcium response within 5 minutes. On the contrary, astrocytes are completely deaf to NGF, despite the fact that cultured astrocytes express both TrkA and p75NTR receptors.

This surprising striking result shows that cultured astrocytes can respond very rapidly to an acute reduction of the NGF levels that they secrete themselves, but not to an acute increase of NGF levels.

6.7 The Ca^{2+} involved in anti-NGF dependent calcium waves derives from ER-stores

What is the source of the calcium ions involved in the oscillations induced by acute anti NGF treatment?

Intracellular Calcium can increase from Calcium stores located in the ER (Endoplasmic Reticulum) or from the extracellular medium. In order to address this question, I pretreated the astrocytes, respectively, with thapsigargin⁴⁸ (to block ER calcium stores) or with the Calcium chelator EGTA (to block extracellular Calcium and prevent it from entering the cell via Voltage gated Calcium Channels) before evoking calcium oscillations by adding anti NGF antibodies.

First of all, I examined whether calcium responses in astrocytes evoked by 800 ng/ml of α D11 were affected by the administration of thapsigargin. To do that, I induced the calcium oscillation as described above; after 20 minutes I treated the cells with thapsigargin (1 μM) and observed that the increase in calcium oscillations was strongly abolished and the number of responding cells was comparable with the baseline activity (fig 6.8).

Moreover, the depletion of intracellular Ca^{2+} ions determined by a pretreatment with thapsigargin ($1\ \mu\text{M}$) 30 min before the beginning of the registration did not affect the baseline calcium response but made the astrocytes unresponsive to αD11 antibody (fig 6.8).

Under no circumstances the treatment with EGTA prevented or abolished the calcium oscillations, like PBS solvent control and V5 antibody control (data not shown).

Thus, I demonstrated that the calcium ions involved in the oscillations induced by NGF deprivation derive from intracellular Calcium stores located in the ER.

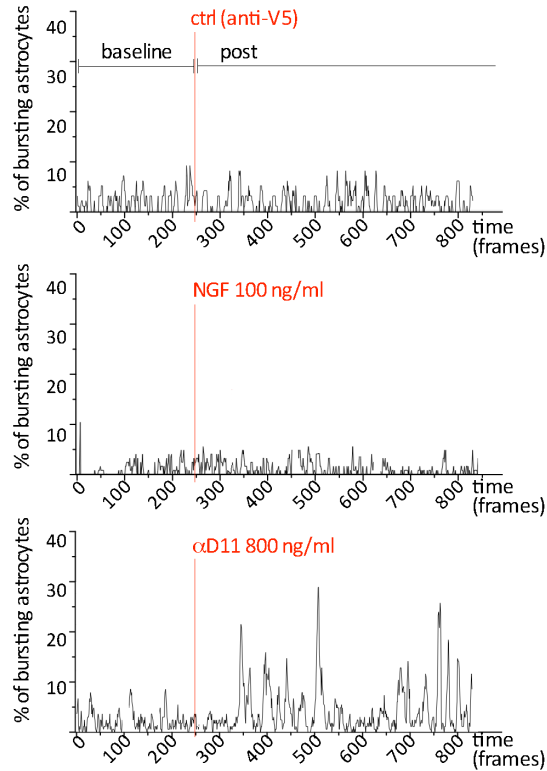
Ca⁺⁺ oscillations in cultured astrocytes

Fig 6.8 – panel 1 of 3. The NGF depletion increases astrocyte calcium oscillations

The calcium oscillations of plated astrocytes are recorded and graphicated above. No increase in frequency or amplitude is recorded with NGF nor V5-control antibody administration. On the contrary, αD11 causes a fast and durable increase.

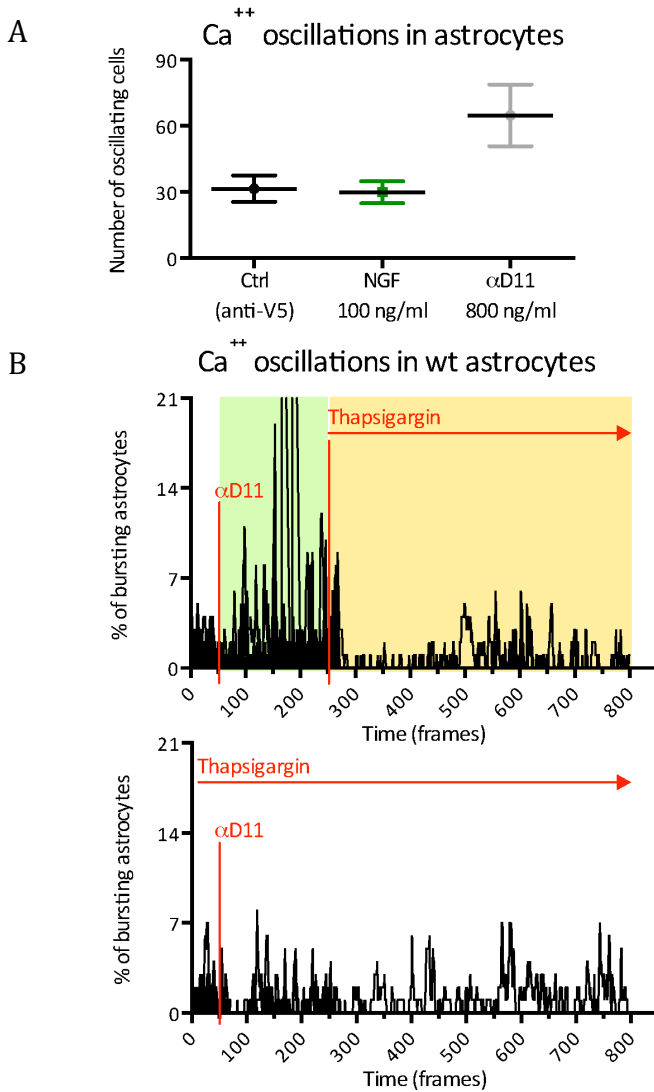


Fig 6.8 – panel 2 of 3. The NGF depletion increases astrocyte calcium oscillations.

(a) quantifications of previous;

(b) Thapsigargin abolishes and prevents the α D11-induced calcium oscillations.

6.8 Calcium oscillations induced by anti NGF antibodies are abolished if TrkA expression is chemogenetically inhibited in astrocytes

What is the trigger of the calcium oscillations induced by acute anti NGF treatment?

Since I demonstrated that the α D11 anti-NGF antibody is able to induce calcium oscillation in astrocytes, I postulated that the NGF secreted by astrocytes (see above) might stimulate TrkA receptors on astrocytes in an autocrine or a paracrine way.

In order to investigate the relationship between TrkA NGF receptors and their effect on calcium oscillations induced by anti NGF antibodies, I exploited a chemogenetic approach, taking advantage of the Ntrk1tm1Ddg/J mice⁴⁹. These mice carry a floxed F592A mutation in exon 12 of the mouse NTRK1 (TrkA) gene. The mutation in the floxed allele encodes a TrkA receptor that is sensitive to a family of small-molecule inhibitors, including 1NMPP1, which acts selectively, rapidly and reversibly to inhibit TrkA activation⁴⁹.

I cultured the astrocytes from these TrkA inducible knock out mice and incubated them in the presence or absence of the inhibitor 1NMPP1 10 μ M (fig 6.8 panel 3).

In the absence of 1NMPP1, the treatment with α D11 anti NGF induced a fast and durable increase of calcium oscillations in astrocytes from Ntrk1tm1Ddg/J mice, similarly to what happens in wt astrocytes.

This calcium activity was completely blocked if the astrocytes, treated with α D11, were pre-incubated with 1NMPP1 (see fig 6.8 panel 3).

Thus, I concluded that α D11 anti-NGF antibodies induce calcium oscillation via the activation of TrkA receptors.

Ca⁺⁺ oscillations in Ntrk1DG astrocytes

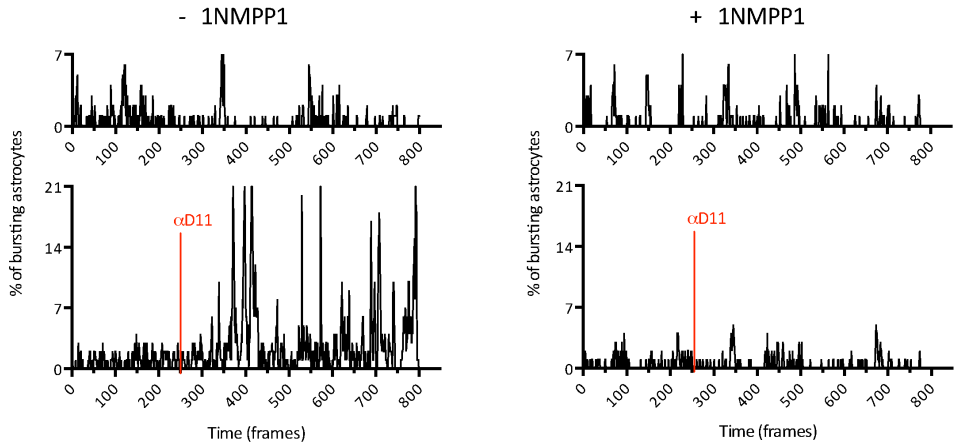


Fig 6.8 – panel 3 of 3. Calcium oscillations induced by anti-NGF antibodies are abolished if TrkA expression is chemogenetically inhibited in astrocytes

The aD11-induced calcium oscillations are also recorded in astrocytes from Ntrk1DG mice. When the TrkA-silencing compound 1NMPP1 is added, the aD11-induced calcium oscillations are not observed.

6.9 Transcriptomic changes at 8, 24 and 48 hours after anti-NGF antibody administration

I described above the genes modulated after 8 hours of incubation with α D11.

What are the transcriptomic changes affecting the astrocytes at different times after anti-NGF antibody administration?

When I analysed the effects after 24 hours (differently from 8 h and 48 h) from the beginning of the incubation (for experimental details see M&M), I found that the changes in astrocyte morphology are accompanied by transcriptomic changes which identify a transcriptional fingerprint typical of reactive type A1 neurotoxic astrocytes⁷⁰.

I verified the expression of the A1 neurotoxic markers and of the A2 neuroprotective markers in the transcriptomic datasets acquired from astrocytes treated with anti NGF antibodies for 8, 24 and 48 hours. I found that at 24 hours (but not at 8 or 48 hours) most A1-specific markers were upregulated in anti NGF treated astrocytes.

On the other side, at 24 hours (but not at 8 or 48 hours) most A2-specific markers were downregulated in anti NGF treated astrocytes.

Gene:	fold at time: (ns = non-significant)		
	8h	24h	48h
<u>Pan reactive</u>			
Lcn2	+1,16 ns	+1,08	+0,1 ns
Steap4	-	+1,58	-
S1pr3	-0,15 ns	+0,73	-0,4 ns
Timp1	-0,65 ns	-1,40	-0,63 ns
Hspb1	-0,66 ns	-1,76	-0,38 ns
Cxcl10	+0,08 ns	+2,46	-0,08 ns
Cd44	+0,02ns	-0,69	-0,25 ns
Osmr	+0,34 ns	+0,75	-0,12 ns
Cp	+0,09 ns	+1,8	-0,33 ns
Serpina3n	+0,17 ns	-0,32	-0,17 ns
Aspg	+0,23 ns	-0,89	+0,71 ns
Vim	+0,04 ns	+0,39	+0,09 ns
Gfap	+0,11 ns	+0,59	-1,28
<u>A1specific</u>			
H2-T23	-0,02 ns	+1,37	+0,13 ns
Serping1	+0,15 ns	+1,26	+0,21 ns
H2-D1	+0,1 ns	+1,07	-0,1 ns
Ggta1	-	+0,86	-
Ligp1	-	-	-
Gbp2	+0,11ns	+1,87	+0,09ns
Fbln5	+0,07ns	+1,01	+0,48ns
Ugt1a1	+0,1ns	-0,24	+0,26ns
Fkbp5	+0,30ns	-0,25	+0,08ns
Psemb8	-0,16ns	+1,16	+0,04ns
Srgn	-0,12ns	+0,74	+0,04ns
Amigo2	-0,63ns	-0,07	-0,21ns

A2 specific

Clcf1	+0,14ns	-2,39	+0,04ns
Tgm1	-	-1,06	-
Ptx3	-	-2,11	-
S100a10	+0,07ns	-0,96	-0,09ns
Sphk1	-0,21ns	-1,02	+1,12
Cd109	+0,20ns	-0,60	+0,12ns
Ptgs2	+0,41ns	-2,64	+0,11ns
Emp1	+0,12ns	-1,14	+0,16ns
Slc10a6	-	-	-
Tm4sf1	+0,01ns	+0,00	+0,1ns
B3gnt5	-	-0,83	-
Cd14	+0,44ns	+0,21	+0,25ns

Table 2: modulation of markers for neurotoxic and neuroprotective astrocyte phenotype in astrocytes after 8, 24 and 48 hours with the aD11 anti NGF antibody.

As reported in table 2, the RNA modulation occurring 24 hours after the exposure to the α D11 anti-NGF antibody was consistent with a pan reactive phenotype and, in particular, with a full A1-like neurotoxic phenotype.

6.10 In astrocyte-neuron co-cultures, the NGF starvation leads to neuronal impairment and death

What happens to neurons, in astrocytes-neuron co-cultures, when astrocytes react to NGF starvation?

Given the demonstration that incubation with anti NGF antibodies leads to the acquisition of an A1 neurotoxic phenotype, it seemed important to investigate how this important and unexpected finding could influence neuronal physiology.

To this aim, I performed astrocytes-neurons co-cultures. I separately cultured astrocytes for 2 weeks and hippocampal neurons for 1 week, as described in the M&M section. I cultured the two cellular types separately to be sure to obtain a high grade of purity of each culture type. Of note, hippocampal neurons do not express TrkA receptors (Capsoni et al., 2017).

At the end of the two respective periods of culture I joined the two cultures, re-plating the detached astrocytes onto the neuronal culture with proportion between neurons and

astrocytes of 1:1. After a week of co-culture, the two cultures perfectly integrate (see fig 6.9 F) and I started the treatments.

I first treated hippocampal neurons, alone or cultured with hippocampal astrocytes, with NGF (100 ng/ml), anti-V5 (as a control for antibody 800ng/ml), α D11 (800 ng/ml), NGF followed by α D11 (NGF and then α D11, 3 days delay, respectively 100 ng/ml and 800 ng/ml).

In order to evaluate the presence of possible neuronal degeneration, the experimental readout on the neuronal culture was evaluated looking at morphological alterations commonly found in degenerating cells⁶³.

Neurons were identified by MAP2 immunoreactivity and were considered healthy if none of the following parameters was met: i) degenerated soma, with or without detached dendrites, ii) blebbing of dendritic membrane or iii) dendrite degeneration and rupture.

The percentage of healthy hippocampal neurons cultured alone is comparable to that for neurons co-cultured with astrocytes.

In neurons co-cultured with astrocytes, incubation with NGF or with control anti V5 antibody determines no change. On the contrary, the treatments with α D11 or with NGF

followed by α D11, determined (after 2 days) a dramatic decrease of healthy neurons.

I also evaluated the amount of cleaved caspase 3 in neurons plated with astrocytes after the treatments with NGF (100 ng/ml), anti V5 (800 ng/ml), α D11 (800 ng/ml), NGF followed by α D11 (after 3 days, respectively 100 ng/ml and 800 ng/ml) and also treating the neurons cultured alone with the supernatant of astrocytes previously treated (within 24 hours) with α D11 (800 ng/ml). In the cases of α D11 and NGF followed by α D11, the caspase 3 cleavage increased up to 4-fold (fig 6.9 A).

The results that I obtained counting the percentage of TUNEL+ neurons after the same treatments are superimposable to the ones discussed above (fig 6.9 A).

This demonstrates that the NGF neutralization leads to a neuronal impairment, but only if the neurons are co-cultured with astrocytes.

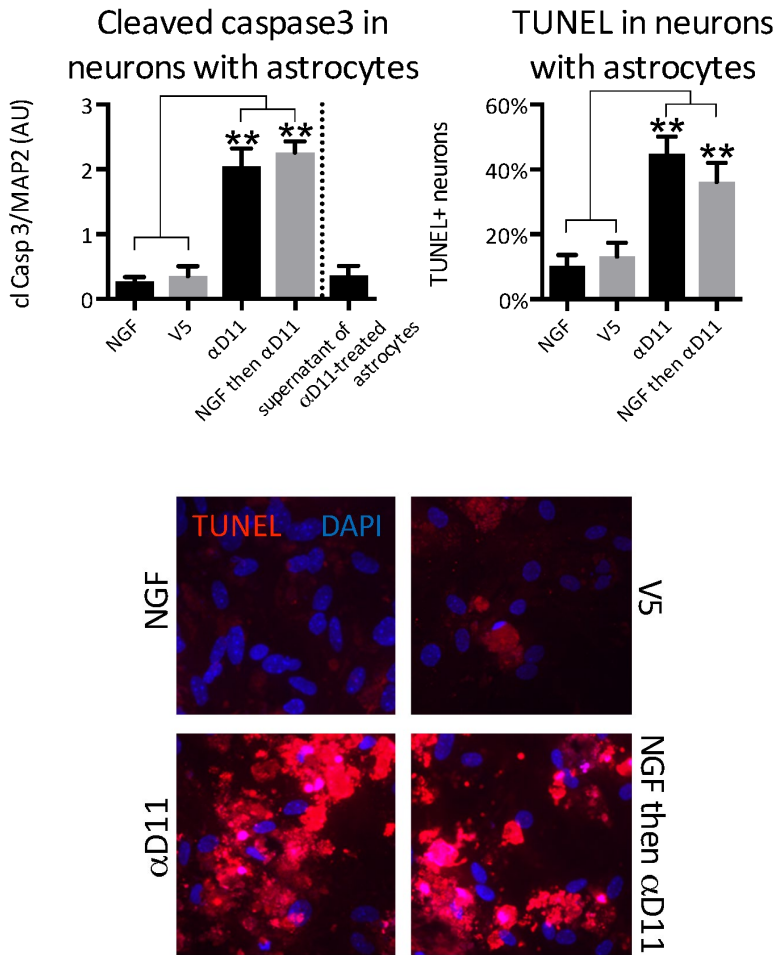


Fig 6.9 Atrophic astrocytes becomes neuro-toxic

Panel A.

Top-right: Amount of cleaved caspase 3 in neurons plated with astrocytes after the treatments with NGF (100 ng/ml), anti V5 (800 ng/ml), α D11 (800 ng/ml), NGF followed by α D11 (after 3 days,

respectively 100 ng/ml and 800 ng/ml) and also treating the neurons cultured alone with the supernatant of astrocytes previously treated (within 24 hours) with aD11 (800 ng/ml).

In the cases of aD11 and “NGF then aD11”, the caspase 3 cleavage increased up to 4-fold).

Top-right and bottom: The results depicted above are superimposable with the ones that I obtained counting the percentage of TUNEL+ neurons after the same treatments (NGF, V5, aD11, NGF then aD11).

6.11 The effects of NGF deprivation onto astrocytes might imply the production of β amyloid oligomers or glutamate excitotoxicity, impairing neurons

What are the possible mechanisms that couple astrocytes and neuron impairment?

I postulated that the death of hippocampal neurons co-cultured with anti NGF-treated astrocytes might be executed by amyloid β oligomers, the known toxic form of the A β peptide. In order to test this hypothesis, I exploited the recombinant antibody fragment scFvA13, generated in the lab, that specifically recognizes the oligomeric forms of the A β peptide, and not A β monomers nor A β fibrils (Meli et al (2009) Journal of Molecular Biology).

I also tested the hypothesis that the neuronal death might be due to glutamate excitotoxicity.

To answer to these pivotal questions, I treated hippocampal neurons, alone or cultured with hippocampal astrocytes, with α D11 + A13 (a highly specific anti- β amyloid antibody against oligomers of this peptide, respectively 800 ng/ml and 1:300 dilution) and with α D11 + kynurenic acid

(KynA, antagonist of the glutamate ionotropic excitatory amino acid receptors, respectively 800 ng/ml and 50 μ M). Fig 6.9 B and C.

The results of this experiment demonstrated that the neuronal impairment is reduced when NGF is neutralized concomitantly with the amyloid β neutralization with A13⁶² or concomitantly with the glutamate ionotropic receptors blockade (fig 6.9 B and C), thus indicating that the effects of deprivation of NGF might imply the production of β amyloid oligomers and excitotoxicity.

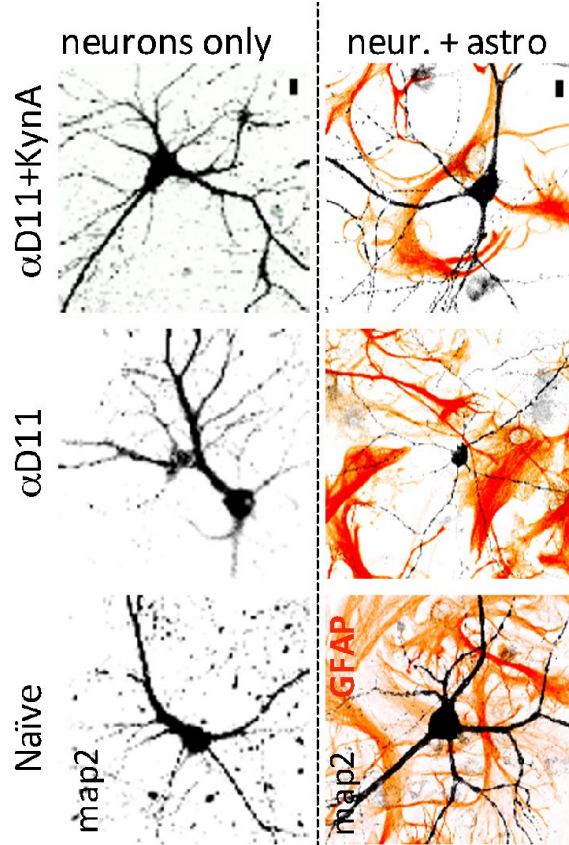


Fig 6.9 Atrophic astrocytes becomes neuro-toxic

Panel B.

The percentage and morphology of healthy neurons cultured alone is comparable to the one calculated for neurons co-cultured with naïve astrocytes (bottom). In neurons co-cultured with astrocytes, the treatments

RESULTS - NMC - SNS

with aD11 determined (after 2 days) a dramatic decrease of healthy neurons. This effect was reduced adding also KynA.

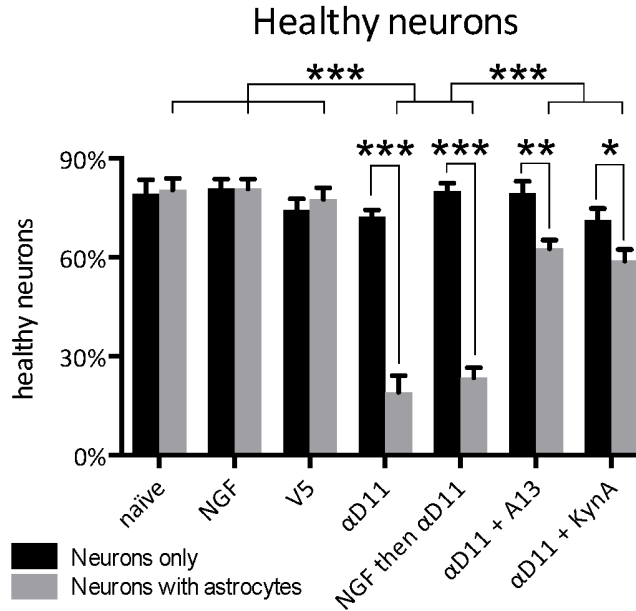


Fig 6.9 Atrophic astrocytes becomes neuro-toxic

Panel C.

In neurons co-cultured with astrocytes, the treatments with αD11 and NGF followed by αD11, but none NGF alone or anti-V5, determined (after 2 days) a dramatic decrease of healthy neurons. This effect was reduced when αD11 was co-incubated with A13 or KynA.

6.12 The astrocyte Ca^{2+} elevations induced by NGF starvation trigger Ca^{2+} hyper-activation in neurons

It is well demonstrated that a cooperation between astrocytes and neurons is a prerequisite to support ictal (seizure-like) and interictal epileptiform events⁶⁴.

During these events, neurons engage astrocytes in a recurrent excitatory loop, possibly involving gliotransmission, that promotes seizure ignition and sustains the ictal discharge⁶⁵ and, possibly, neuronal death.

Does the astrocyte Ca^{2+} elevations induced by NGF starvation might trigger the observed Ca^{2+} hyper-activation in neurons?

For this purpose, I treated neuronal-astrocytes co-culture with αD11 (800 ng/ml) of anti V5 (800 ng/ml), and I measured the average number of Ca^{2+} oscillations after 400 seconds of each treatment.

The experimental plane and the results are summarized in fig 6.9 D-E. I measured a statistically significant increase in the Ca^{2+} transient average number after the αD11 administration. I also co-cultured wild type neurons with TrkA KO-inducible astrocytes from $\text{Ntrk1}^{\text{tm1Ddg}}/\text{J}$ mice and

observed that the increase in Ca^{2+} transients was prevented by the 1NMPP1 treatment.

This compound, given concomitantly with αD11 in wt neuron / wt astrocytes, did not impair the αD11 effects.

These results demonstrate that the fast increase in the astrocytes Ca^{2+} oscillations that follows the NGF neutralization is mediated by the TrkA and leads to an alteration in neuronal Ca^{2+} activity and leads neuronal death.

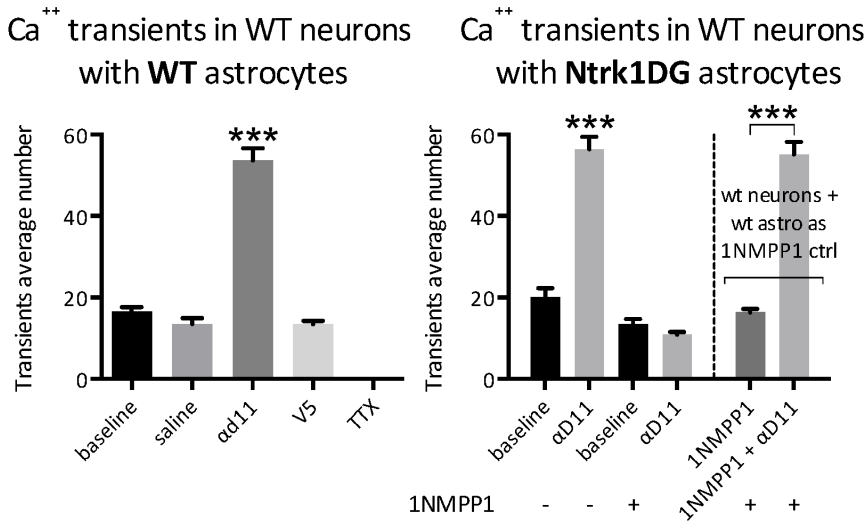


Fig 6.9 Atrophic astrocytes becomes neuro-toxic

Panel D.

Left: I treated neuronal-astrocytes co-culture with aD11 (800 ng/ml) of anti V5 (800 ng/ml), and I measured the average number of Ca²⁺ after 400 seconds of each treatment.

I measured a statistically significant increase in the Ca²⁺ transient average number after the aD11 administration. Neither co-culture treated with saline nor the ones treated with V5 differ from normal calcium behavior. TTX completely abolishes the calcium waves as expected.

Right: I also co-cultured wt neurons with TrkA KO-inducible astrocytes from Ntrk1tm1Ddg/J mice and observed that the increase in Ca^{2+} transients was prevented by the 1NMPP1 treatment.

This compound, given concomitantly with aD11 in wt-neuron/wt-astrocytes, did not impair the aD11 effects.

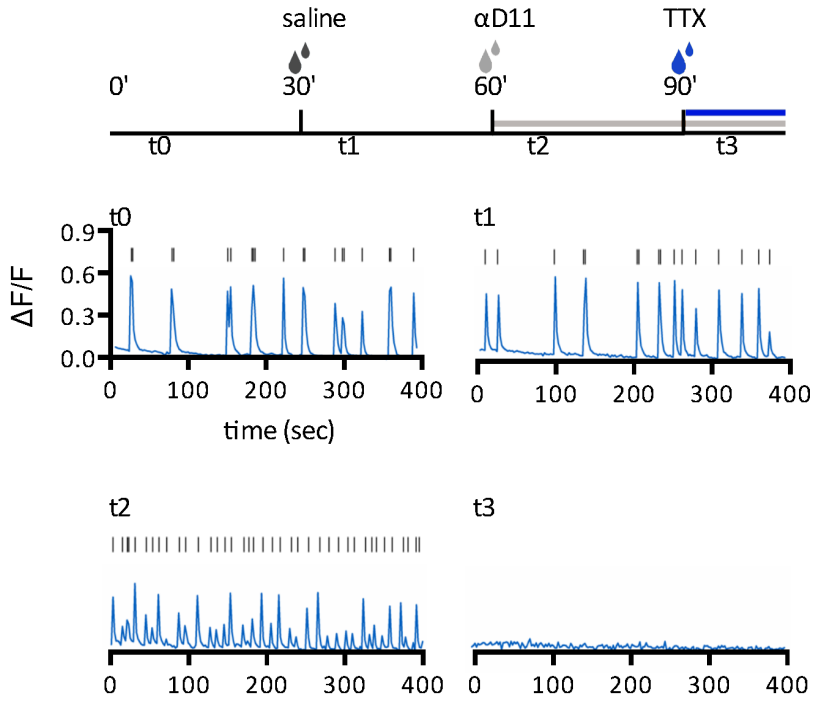


Fig 6.9 Atrophic astrocytes becomes neuro-toxic

Panel E.

Here is reported a typical calcium waves experiment frame. At t1, saline solution did not cause any change; at t2, calcium waves strongly increased when αD11 was added. As washout and internal control, TTX immediately abolishes the trace (t3).

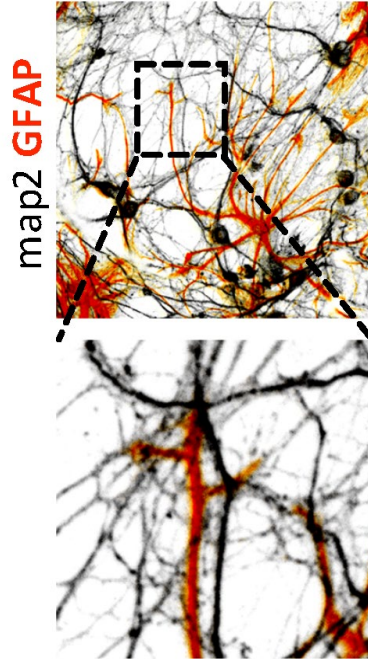


Fig 6.9 Atrophic astrocytes becomes neuro-toxic

Panel F.

Images from neuron-astrocyte co-cultures. The bottom picture is the magnification of the widest one above circumscribed within the dotted square. The integration among the two populations was strong and neurons - astrocytes showed synaptic integration areas (naïve untreated).

6.13 *In vivo* rescue of astrocytes atrophy by NGF in different AD models

The initial experimental observation that triggered this PhD thesis was a description of the *in vivo* asthenic phenotype of astrocytes in the hippocampus of AD11 and TgproNGF#3 mice (fig 6.1 and 6.4). In those models that phenotype is NGF-dependent and can be rescued by NGF intranasal delivery (fig 6.10).

Based on this result, I was able to develop an *in vitro* model that reproduced the phenotype observed *in vivo*. This *in vitro* model allowed me to identify ambient extracellular levels of NGF as a key parameter that regulates, in a homeostatic way, the acquisition of the astrocyte phenotype that could be characterized as the A1 neurotoxic astrocyte phenotype.

This astrocyte asthenic phenotype has been already described for several neurodegeneration models, such as 3xTG-AD, and 5xFAD mouse models, as well as in human AD patients^{34,38}.

It was therefore of interest to verify whether this asthenic neurotoxic phenotype of astrocytes, found in neurodegeneration models independent of NGF deficits, can also be reverted by NGF delivery *in vivo*.

Can this atrophy in 3xTG-AD mice be reverted by the administration of NGF?

To address this point, I performed an intranasal NGF treatment on AD11 and 3xTG-AD mice from 1,5 to 2 months of age. The treatment lasted for 2 weeks and consisted of 3 administrations per week of murine NGF, intranasally delivered.

The morphology was evaluated once again by the analysis of 4 cell parameters such as Volume, Area, number of Branching Points and Length of the filaments on GFAP labelled hippocampus slices. For 3 of these 4 parameters I observed a statistically significant amelioration (i.e. increase in morphological complexity) after the treatment with NGF, compared to saline administration (see fig 6.10). The filaments became longer, determining an increase of area and a tendency increase of volume.

These results demonstrate that the astrocytes atrophy can be reverted by NGF nasally administered. I found the same results with both AD11 and 3xTg-AD mice.

Particularly remarkable is that the 3xTg-AD is a model in which the onset of the Alzheimer neurodegeneration phenotype - and the astrocyte atrophy - is not due to an NGF imbalance as it is in AD11, but in both the intranasal NGF administration is sufficient to ameliorate the astrocytes morphology.

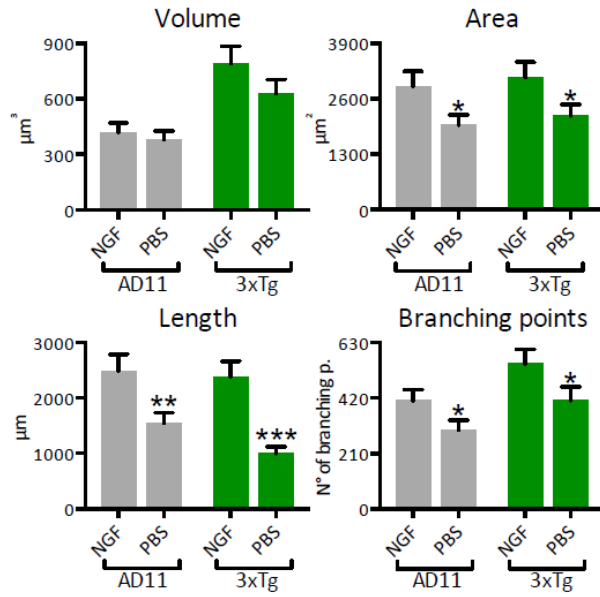


Fig 6.10 In vivo rescue of astrocytes atrophy, by NGF intranasally delivered, in different AD models

6.14 NGF modulate astrocyte calcium activity *in vivo*

In paragraphs 6.6, 6.7 and 6.12, I presented data suggesting that primary cultured astrocytes are able to sense the extracellular levels of NGF and respond to NGF deprivation via calcium transients, becoming neurotoxic. Due to the intrinsic nature of *in vitro* work, which could be biased by differences in the activation state of primary astrocytes (Guttenplan & Liddelow, 2019), it was then of paramount importance and interest to study whether and how modulations of NGF levels affect astrocytes also in their natural environment: the brain parenchyma.

For these reasons in our lab, based on my work, my colleague Dr. Alexia Tiberi carried out the *in vivo* experiments necessary to unveil the role of astrocytes in their natural environment. The experiments were discussed by Alexia, me and our supervisors, and were carried out in the Dr. Wen-Biao Gan lab at Skirball Institute and Department of Physiology and Neuroscience of the New York University.

I will report here, in this and in the following paragraphs, selected findings from these experiments, for their tight connection with my work and their pivotal role in

depicting a complete scenario around the finding that we are unveiling.

As described in Material and Methods Chapter, to answer to the question:

Can NGF levels modulate astrocyte calcium activity also in vivo?

We exploited adeno-associated viruses to induce the expression of a calcium reporter, Gcamp6, in astrocytes in the motor cortex of WT mice and measured the acute response of astrocytes to modulations of NGF levels.

We first sought to investigate whether astrocytes could respond to changes in levels of NGF by applying the neurotrophin exogenously or by decreasing its levels via the neutralizing antibody α D11. In anesthetized mice, which were infected with AAV5-GfapABC1D-cyto-GCaMP6f-SV40 virus (GFAP.GCaMP6.cyto) to drive GCaMP6 expression in astrocytes, we imaged astrocyte calcium levels both as baseline activity and in response to an α 1-receptor agonist phenylephrine (PE), which is capable of instantly inducing a strong calcium wave in astrocytes (Ding et al., 2013). PE is used to activate astrocytes that otherwise, in the anesthetized mouse, are more or less silent, in order to detect the global

activation capacity of these glial cells. Treatments were diluted in ACSF (NGF 1 μ g/ml, α D11 8 μ g/ml, PE 100 μ M) and applied directly onto the cortical surface through a small cranial window over the motor cortex. Imaging began right after the application of the drugs.

Astrocytic Ca²⁺ responses were first measured in the fine processes of the astrocytes during baseline activity (fig. 6.11 a). The effect of treatments on Ca²⁺ activity of astrocytes was monitored right after their application (t0), then after 5 (t5) and 10 minutes (t10). At any time-point, NGF did not induce any change in the Ca²⁺ baseline activity of astrocytes – data was thus pooled into a single bar (fig. 6.11 b).

Interestingly though, decreasing the levels of NGF via α D11 treatment significantly increased astrocytic Ca²⁺ responses in fine processes (fig. 6.11 b). We then measured the bulk activation response of astrocytes, pretreated with NGF or α D11 10 for 10 minutes, to the adrenergic agonist PE (fig. 6.11 c).

We found that PE treatment induced a much larger astrocytic Ca²⁺ response in α D11 treated mice as compared with non-treated controls (fig. 6.11 d, e), while no difference was detected in the NGF treated cohort.

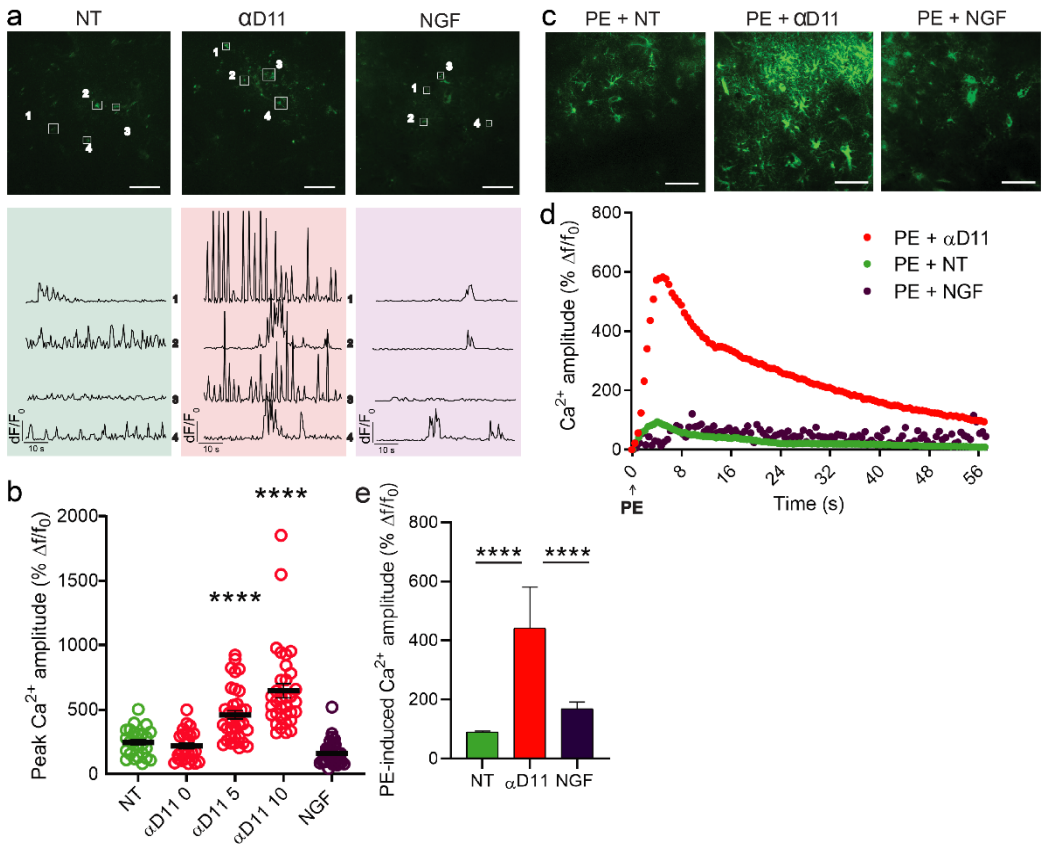


Fig 6.11 Lack of NGF increases astrocyte calcium

(a) Representative two-photon images and traces of Ca^{2+} response in astrocytic processes expressing GCaMP6s before (NT) and after NGF ($1\mu\text{g}/\text{ml}$) or α D11 ($8\mu\text{g}/\text{ml}$) application in the motor cortex of an anesthetized mouse.

(b) Quantification of the peak amplitude of Ca^{2+} transients in astrocytic processes during baseline (NT), right after (α D11 t_0), after 5 min (α D11 t_5) and 10 min (α D11 t_{10}) of α D11 ($8\mu\text{g}/\text{ml}$) application

RESULTS - NMC - SNS

(One-way ANOVA, NT vs. aD11 NF t5 $p < 0.0001$; NT vs. aD11 t10 $p < 0.0001$, $n=4$ per group, ~ 20 processes per animal).

(c) Representative images of non-treated (NT), aD11 and NGF treated astrocytic response to phenylephrine (PE) 100 μM .

(d) Representative traces of the bulk astrocytic response to PE administered at t0.

(e) Quantification of the astrocytic response to PE 100 μM

(One-way ANOVA, NT vs aD11, $p=0.0001$; NT vs NGF, n.s.; NT aD11 vs NGF, $p=0.0001$; $n=3$, 10 cells per animal).

6.15 Reducing NGF levels increases astrocyte calcium in the awake behaving animal

Since the lack of NGF in cortical tissue relayed such a powerful response from astrocytes we decided to focus on this treatment, switching to the more complex system of the awake behaving animal.

Can NGF levels modulate astrocyte calcium activity also in vivo, in awake behaving animals?

We performed 2-photon imaging in mice previously injected with AAV5-GfapABC1D-cyto-GCaMP6f-SV40 virus (GFAP.GCaMP6.cyto) to drive Gcamp6f expression in astrocytes. We then imaged the astrocytic calcium response in the mouse motor cortex during a running task (120 seconds total, running 20-100).

It has already been reported that astrocytes can respond to running with a wide and global calcium response that interests both soma and fine processes.

We thus quantified the response to such task under the influence of α D11 or NT conditions.

In a similar manner to anesthetized conditions, in the

awake behaving animal, lack of NGF increases astrocytic activity both in the soma (fig. 6.12 b, c) and processes (fig. 6.12 d, e).

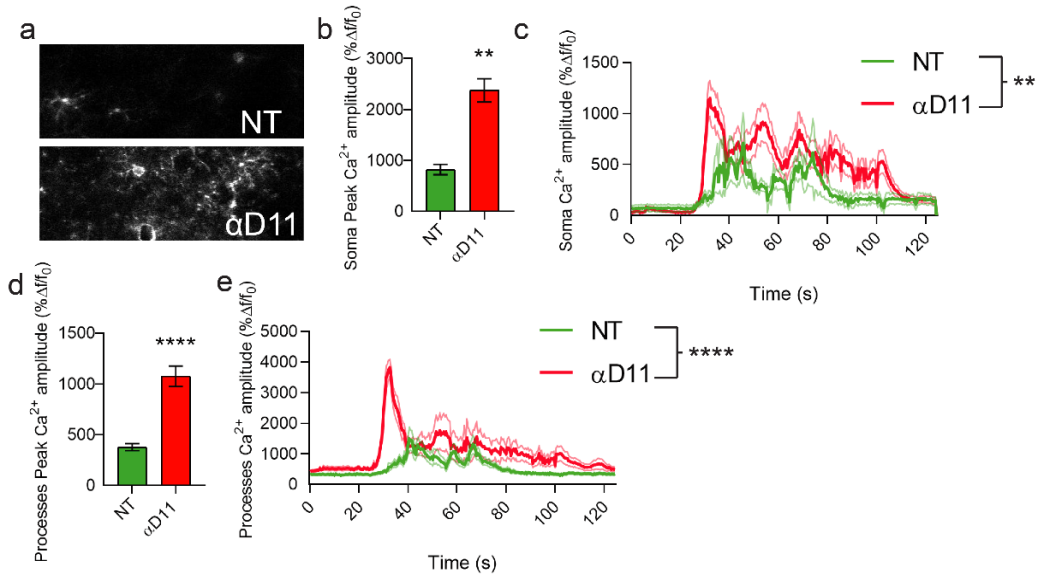


Figure 6.12 Lack of NGF increases astrocytic activity in the awake behaving animal

- (a) Representative images of the astrocytic responses.
 (b) Soma peak amplitude (2tailed t -test, $p=0.0012$) and
 (c) traces (2way ANOVA, $p<0.0001$) to running in NT and α D11 treated conditions.
 (d) Process peak amplitude (2tailed t -test, $p<0.0001$) and
 (e) traces (2way ANOVA, $p<0.0001$) to running in NT and α D11 treated conditions ($n=4$ per group, ~ 10 cells per animal).

Next, we used another NGF inhibitor, the commercial TrkAFc, to further confirm the effect of the lack of NGF onto astrocyte calcium levels. As for α D11, TrkAFc was able to consistently increase astrocyte calcium in their processes (fig. 6.13 d, e).

In conclusion, we have tackled the *in vivo* extension of the *in vitro* data by using in vivo 2-photon microscopy.

We monitored the effects of NGF on astrocyte physiology, by monitoring the changes in calcium activity of these cells during modulations of NGF levels in the extracellular environment.

We discovered that, also in vivo, while NGF exerted no effect, a lack of the neurotrophin, induced by acute anti NGF injection, increased astrocyte calcium activity in the anesthetized mouse as well as in the awake behaving animal.

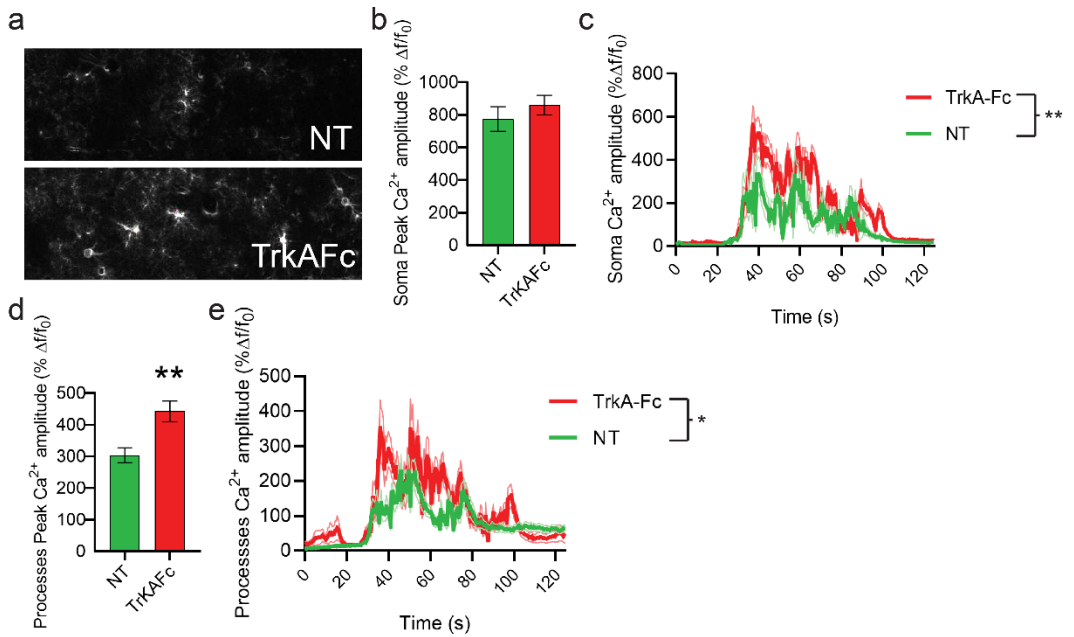


Figure 6.13 Inhibition of NGF via TrkAFc increases astrocytic calcium activity

(a) Representative images of the astrocytic response to TrkAFc.

(b) Soma peak amplitudes (2tailed *t* test, *n.s.*) and

(c) traces (2way ANOVA, $p = 0.0016$) of the astrocytic Ca²⁺.

(d) Process peak amplitudes (2tailed *t* test, $p = 0.001$) and

(e) traces (2way ANOVA, $p = 0.0103$)

($n = 3$ per group, ~ 10 cells per animal).

6.16 Upregulation of NGF translation after 5 min of NGF deprivation

What adaptive or homeostatic function could potentially be fulfilled by A1 astrocytes, in their natural context, remains an open question. We should consider the A1 neurotoxic phenotype as a state reached by the astrocytes after a prolonged chronic insult and after the homeostatic responses of astrocytes, to react to different stress insults, have been exhausted. But what are the early events after an acute NGF starvation?

If these are the premises, the short-term calcium response of astrocytes to anti NGF could be considered as the triggering of a rapid homeostatic alert signal. If the NGF deprivation is read by astrocytes as an insult signal, to which a homeostatic response should be provided, we argued that astrocytes might react also attempting to restore the NGF levels.

What are the early events after an acute NGF starvation? Does the astrocyte react to acute NGF deprivation also translating new NGF protein?

To answer this question, (in cultured astrocytes, as above and M&M) I measured the astrocyte intracellular NGF protein after 5 minutes of acute exposure to α D11 (800 ng/ml) or anti V5 (800 ng/ml) antibodies, plus or minus the protein synthesis inhibitor geneticin (G418, 300 μ g/ml). Cell extracts were immunoprecipitated and analyzed by and immunoblotting technique (for details, see M&M paragraph 8.17).

Geneticin (G418), an aminoglycoside antibiotic, is an elongation inhibitor of 80 S ribosomes that blocks polypeptide synthesis by inhibiting the elongation step in both prokaryotic and eukaryotic cells.

An NGF pulse clearly appears after only 5 minutes from acute NGF starvation by α D11 antibody.

The NGF pulse was absent in naïve untreated and in anti- V5 treated astrocytes (fig 6.14). The geneticin was also able to abolish the NGF pulse elicited by α D11 administration, demonstrating that the NGF pulse is newly synthesized NGF i.e. not an amount previously stored in intracellular compartment (fig 6.14).

This pulse of NGF synthesis results from the translational activation of the NGF mRNA, as a homeostatic response of the astrocyte to the lower ambient levels of NGF.

As a consequence of this finding, we can draw a picture whereby astrocytes would have a pool of NGF mRNA readily available, but in a state of translational repression. The mechanism of this translational repression remains to be investigated, but could involve specific microRNAs, polyadenylation control or specific translation initiation factors.

Elucidating this mechanism of translational control will be the object of future research. One can postulate that the Calcium signal rapidly activated upon anti-NGF addition might provide a signal to induce the synthesis of NGF.

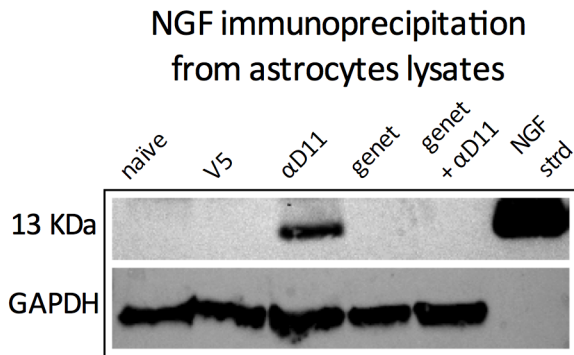
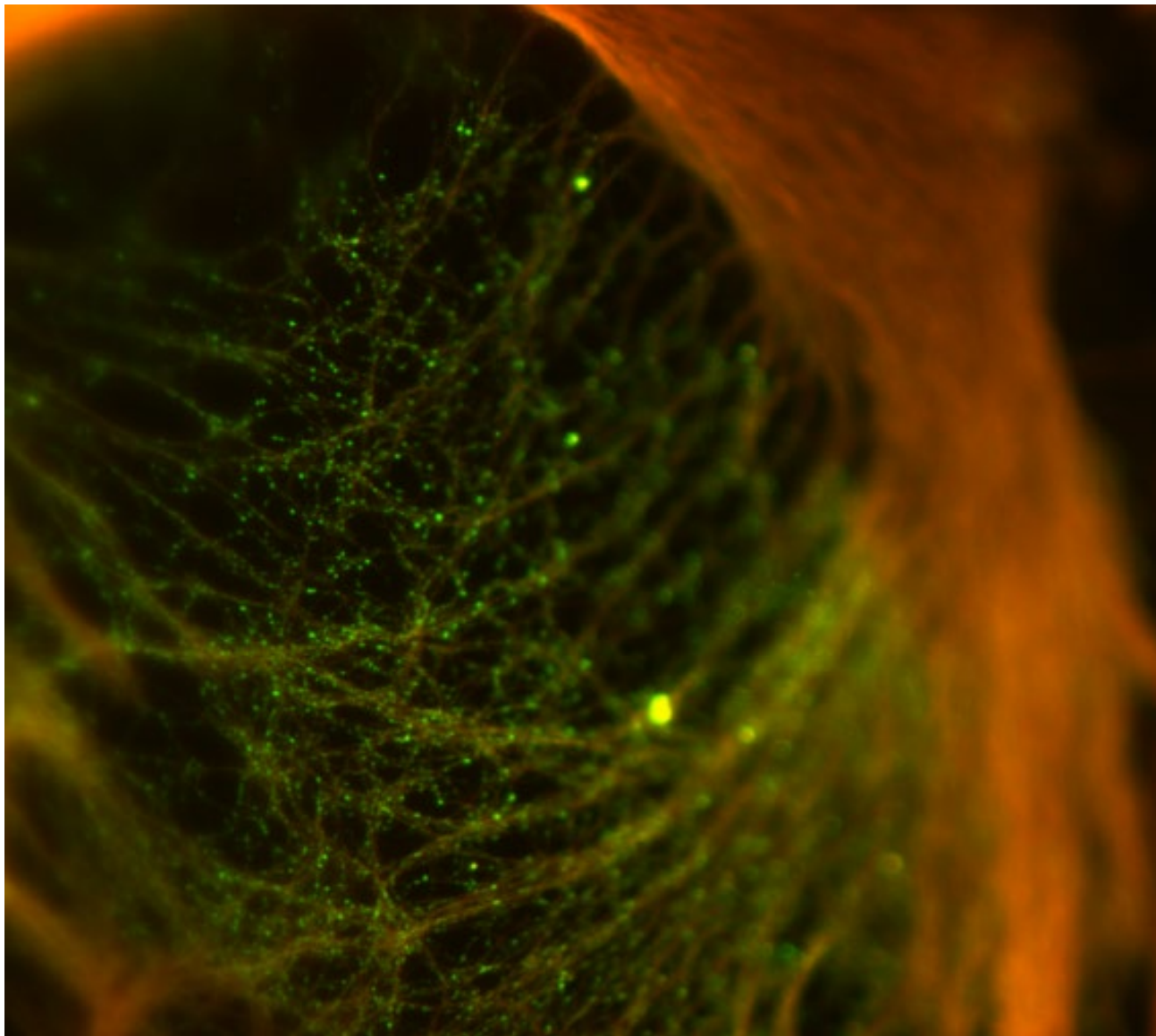


Figure 6.14 Upregulation of intracellular NGF translation after 5 min of extracellular NGF starvation

The astrocytes react to NGF starvation translating NGF: WB after Immunoprecipitation.

Intracellular NGF protein after 5 minutes of acute exposure to α D11 (800 ng/ml), or-V5 (800 ng/ml) antibodies, geneticin (G418, 300 μ g/ml) and geneticin (G418, 300 μ g/ml) + α D11 (800 ng/ml).

The last lane shows NGF standard immunoreactivity as internal control.



Phospho TrkA marked intracellular vesicles, blebbing from Endoplasmic Reticulum in an NGF-starved astrocyte.

Green is pTrkA, red is GFAP. Confocal microscopy.

Credit: Nicola Maria Carucci, 2015

7. Discussion

The neurotrophin Nerve Growth Factor (NGF) promotes a variety of responses, including increased transmitter production, Trk receptor production, neurite outgrowth, and enhanced neuronal survival (Barker and Murphy, 1992; Yuen et al., 1996; Frade and Barde, 1998; Gustilo et al., 1999). In the brain it is believed to act mainly on cholinergic neurons of the basal forebrain (Hefti, 1986).

Astrocytes have been implicated in the trophic support of developing neurons, and influencing the structure of mature

neurons (Jordan, 1999). In addition, astrocytes have been proposed to function in inducing and stabilizing the formation of new synapses (Ullian et al., 2001), being required for synapse formation and maintenance.

7.1 Astrocytes and NGF: secretion, signalling and mouse models

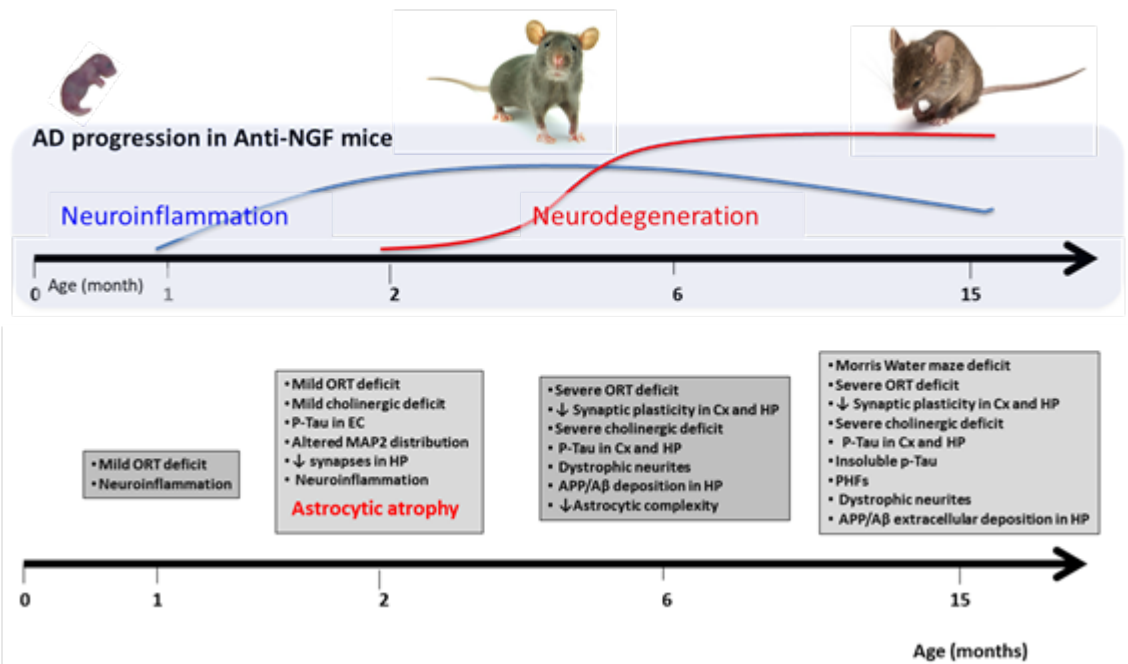
Whether NGF can be produced in physiological conditions by astrocytes and if astrocytes express NGF high affinity (NTRK1) and low affinity (p75NTR) receptors in vivo and in vitro are non-matter of debate anymore. Indeed, NGF synthesis by astrocytes was initially believed to occur only in pathological conditions to support regeneration of neuronal processes and influence synaptic rearrangements (Althaus and Richter-Landsberg, 2000).

In my thesis I demonstrate that NGF can be produced by astrocytes in vitro and that both TrkA and p75NTR NGF receptors are expressed on cultured astrocytes.

To study whether NGF can influence astrocyte physiology I first relied on the AD11 mouse model in which mature NGF biological activity is blocked by the expression of a recombinant neutralizing antibody, leading to an imbalance

between NGF/proNGF signalling (Ruberti 2000, Capsoni 2000, Capsoni 2010 PNAS, Capsoni & Cattaneo 2006).

In this mouse model I showed that astrocytes stained with an antibody against GFAP have a reduced morphological complexity (max diff at 2 m.o.a.), due to reduced volume and



ramifications.

Fig 7.1 AD-like progression in AD11 mice

The major hallmarks are pointed out at specific times. Note the astrocytic atrophy at 2 months of age, when other AD hallmarks are not still present.

The collected evidence leads to the conclusion that the morphological changes observed in astrocytes are really due to a structural change of these cells and could not be explained by a fluctuation of cell marker expression. The astrocytes in AD11 mice are clearly atrophic: they show a marked shrinkage at 2 months of age i.e. in an early pre-symptomatic phase when other AD hallmarks are not still present in these animals (fig 7.1).

7.2 Pathological implications of atrophic astrocytes

Morphological atrophy of astrocytes at the early stages of the AD may have several pathologically relevant consequences. First and foremost, this may result in decrease of astroglial synaptic coverage. Perisynaptic glial membranes that enwrap most (~70% in hippocampus) of the synapses in the CNS form “astroglial cradle” fundamental for maintenance of synaptic transmission through multiple molecular cascades sustaining homeostasis of the synaptic cleft and supplying neuronal terminals with neurotransmitter precursors (Nedergaard and Verkhratsky 2012; Verkhratsky and Nedergaard 2014). Reduced synaptic coverage may therefore compromise synaptic strength and even promote synaptic loss.

This synaptic loss is generally considered to represent the earliest morphological symptoms of AD responsible for early signs of cognitive deficit (Coleman and others 2004; Terry 2000). The degree of synaptic loss has been claimed to correlate with the severity of dementia (DeKosky and Scheff 1990; Samuel and others 1994). In addition, asthenic astrocytes cannot support synaptogenesis (Eroglu and Barres 2010) thus affecting regeneration.

Comparable astrocyte asthenia has been already described in Alzheimer's mouse models such as, for example, 3xTG-AD34,38 mice as well as in human AD patients, but the signals that determine this phenotype have not been understood. Astroglial reactivity (defined by an increase in GFAP or S100 β expression) was frequently described in the AD post-mortem tissues (Beach and McGeer 1988; Griffin and others 1989; Meda and others 2001; Mrazek and Griffin 2005), and even some correlation between increased GFAP levels and the Braak stage of AD were claimed (Simpson and others 2010). I found the same results with both AD11 and 3xTg-AD mice.

Particularly remarkable is that the 3xTg-AD is a model in which the onset of neurodegeneration - and the astrocyte atrophy - is not due to an NGF imbalance as in AD11. Yet, in

both AD11 and 3xTg-AD mice, the intranasal NGF administration is sufficient to ameliorate the astrocytes morphology.

7.3 Early events after NGF deprivation

To understand the consequences of this astrocytic atrophy I replicated this phenotype in vitro. This step has been fundamental to show that atrophic astrocytes are indeed reactive cells. The first evidence came from the fact that NGF deprivation in cultured astrocytes causes fast and durable calcium oscillations within 5 minutes. This data fits with the fact that reactive astrocytes generate aberrant Ca^{2+} signals represented by spontaneous Ca^{2+} oscillations and abnormal Ca^{2+} waves (Kuchibhotla and others 2009). On the contrary, I found that astrocytes, cultured in the same conditions, are deaf to NGF.

Molecular mechanisms triggering astroglial reactivity and Calcium responses remain debated and should be more intensely addressed. There are indications that soluble β -amyloid induces abnormal Ca^{2+} oscillations in cultured primary astrocytes (Abramov and others 2003; Abramov and others

2004), although these results were not universally confirmed (Grolla and others 2013; Ronco and others 2014). Chronic exposure of cultured astrocytes to β -amyloid resulted in significant changes in the Ca^{2+} signalling toolkit in the hippocampus but not in the entorhinal cortex (Grolla and others 2013).

In addition to that, I found that the changes in astrocyte morphology are accompanied by transcriptomic changes which identify the astrocytes resulting from anti NGF treatment as harbouring a transcriptional fingerprint typical of reactive type A1 neurotoxic astrocytes⁷⁰. The RNA modulation occurring 24 hours after the exposure to the α D11 anti-NGF antibody was consistent with a pan reactive phenotype and, in particular, with a full A1-like activation. On the other side, there was a downregulation of the mRNAs linked to a A2-specific neuroprotective phenotype. Altogether, I conclude that a long exposure of astrocytes to reduced levels of NGF activates a neurotoxic A1 phenotype. This neurotoxic phenotype of astrocytes has been described as the executor of the neurodegeneration process in the course of Alzheimer's disease and other neurodegenerative diseases.

7.4 Long term events after NGF deprivation

The identification of the “killer” molecule(s) secreted from neurotoxic A1 astrocytes is currently a top priority in the field. I have developed in this thesis an in vitro model to reproducibly induce the neurotoxic A1 phenotype by a simple “negative” signal (anti NGF antibodies) and this forms a solid basis to set up a screening functional assay for the identification of the killer molecule(s) produced by A1 neurotoxic astrocytes.

At the beginning, transcriptomic analysis of microglia in neurodegenerative models has provided some valuable starting points for how these cells respond locally at neurodegenerative foci, giving rise to the idea of disease-associated microglia (DAM) or of the microglial neurodegenerative (MGnD) phenotype. Interestingly, these microglia differentially express markers that are nowadays traditionally associated with both M1 and M2 microglia - i.e., markers from both populations are either upregulated or downregulated (Shi & Holtzman, 2018). At a broad level, this signature is associated with increased expression of phagocytic and inflammatory genes, as well as regulators of microglial ontogeny, specifically colony stimulating factor 1 (Csf1).

Coming back to astrocytes, transcriptional analysis has demonstrated subtype heterogeneity among reactive astrocytes that depends heavily on the extracellular environment and type of injury. For example, reactive astrocytes produced in the context of either neuroinflammation induced by systemic LPS injection or middle cerebral artery occlusion (MCAO) upregulate transcription of a core set of “pan-reactive” genes. However, sub-populations of reactive astrocytes differentially regulate transcriptional modules, enabling them to be further categorized and robustly discriminated. Subsequent research has designated the reactive sub-populations induced by neuroinflammation (LPS) and ischemia (MCAO) as the “A1” and “A2” reactive astrocyte subtypes⁶⁹. Very interestingly, astrocyte-conditioned medium from A1 astrocytes (A1-ACM) is potentially neurotoxic⁶⁹.

7.5 Adaptive homeostatic functions of astrocytes

What adaptive or homeostatic function could potentially be fulfilled by A1 astrocytes remains an open question. The removal of unsalvageable neurons from neural circuits is one potential evolutionary reason for their existence, i.e. eliminating those which have lost functional synaptic

connections or have become virally compromised. Eliminating unsupported neurons could also have significance during development.

One can also consider the A1 neuroxic phenotype as a state reached by the astrocytes after a prolonged chronic insult has worn them out and their homeostatic responses to combat the stress insult have been unsuccessful. In this respect, the short-term calcium response of astrocytes to anti NGF could be considered as the triggering of a rapid homeostatic alert signal. This homeostatic response results in the translational activation of the NGF mRNA, as a response of the astrocyte to the lower ambient levels of NGF (fig 6.14).

If the NGF deprivation becomes chronic, I propose that the homeostatic response of astrocyte fails, and the astrocytes start acquiring a neurotoxic phenotype. Microglia are actively involved with synaptic pruning during neurodevelopment and A1 astrocytes could plausibly serve a complementary or parallel function (Hinkle et al., 2019). Regardless of their ontological basis, A1 phenotype regulators should likely be seen as candidate targets for therapeutic interventions.

Recent evidence established a clear link between immune cell - induced reactive astrocyte function that leads to neuronal and oligodendroglial cell death. Most strikingly, reactive astrocytes are localized to regions of degeneration in

human AD patient post-mortem tissue⁶⁹, mouse models of tauopathy (Shi et al., 2017), and many other neurodegenerative diseases⁶⁹ (Rothhammer et al., 2018; Yun et al., 2018; Sadick and Liddelow, 2018).

Couple of dozens of mice AD-like strains have been produced in a recent decade; all of them bear mutant genes associated with family AD in different combinations (Gotz and others 2012; Oddo and others 2003). Most of these mice express mutant genes for amyloid precursor proteins and or presenilins, which allows production of β -amyloid in animals, wild types of which are lacking this pathway. Reduction of astroglial profiles together with decrease in astroglial complexity and number of principal and secondary processes have been quantified in hippocampi from mice with experimental amyloidosis (the PDAPP-J20 mice expressing mutant APP; Beauquis and others 2013; Beauquis and others 2014) and in 3xTg-AD mice that display senile plaques and tangles (Olabarria and others 2010; Verkhratsky and others 2010). Importantly, these atrophic changes occurred before the emergence of amyloid plaques, i.e., before 12 months of age for 3xTG-AD mice). Signs of astroglial atrophy have been found in different regions of the brain (Verkhratsky and others 2014). In AD animal models, astro-degenerative changes are complemented by astroglial reactivity. Reactive, hypertrophic

astrocytes occur in hippocampus in response to development of senile plaques and perivascular β -amyloid deposits, with which reactive astrocytes are associated (Olabarria and others 2010).

Several studies have demonstrated that the survival/death choice of NGF-dependent neurons is a complex mechanism since it depends upon an intricate balance between proNGF/mature NGF and on the spatio-temporal expression of their receptors TrkA, p75NTR and Sortilin66. However, all these data point to mechanisms that do not take into account the fact that in the brain a large population of cells are of glial nature and do not take into account the interaction between neurons and glial cells, particularly astrocytes.

7.6 A new mechanism of neuronal death mediated by NGF-deprived neurotoxic astrocytes

Here I propose a further complexity and regulatory step provided by the astrocytes that could explain this and other phenomena already observed.

For example, it has been reported that primary hippocampal neurons, that do not express NGF receptors,

after 48 h of NGF exposure die following NGF withdrawal. This result has not been explained and are still poorly understood but could be explained considering the mechanism that I propose, i.e. that NGF deprivation induces the A1 phenotype in astrocytes and in turn they trigger neuronal degeneration.

I set up neuron and astrocytes cultures and co-cultures and I demonstrated that the NGF neutralization leads to a neuronal impairment only if the neurons are co-plated with astrocytes.

This experimental approach gave me the opportunity to gain insights into the mechanism of neuronal death mediated by NGF-deprived neurotoxic astrocytes. I postulated that the cell death might involve the production of the toxic species of A β peptide, the so called A β oligomers. To test this hypothesis, I exploited a recombinant small antibody fragment scFvA13 (Meli et al 2009 JMB, 2014 Nat Comm), that binds selectively A β oligomers with no binding affinity for A β monomers nor for A β fibrils (Meli et al 2009 and 2014). Interestingly, the neuronal impairment is reduced when NGF is neutralized concomitantly with the amyloid β oligomers neutralization with A13 antibody, or concomitantly with the glutamate ionotropic receptors blockade exerted by kynurenic acid.

This indicates that the neurotoxic effects of deprivation of NGF, mediated by the astrocytes, might imply the production of β amyloid oligomers or excitotoxicity.

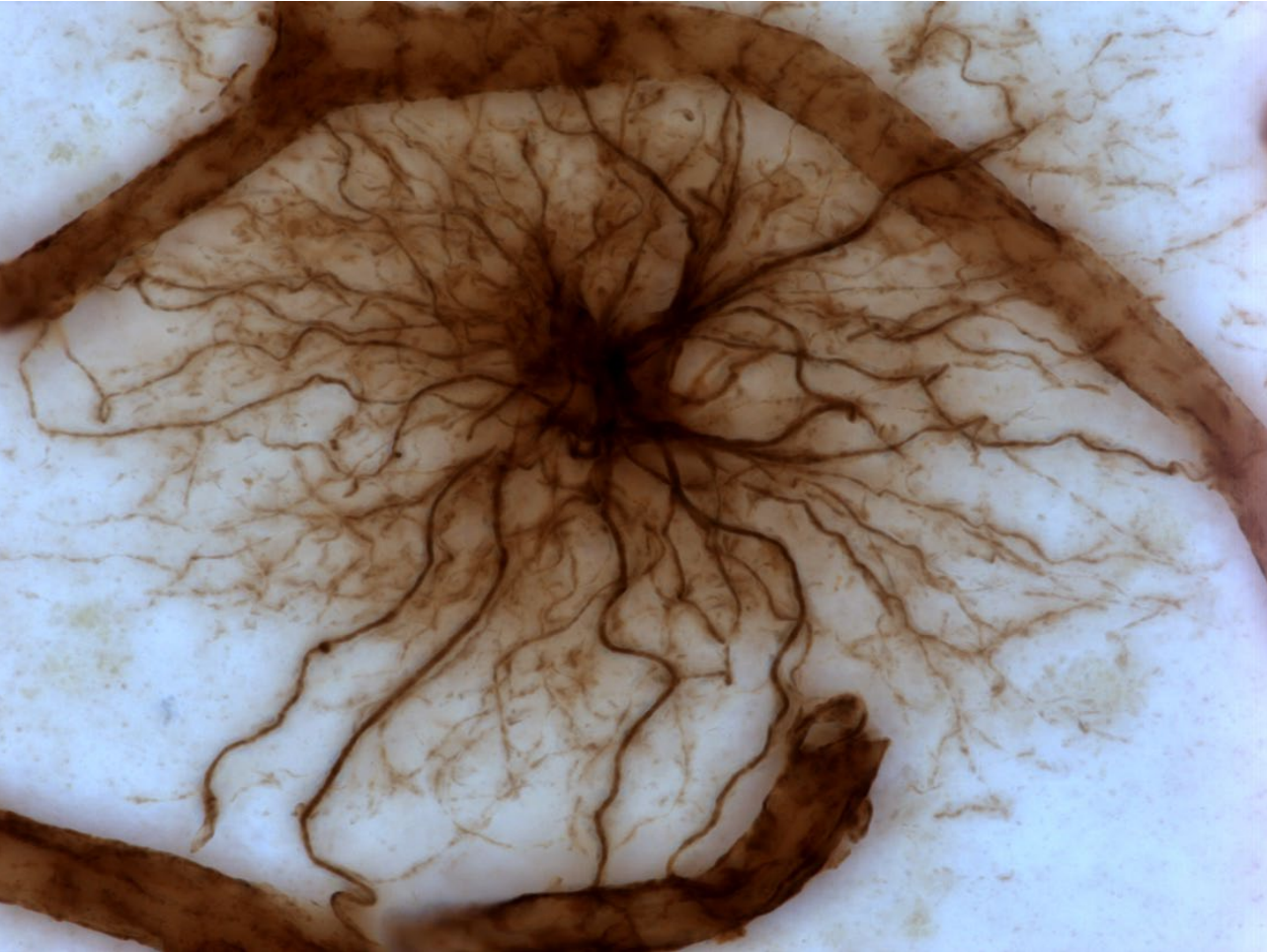
Is this relevant for AD neurodegeneration? Increasing evidence indicates that astrocyte glutamatergic homeostasis is disrupted in AD and, more in general, in neurodegenerative diseases. Reduced glutamate transporters in association with increased levels of glutamate in the CSF are potential biomarkers to identify early changes. Excitotoxicity has been implicated in several other brain disorders, but early astrocyte glutamatergic dysfunction in brain regions commonly associated with AD provides an interesting avenue with plenty of potential biomarker targets (Carter et al., 2019).

We have tackled the *in vivo* extension of the *in vitro* data by using *in vivo* 2-photon microscopy. We monitored the effects of NGF on astrocyte physiology, by monitoring the changes in calcium activity of these cells during modulations of NGF levels in the extracellular environment. We discovered that, also *in vivo*, while NGF exerted no effect, a lack of the neurotrophin, induced by acute anti NGF injection, increased astrocyte calcium activity in the anesthetized mouse as well as in the awake behaving animal.

7.7. Widening the potential clinical application of NGF

Taken all together, the data shown in this thesis strongly suggest NGF as potential treatment for neurodegeneration. NGF has been considered to have therapeutic potential for Alzheimer's disease due to its neuroprotective action on cholinergic neurons.

Here I show that the extracellular levels of NGF influence the reactive states of astrocytes and thus restoring its levels might reduce the pro-neurodegenerative state of these cells. Importantly, the latter statement applies not only to Alzheimer's disease but also to human several diseases in which astrocytes contribute to neurodegeneration, thus widening the potential clinical application of this neurotrophin.



Human astrocyte contacting blood vessels.

Credit: Liam O'Leary, The Douglas Research Centre.

8. Methods

8.1 Animals

B 6129 mice were purchased from The Jackson Laboratory (Bar Harbor, ME). AD11 mice, VH mice control (Ruberti, Capsoni et al. 2000) and proNGF mice (Tiveron et al., 2013) from an in-house colony were used. For experiments involving AD11 mice, littermates were used as controls for the IHC, since AD11 has a C57BL/6 x SJL background.

The 3xTG mice are homozygous triple-transgenic AD mice possessing PS1_{M146V}, A β PP_{swe}, and *tau*_{P301L} transgenes purchased from The Jackson Laboratory (Bar Harbor, ME).

Genotyping was performed by PCR analysis of tail DNA according to the best genotyping procedure specific for each strain.

All experiments with mice were performed according to the national and international laws for laboratory animal welfare and experimentation (EU directive n. 2010/63/EU and Italian DL n. 26 04/03/2014).

Mice were kept under a 12-h dark to light cycle, with food and water *ad libitum*.

8.2 Intranasal Delivery

Intranasal administration was performed on anaesthetized mice as follows. First, 2,2,2-tribromethanol (Sigma–Aldrich) was dissolved in absolute ethanol at the concentration of 1 g/ml and stored at -20°C in the dark. After dilution in 0.9% NaCl at the final concentration of 2.5%, it was injected i.p. at the dosage of 10 μ l/g of body weight to induce anesthesia, which followed within 5–10 min after injection.

After anesthesia, mice were laid on their back, with the head in upright position. The experiment required 10 μ M solution of mouse NGF in PBS administered intranasally to mice, 3 μ l at a time, alternating the nostrils, with a lapse of 2 min between each administration, for a total of 14 times in a single session.

The treatment lasted for 2 weeks and consisted of 3 sessions per week. During these procedures, the nostrils were always kept open. As control, mice were treated with PBS.

8.3 Cell cultures

All primary cell cultures were grown and maintained in DMEM/F12 or RPMI (Thermo Fisher Scientific, MA, USA #11835-063) medium containing 1% penicillin/streptomycin (Euroclone, MI, Italy #ECB3001D), 1% Glutamax (Thermo Fisher Scientific, MA, USA; #35050-038) and 10% fetal bovine serum (FBS) (Euroclone, MI, Italy #ECS0180l) in 5% CO₂ at 37°C incubator.

Primary astrocyte cells were derived from the brains of B6129 at postnatal day 3-4 as described by Butovsky et al., 2014. Astrocytes were maintained in Dulbecco's modified Eagle's medium (DMEM/F12) (Thermo Fisher Scientific, MA,

USA #21331-020) containing 1% penicillin/streptomycin, 1% Glutamax and 10% FBS in 5% CO₂ pH 7.4 at 37 °C. Microglia were eliminated from the mixed primary glial cultures by mild shaking. Astrocytes, after 14 days in culture, were detached by mild trypsinization (10 min, 0.01% of trypsin (Thermo Fisher Scientific, MA, USA), then collected and re-suspended in DMEM/F12 with 1% penicillin/streptomycin, 1% Glutamax and 10% FBS and plated on the appropriate support 24hrs before the experiments to allow cells to attach to the substrate.

Primary cortical and hippocampal neurons were prepared at postnatal day 0 as described by Beaudoin et al., 2012. Briefly, animals were decapitated, the brain was rapidly excised and placed into ice-cold Hanks Buffered Saline Solution (HBSS) (Thermo Fisher Scientific, MA, USA; #14180046). Hippocampi and/or cortex were removed and digested for 15 min at 37°C in DMEM-F12 containing 0.1% of trypsin (Thermo Fisher Scientific, MA, USA). Thereafter, tissue was transferred in culture medium containing 10% FBS and gently disrupted using a polished Pasteur pipette. Following centrifugation at 4°C for 8 min at 800 r.p.m. cells were resuspended in fresh DMEM containing 1% Glutamax, 10% FBS, 2% B27 supplement (Gibco, MA, USA, #17504044), 6 mg/ml Glucose, 12,5 uM Glutamate, 10 ug/ml

Gentamicin (Gibco, MA, USA, #15710-049) and plated at a density of approx. 150,000 cells per coverslip after proper poly-D-lysine coating (Sigma Aldrich, MO, USA, #P1024).

Cells were kept at 37°C in 5% CO₂. After 12-24 hours, medium was replaced with pre-warmed Neurobasal A medium (Thermo Fisher Scientific, MA, USA #10888-022) containing 2% of B27 supplement, 2.5 uM Glutamax, and 10 ug/ml Gentamicin. The experiments were performed at DIV 17-19.

8.4 Immunoblot analysis

Primary astrocytes were plated in 6 well plates at a density of 5×10^5 /well in culture medium. Cells were treated with the different drugs as mentioned in each corresponding paragraph and sequentially collected and lysed in ice-cold RIPA buffer (50 mM Tris-HCl, pH 7.6, 150 mM NaCl, 1% Igepal, 1 mM EDTA, 1% SDS, 0.5% sodium deoxycholate, 1x protease and phosphatase inhibitor cocktails (Roche, Basel; CH)). After sonication, cells were collected by centrifugation for 15 min at 4°C (13,000 r.p.m.).

Protein concentrations of the cell lysates were measured using the Bradford method. Lysates (20 to 50 ug) were then separated on a 10% SDS-PAGE, transferred to a nitrocellulose membrane, and analyzed by Western blotting.

After transfer in nitrocellulose, the membrane was blocked for 1h and incubated with the appropriate primary antibodies. Inhibitors of NGF-receptors used: 200 nM K252a (Abcam, Cambridge, UK; #ab120419), TAT-pep5 p75NTR (Millipore, CA, USA; #506181) (Yamashita Tohyama, 2003), were added 30 min before treatment.

The following primary antibodies were used: anti-TrkA 1:1000 (Millipore, CA, USA; #06-574), anti-pTrkA 1:1000 (Y794) (Rajagopal, Chen, Lee, Chao, 2004) kindly provided by M. V. Cao (New York University School of Medicine, New York, USA) anti Akt 1:1000 (Cell Signaling Technology, MA, USA; #C67E7) , anti p-Akt 1:1000 (Cell Signaling Technology #130386), anti-Erk 1:1000 (Promega, WI, USA; #V114A), anti-pErk 1:1000 (Cell Signaling Technology, MA, USA; #4370S), anti-c-Jun 1:1000 (Cell Signaling Technology, MA, USA; #60A8), anti-phospho-c-Jun 1:1000 (Cell Signaling Technology, MA, USA; #9261), anti-p75 1:1000 (Millipore, CA, USA; AB1554), anti-GAPDH 1:20000 (Fitzgerald, MA, USA; #10R-G109a), anti-tubulin 1:20000 (Sigma Aldrich, MO, USA; #T5168). After incubation with the appropriate HRP-conjugated secondary antibody (Santa Cruz, TX, USA; anti-mouse #sc-2005, anti-rabbit #sc-2004), membranes were developed using ECL-enhanced chemiluminescence kit (Bio-Rad, CA, USA).

Densitometric analyses were performed using the NIH ImageJ 1.44p software.

8.5 Immunocytochemistry

Primary astrocytes were plated on coverslips in 24-well plates coated with poly-D-lysine (1×10^5 cells/well) in culture medium. After 18 hrs, cells were fixed with 2% PFA, and blocked for 1 hr at room temperature. Coverslips were incubated overnight at 4°C in primary antibody: rabbit anti-Glial Fibrillary Acidic Protein (Dako, Cytomation, Glostrup, Denmark, Z0334, 1: 500) or goat Anti-Glial Fibrillary Acidic Protein (Santa Cruz Biotechnology, California, USA, sc-6170, 1:300) 1:500 anti-TrkA 1:100 (MNAC13 (Covaceuszach, Cattaneo, Lamba, 2005)), anti-p75 1:500 (Millipore, CA, USA; AB1554).

After three washings, cells were incubated for 1 hr with appropriate secondary antibodies (1:500) anti-rabbit Alexa-Fluor 555, anti-mouse Alexa-Fluor 488, Thermo Fisher Scientific, MA, USA; A-21428; A-21201). Coverslips were mounted on glass slides in Fluoromount (Sigma Aldrich, MO, USA #F6057) and confocal images were acquired using a Leica SP2 confocal microscope (Leica Microsystems, Wetzlar, Germany).

8.6 Immunofluorescence on slice

Mice were sacrificed with a lethal dose of carbon dioxide and immediately underwent a perfusion procedure. Blood was firstly transcardially washed out with cold phosphate buffer saline solution (PBS), then tissues were fixed with cold 4% paraformaldehyde in 0.1 M pH 7.4 phosphate buffer (PBS) with a peristaltic pump for 10 minutes.

Brains were dissected, post-fixed for 48 hrs at 4°C, washed from paraformaldehyde with PBS and cryoprotected in 30% sucrose/PBS at 4°C overnight. Dry ice frozen brains were cut into 40 um coronal sections with a cryostat microtome (Leica Microsystems, Wetzlar, Germany) at -20°C. Sections were rinsed for three times in PBS and incubated with a mix of primary antibodies in PBS 0.3% Triton X-100 (Applichem, BioChemica, Darmstadt, Germany) overnight at room temperature.

Astrocytes were stained with rabbit anti-Glial Fibrillary Acidic Protein (Dako, Cytomation, Glostrup, Denmark, Z0334, 1: 500) or goat Anti-Glial Fibrillary Acidic Protein (Santa Cruz Biotechnology, California, USA, sc-6170, 1:300). NGF receptors were identified by anti-TrkA (clone MNAC13, 1:300, (Cattaneo et al., 1999)) and anti-p75 (Promega Corporation, Madison, WI, USA, G3231, 1:300). After three

10 min rinses in PBS at RT, sections were incubated for 2 hrs at RT in a mix of the appropriate secondary antibodies - anti-mouse/rabbit/goat/rat Alexa-Fluor 488/555/649 conjugated (Thermo Fisher Scientific, MA, USA; A-21428 diluted 1:500) followed by three 10 min rinses in PBS. DAPI was applied for 5 min in the second rinse, dissolved in the PBS solution.

To exclude non-specific signals of secondary antibodies, sections from each group of animals have also been stained with secondary antibody alone, following the same experimental procedure but omitting the primary antibodies.

8.7 Flow cytometry

Primary astrocytes were plated in 6 well plates at a density of 5×10^2 cells/well.

Cells were washed with PBS and collected for analysis. Data acquisition: A Sorter S3 (BioRad, CA, USA) with a single 488 nm (100 mW) excitation laser was used. The gating strategy

was decided on the FSC and SCC scatter plots, in order to gate out debris. Filters are based on the emission spectra of the fluorochromes RhodamineB or DyeRed.

The analysis was performed using the FlowJo software (FlowJo, LLC, Ashland, Ore., USA).

8.8 Microarray transcriptome analysis

Primary astrocytes were treated with drugs as described in the experimental paragraphs. RNA isolation, amplification, and labeling were performed using a RNeasy mini kit according to manufacturer's protocol (Qiagen). Total RNA was isolated from these cells using Trizol (Invitrogen) and DNase treated by Qiagen columns. Quality and integrity of each sample was checked using the Agilent BioAnalyzer 2100 (Agilent RNA 6000 nano kit): samples with an RNA Integrity Number (RIN) index lower than 8.0 were discarded. All the experimental steps involving the labeling, hybridization, and washing of the samples were done following the standard one-color micro Agilent protocol.

The gene expression profiling was performed using the Microarray Agilent Platform. 200ng of RNA was labeled with Low Input Quick Amp Labeling Kit One-Color (Agilent Technologies), purified and hybridized overnight onto the Agilent 8X60K whole mouse genome oligonucleotide microarrays (Grid ID 028005) according to the manufacturer's instructions for one-color protocol.

The Agilent DNA microarray scanner (model G2505C) was used for slide acquisition and spot analysis was performed with Feature Extraction software ver 10.7 (Agilent

Technologies). Data filtering and analysis were performed using R-Bioconductor and Microsoft Excel. All the features with the flag `gIsWellAboveBG=0` (too close to background) were filtered out and excluded from the following analysis. Filtered data were normalized by aligning samples to the 75th percentile. Differentially expressed genes were selected by a combination of fold change and moderated T-test thresholds (R Limma test $p_{0.05}$; $|\text{Log}_2 \text{ fold-change}| > 1.0$). Principal Component Analysis, Multi-Dimensional Scaling, Hierarchical Clustering of samples and volcano plots were computed using the open source R Studio (Boston, MA, USA).

8.9 Neuron/astrocytes co-cultures

For neuron/astrocytes co-cultures, at DIV 17-19 for neurons, primary astrocytes were seeded onto cultured hippocampal neurons (1×10^5 cells/well).

The culture was maintained in Neurobasal-A supplemented with 2% B27, 2mM L-Glutamine and 10 ug/ml gentamicin and used after 24 hrs for experiments. Co-cultures, treated as described in the experimental part, were fixed in 2% PFA and 5% sucrose for 10 min, washed in PBS and blocked for 1 hr at room temperature in BSA 1%. Incubation with primary antibody was performed at the following

concentrations: anti-PSD95 1:500 (Abcam Cambridge, UK; ab9909), anti-actin 1:500 (Sigma Aldrich, MO, USA A-3853), rabbit anti-Glial Fibrillary Acidic Protein (Dako, Cytomation, Glostrup, Denmark, Z0334, 1: 500) or goat Anti-Glial Fibrillary Acidic Protein (Santa Cruz Biotechnology, California, USA, sc-6170, 1:300). For image acquisition, coverslips were mounted on glass slides in Fluoromount (Sigma Aldrich, MO, USA, F4680-25ML).

8.10 Confocal microscopy and image analysis

Image Analysis Images from AD11, VH and WT mice were acquired with a confocal laser scanning microscope (TCS SP2; Leica Microsystem, Wetzlar, Germany) on slices labelled as previously described for GFAP detection. 10 stacks per region per mice were obtained. On the Z axis, images were taken every 0.4 μm . Region of interest for morphological changes were the hippocampus. Image elaboration and analysis was conducted using Bitplane software Imaris (Zurich, Switzerland). Images were acquired with a confocal microscope (Leica TCS SP2) using an oil objective: HCX PL APO 63.0X OIL (NA=1.40), and pinhole was set to 1 AU. Sequential illumination with Ar 561 and Ar 488 laser lines was used to detect the immunofluorescence.

Points of colocalization were localized when a merging area in the same cell was evident, showing a yellow resulting color from the overlap of two green-red signals, and they were verified by analysis on the z-axes with 1 μ m-stacks using the Pearson index tool provided from ImageJ 1.44p software (ImageJ.nih.gov).

8.11 Data Analysis and statistics

Data are presented as means \pm s.d. unless otherwise noted, using Origin (OriginLab Corporation, MA, USA) and Prism (GraphPad Software, San Diego, CA, USA). Means were compared using the unpaired or paired t-test.

Multiple comparisons were made using one-way ANOVA test, followed by a post-hoc Bonferroni test.

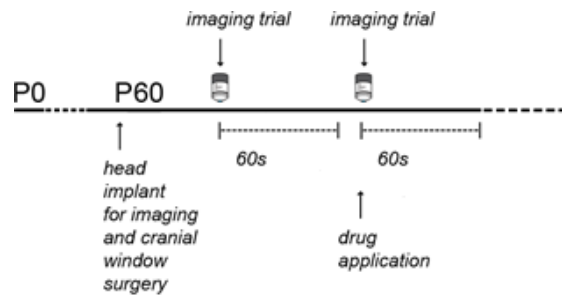
The variance of each dataset was measured with an F test; * $p \leq 0.05$, ** $p \leq 0.01$ and *** $p \leq 0.001$.

8.12 Transgenic mice for *in vivo* Ca²⁺ experiments

Wild-type mice (C57J\BL) were used for viral injection at 1-1.5 month of age to achieve expression of GCamp6f in astrocytes. Mice were group-housed (5 per cage) in the Science Building Animal Facility at New York University Medical Center.

Mice were maintained at 22 C± 2°C with a 12-h light:dark cycle. All experiments were conducted during the light cycle between 08:00-18:00. Food and water were available at libitum. 1-1.5-month-old animals of both sexes were used for all the experiments in accordance with ethical regulations and the New York University Medical Center (NYUMC) guidelines, and approved by the Institutional Animal Care and Use Committee (IACUC) at NYUMC. No association was found between animals' sex and experimental results.

8.13 In vivo imaging with two-photon microscopy in the anesthetized mouse



GCamp6f astrocytes were imaged by two-photon microscopy, through a small craniotomy (Grutzendler, Kasthuri, & Gan, 2002).

Briefly, adult transgenic mice were anesthetized intraperitoneally with ketamine (200 mg/kg body weight) and xylazine (30 mg/kg body weight) in 0.9% NaCl solution. For imaging through a window in the skull, a thinned region (1–2 mm in diameter) was opened either with needle or forceps.

A drop (200 μ l) of artificial mouse cerebrospinal fluid (ACSF, 125 mM NaCl, 26 mM NaHCO₃, 1.25 mM NaH₂PO₄, 2.5 mM KCl, 1.0 mM MgCl₂, 2.0 mM CaCl₂, 25 mM glucose; Bubble 95% O₂ and 5% CO₂ through the solution) was applied on the exposed region for the duration

of the experiment. The skull surrounding either the thinned region or the open skull window was attached to a custom-made steel plate to reduce respiratory-induced movement. The animal was placed under either a Bio-Rad multi-photon microscope (Radiance 2001) or a custom-made two-photon microscope described previously. The Ti-sapphire laser was tuned to the excitation wavelength for GFP (920 nm).

A stack of image planes with a step size of 0.75–2 μm was acquired using a water-immersion objective (Olympus 60x, 0.9 N.A.; Olympus 25X, N.A. 1.1) at zoom of 1.0–3.0. The maximum imaging depth was ~ 200 μm from the pial surface.

8.14 Surgical preparation for imaging awake, head-restrained mice

Ciao We performed imaging in awake, head restrained mice through a cranial window. 24 h prior to imaging, mice underwent surgery to attach a head holder (G. Yang, Pan, Chang, Gooden, & Gan, 2013). Specifically, mice were deeply anesthetized with an intraperitoneal injection of ketamine (100

mg/g) and xylazine (10 mg/g). The mouse head was shaved, and the skull surface was exposed with a midline scalp incision.

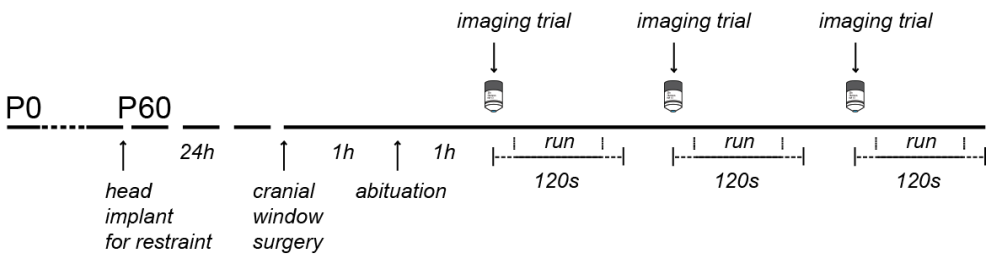
The periosteum tissue over the skull surface was removed without damaging the temporal and occipital muscles. Two parallel micro-metal bars were attached to the animal's skull to serve as the head holder to help restrain the animal's head and reduce motion-induced artifact during imaging.

A skull region of 0.2 mm in diameter was located over the primary motor cortex based on stereotactic coordinates (at 0.2 mm anterior to bregma and 1.2 mm lateral to midline) and marked with a pen. Next the head holder was mounted with dental acrylic cement (Lang Dental Manufacturing Co., IL, USA) such that the marked skull region was exposed between the two bars.

The marked region for imaging was kept exposed, uncovered with dental acrylic cement. The next day, we created the cranial window over the marked region. Briefly, the head holder was screwed to two metal cubes that were attached to a solid metal base.

A high-speed drill was used to carefully reduce the skull thickness under a dissecting microscope (skull thickness 20 μ m). The skull was immersed in artificial cerebrospinal fluid (ACSF) during drilling. For open skull preparation a small

circular craniotomy (1.0-1.5 mm diameter) was made and covered with a round glass coverslip (World Precision Instruments, coverslips, 5mm diameter) custom-made to the size of the bone removed.



The coverslip was glued to the skull to reduce motion of the exposed brain. Before imaging, mice were given 1 day to recover from the surgery related anesthesia and habituated for a few times (10 min each) in the imaging apparatus to minimize potential stress effects due to head restraining and awake imaging.

8.15 Drug through an open window in the skull

Various reagents were dissolved in ACSF (artificial cerebrospinal fluid), and a small drop of the solution (200 μ l) containing the compound of interest was applied directly onto the cortex through the open window after removing the dura.

Imaging started either right away for anesthetized experiments or 10 min after drug application for awake head restrained experiments. Drugs: NGF (200-1000ng/ml), proNGF (400-1000 ng/ml), Phenylephrine (Sigma, 100 nM), anti-NGF clone α D11 (8 μ g/ml), anti- TrkAFc (1 μ g/ml, R&D Systems). The NT condition in all in vivo experiments stands for “ACSF only”.

8.16 Statistical analyses for *in vivo* Ca²⁺ experiments

All imaging data were presented as mean \pm s.e.m. Student's t-test (two-tailed) was used to test for differences between groups whose distributions passed tests for normality (Kolmogorov–Smirnov).

Wilcoxon matched-pairs signed rank test and Mann–Whitney U test were used to analyze those groups whose distributions did not pass tests for normality.

1way ANOVA was used when confronting groups $n > 2$.
2way ANOVA was used when confronting traces to take into account time, treatment and replicates.

Significant levels were set at $P \leq 0.05$. All statistical analyses were performed using the GraphPad Prism.

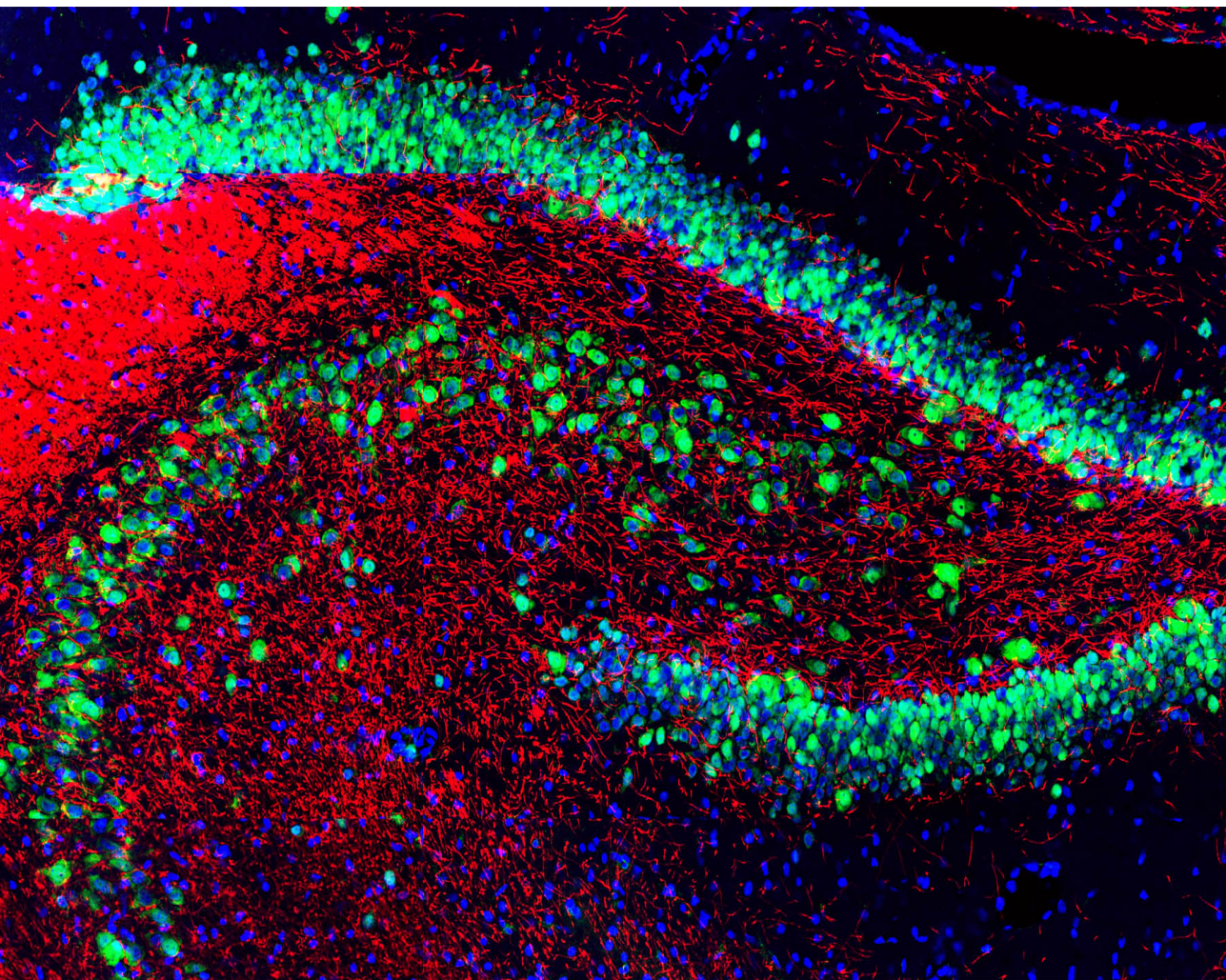
8.17 NGF immunoprecipitation and Western Blot

The scraped astrocytes (see the M&M 8.4 paragraph for the input cells treatment and collection) were sonicated, incubated in ice for 30 min, and centrifuged at $15,000 \times g$ for 30 min at 4°C . Protein concentration in the supernatant was quantified using the Bradford method (Bio-Rad).

Four milligrams of protein were immunoprecipitated with an excess of anti-NGF αD11 antibody in NET Gel Buffer (Tris-HCl, pH 7.5, 50 mM; NaCl 150 mM; 0.1% Nonidet P-40; EDTA, pH 8, 1 mM; 0.25% gelatin; and 0.02% NaN).

After immunoprecipitation, total lysates were loaded on 12% acrylamide gels and blotted using nitrocellulose membranes. The primary antibody was anti-NGF M20 (1:500; Santa Cruz Biotechnology), the secondary antibody was goat anti-rabbit HRP-conjugated (1:500; Santa Cruz

Biotechnology). Blot images were acquired using a ChemiDoc System (Bio-Rad), and the optical density was quantified using ImageJ (NIH).



Rat hippocampus stained with antibody to NeuN (green), myelin basic protein (red) and DAPI (blue).

Credit: GerryShaw, 2015.

9. References

1. Verkhratsky, A., Nedergaard, M. & Hertz, L. Why are Astrocytes Important? *Neurochem. Res.* 40, 389–401 (2014).
2. Gallo, V. & Deneen, B. Glial development: The crossroads of regeneration and repair in the CNS. *Neuron* 83, 283–308 (2014).
3. Allen, N. J. & Barres, B. A. Neuroscience: Glia - more than just brain glue. *Nature* 457, 675–677 (2009).
4. Lin, G. G. & Scott, J. G. Glial Development: The Crossroads of Regeneration and Repair in the

- CNS. 100, 130–134 (2012).
5. Molofsk, A. V. *et al.* Astrocytes and disease: A neurodevelopmental perspective. *Genes Dev.* 26, 891–907 (2012).
 6. Zhang, Y. & Barres, B. A. A smarter mouse with human astrocytes. *BioEssays* 35, 876–880 (2013).
 7. He, Q., Johnston, J., Zeitlinger, J., City, K. & City, K. A new subtype of progenitor cell in the mouse embryonic neocortex. *Nat Neurosci* 33, 395–401 (2015).
 8. Simard, M. & Nedergaard, M. The neurobiology of glia in the context of water and ion homeostasis. *Neuroscience* 129, 877–896 (2004).
 9. Schousboe, A., Sarup, A., Bak, L. K., Waagepetersen, H. S. & Larsson, O. M. Role of astrocytic transport processes in glutamatergic and GABAergic neurotransmission. *Neurochem. Int.* 45, 521–527 (2004).
 10. Yi, J. H. & Hazell, A. S. Excitotoxic mechanisms and the role of astrocytic glutamate transporters in traumatic brain injury. *Neurochem. Int.* 48, 394–403 (2006).
 11. Allaman, I., Bélanger, M. & Magistretti, P. J. Astrocyte-neuron metabolic relationships: For

- better and for worse. *Trends Neurosci.* 34, 76–87 (2011).
12. Attwell, D. *et al.* Glial and neuronal control of brain blood flow. *Nature* 468, 232–43 (2010).
 13. Clarke, L. E. & Barres, B. A. Emerging roles of astrocytes in neural circuit development. *Nat. Rev. Neurosci.* 14, 311–21 (2013).
 14. Halassa, M. M. & Haydon, P. G. Integrated brain circuits: astrocytic networks modulate neuronal activity and behavior. *Annu. Rev. Physiol.* 72, 335–55 (2010).
 15. Bergami, M. *et al.* Uptake and recycling of pro-BDNF for transmitter-induced secretion by cortical astrocytes. *J. Cell Biol.* 183, 213–221 (2008).
 16. Bazargani, N. & Attwell, D. Astrocyte calcium signaling: the third wave. *Nat. Neurosci.* 19, 182–9 (2016).
 17. Anderson, M. A., Ao, Y. & Sofroniew, M. V. Heterogeneity of reactive astrocytes. *Neurosci. Lett.* 565, 23–29 (2014).
 18. Colangelo, A. M., Alberghina, L. & Papa, M. Astroglialosis as a therapeutic target for neurodegenerative diseases. *Neurosci. Lett.* 565, 59–

- 64 (2014).
19. Trias, E. *et al.* Phenotypic transition of microglia into astrocyte-like cells associated with disease onset in a model of inherited ALS. *Front. Cell. Neurosci.* 7, 274 (2013).
 20. Wyss-Coray, T. & Mucke, L. Inflammation in neurodegenerative disease - A double-edged sword. *Neuron* 35, 419–432 (2002).
 21. Ruberti, F. *et al.* Phenotypic knockout of nerve growth factor in adult transgenic mice reveals severe deficits in basal forebrain cholinergic neurons, cell death in the spleen, and skeletal muscle dystrophy. *J. Neurosci.* 20, 2589–601 (2000).
 22. Capsoni, S. *et al.* Alzheimer-like neurodegeneration in aged antinerve growth factor transgenic mice. *Proc. Natl. Acad. Sci. U. S. A.* 97, 6826–6831 (2000).
 23. Capsoni, S., Giannotta, S. & Cattaneo, A. Early events of Alzheimer-like neurodegeneration in anti-nerve growth factor transgenic mice. *Brain Aging* 2, 39–40 (2002).
 24. Cattaneo, A., Capsoni, S. & Paoletti, F. Towards noninvasive nerve growth factor therapies for Alzheimer's disease. *J. Alzheimers. Dis.* 15, 255–283

- (2008).
25. Aloe, L., Rocco, M. L., Bianchi, P. & Manni, L. Nerve growth factor: from the early discoveries to the potential clinical use. *J. Transl. Med.* 10, 239 (2012).
 26. Nagele, R. G. *et al.* Contribution of glial cells to the development of amyloid plaques in Alzheimer's disease. *Neurobiol. Aging* 25, 663–674 (2004).
 27. Furman, J. L. *et al.* Mouse Model of Alzheimer's Disease. 32, 16129–16140 (2013).
 28. Garwood, C. *et al.* Review: Astrocytes in Alzheimer's disease and other age-associated dementias; a supporting player with a central role. *Neuropathol. Appl. Neurobiol.* (2016). doi:10.1111/nan.12338
 29. Iram, T. *et al.* Astrocytes from old Alzheimer's disease mice are impaired in A β uptake and in neuroprotection. *Neurobiol. Dis.* 96, 84–94 (2016).
 30. Cornell-bell, A. N. N. H., Finkbeiner, S. M., Cooper, M. S. & Smith, S. J. Glutamate Induces Calcium Waves in Cultured Astrocytes: Long-Range Glial Signaling. 247, 2–5 (1988).
 31. Charles, A. C., Merrill, J. E., Dirksen, E. R. &

- Sanderson, M. J. Intercellular Signaling in Glial Cells: Calcium Waves and Oscillations in Response to Mechanical Stimulation and Glutamate. *6*, 983–992 (1991).
32. Perea, G. & Araque, A. Glial calcium signaling and neuron – glia communication. *38*, 375–382 (2005).
33. Kimelberg, H. K. The problem of astrocyte identity. *Neurochem. Int.* *45*, 191–202 (2004).
34. Olabarria, M., Noristani, H. N., Verkhratsky, A. & Rodríguez, J. J. Concomitant astroglial atrophy and astrogliosis in a triple transgenic animal model of Alzheimer’s disease. *Glia* *58*, 831–838 (2010).
35. Wyssenbach, A. *et al.* Amyloid β -induced astrogliosis is mediated by β 1-integrin via NADPH oxidase 2 in Alzheimer’s disease. *Aging Cell* *1–13* (2016). doi:10.1111/accel.12521
36. Capsoni, S. β -Amyloid Plaques in a Model for Sporadic Alzheimer’s Disease Based on Transgenic Anti-Nerve Growth Factor Antibodies. *Mol. Cell. Neurosci.* *21*, 15–28 (2002).
37. Tiveron, C. *et al.* ProNGF/NGF imbalance triggers learning and memory deficits, neurodegeneration and spontaneous epileptic-like discharges in transgenic mice. *Cell Death Differ.* *20*,

- 1017–1030 (2013).
38. Oddo, S. *et al.* Triple-Transgenic Model of Alzheimer's Disease with Plaques and Tangles Intracellular A β and Synaptic Dysfunction. *Neuron* 39, 409–421 (2003).
 39. Nico, B. *et al.* Nerve growth factor and its receptors TrkA and p75 are upregulated in the brain of mdx dystrophic mouse. *Neuroscience* 161, 1057–1066 (2009).
 40. Cragolini, A. B., Huang, Y., Gokina, P. & Friedman, W. J. Nerve growth factor attenuates proliferation of astrocytes via the p75 neurotrophin receptor. *Glia* 57, 1386–1392 (2009).
 41. Cattaneo, a *et al.* Functional blockade of tyrosine kinase A in the rat basal forebrain by a novel antagonistic anti-receptor monoclonal antibody. *J. Neurosci.* 19, 9687–9697 (1999).
 42. Covaceuszach, S., Cattaneo, A. & Lamba, D. Neutralization of NGF-TrkA receptor interaction by the novel antagonistic anti-TrkA monoclonal antibody MNAC13: A structural insight. *Proteins Struct. Funct. Genet.* 58, 717–727 (2005).
 43. Lee, F. S. & Chao, M. V. Activation of Trk neurotrophin receptors in the absence of

- neurotrophins. *Proc. Natl. Acad. Sci. U. S. A.* 98, 3555–60 (2001).
44. Ronco, V. *et al.* Differential deregulation of astrocytic calcium signalling by amyloid- β , TNF α , IL-1 β and LPS. *Cell Calcium* 55, 219–229 (2014).
 45. Plattner, H. & Verkhratsky, A. The ancient roots of calcium signalling evolutionary tree. *Cell Calcium* 57, 123–132 (2015).
 46. Brawek, B. & Garaschuk, O. Network-wide dysregulation of calcium homeostasis in Alzheimer’s disease. *Cell Tissue Res.* 357, 427–438 (2014).
 47. Shibasaki, K., Ishizaki, Y. & Mandadi, S. Astrocytes express functional TRPV2 ion channels. *Biochem. Biophys. Res. Commun.* 441, 327–332 (2013).
 48. Lee, B. M. *et al.* Extracellular ATP Induces Calcium Signaling in Odontoblasts. *J. Dent. Res.* 22034516671308 (2016).
doi:10.1177/0022034516671308
 49. Chen, X. *et al.* A chemical-genetic approach to studying neurotrophin signaling. *Neuron* 46, 13–21 (2005).
 50. Michal Marzeca, Davide Eletto, Y. A. GRP94: an

- HSP90-like protein specialized for protein folding and quality control in the Endoplasmic Reticulum. 100, 130–134 (2012).
51. Böldicke, T. Blocking translocation of cell surface molecules from the ER to the cell surface by intracellular antibodies targeted to the ER. *J. Cell. Mol. Med.* 11, 54–70 (2007).
 52. Marschall, A. L. J. *et al.* Functional knock down of VCAM1 in mice mediated by endoplasmic reticulum retained intrabodies. *MAbs* 6, 1394–1401 (2014).
 53. Zhang, C. *et al.* Suppression of p75 neurotrophin receptor surface expression with intrabodies influences Bcl-xL mRNA expression and neurite outgrowth in PC12 cells. *PLoS One* 7, (2012).
 54. Pelham, H. R. The dynamic organisation of the secretory pathway. *Cell Struct. Funct.* 21, 413–419 (1996).
 55. Wilson, D. W., Lewis, M. J. & Pelham, H. R. B. pH-dependent binding of KDEL to its receptor in vitro. *J. Biol. Chem.* 268, 7465–7468 (1993).
 56. Kong, H., Boulter, J., Weber, J. L., Lai, C. & Chao, M. V. An evolutionarily conserved transmembrane protein that is a novel downstream target of

- neurotrophin and ephrin receptors. *J. Neurosci.* 21, 176–185 (2001).
57. Huang, E. J. & Reichardt, L. F. Trk Receptors: Roles in Neuronal Signal Transduction. *Annu. Rev. Biochem.* 72, 609–642 (2003).
 58. Chao, M. V. & Hempstead, B. L. p75 and Trk: A two-receptor system. *Trends Neurosci.* 18, 321–326 (1995).
 59. Barker, P. A. & Shooter, E. M. Disruption of NGF binding to the low affinity neurotrophin receptor p75LNTR reduces NGF binding to TrkA on PC12 cells. *Neuron* 13, 203–215 (1994).
 60. Ugolini, G., Marinelli, S., Covaceuszach, S., Cattaneo, A. & Pavone, F. The function neutralizing anti-TrkA antibody MNAC13 reduces inflammatory and neuropathic pain. *Proc. Natl. Acad. Sci. U. S. A.* 104, 2985–2990 (2007).
 61. Hollingworth, P. *et al.* Common variants at ABCA7, MS4A6A/MS4A4E, EPHA1, CD33 and CD2AP are associated with Alzheimer’s disease. *Nat. Genet.* 43, 429–35 (2011).
 62. Meli, G., Visintin, M., Cannistraci, I. & Cattaneo, A. Direct in Vivo Intracellular Selection of Conformation-sensitive Antibody Domains

- Targeting Alzheimer's Amyloid-?? Oligomers. *J. Mol. Biol.* 387, 584–606 (2009).
63. Erturk, A., Wang, Y. & Sheng, M. Local pruning of dendrites and spines by caspase-3-dependent and proteasome-limited mechanisms. *J Neurosci* 34, 1672–1688 (2014).
 64. Gómez-Gonzalo, M. *et al.* An excitatory loop with astrocytes contributes to drive neurons to seizure threshold. *PLoS Biol.* 8, (2010).
 65. Carmignoto, G. & Haydon, P. G. Astrocyte calcium signaling and epilepsy. *Glia* 60, 1227–1233 (2012).
 66. Lu, B., Pang, P. T. & Woo, N. H. The yin and yang of neurotrophin action. *Nat. Rev. Neurosci.* 6, 603–614 (2005).
 67. Matrone, C. *et al.* Tyrosine kinase nerve growth factor receptor switches from prosurvival to proapoptotic activity via A β -mediated phosphorylation. *Proc. Natl. Acad. Sci. U. S. A.* 106, 11358–11363 (2009).
 68. Matrone, C., Ciotti, M. T., Mercanti, D., Marolda, R. & Calissano, P. NGF and BDNF signaling control amyloidogenic route and A β production in hippocampal neurons. *Proc. Natl. Acad. Sci. U. S.*

- A.* 105, 13139–13144 (2008).
69. Liddelow SA, Guttenplan KA, Clarke LE, Bennett FC, Bohlen CJ, Schirmer L, Bennett ML, Münch AE, Chung WS, Peterson TC, Wilton DK, Frouin A, Napier BA, Panicker N, Kumar M, Buckwalter MS, Rowitch DH, Dawson VL, Dawson TM, Stevens B, Barres BA. Neurotoxic reactive astrocytes are induced by activated microglia. *Nature* 2017 Jan 26;541(7638):481-487.
 70. Liddelow SA, Barres BA. Regeneration: Not everything is scary about a glial scar. *Nature* 2016 Apr 14;532(7598):182-3.
 71. Shooter EM. Early days of the nerve growth factor proteins. *nu Rev Neurosci.* 2001; 24:601-29.
 72. Martin A Bruno 1, A Claudio Cuello. Activity-dependent release of precursor nerve growth factor, conversion to mature nerve growth factor, and its degradation by a protease cascade. *Proc Natl Acad Sci U S A.* 2006 Apr 25;103 (17):6735-40.
 73. Fahnstock M, Yu G, Coughlin MD. ProNGF: a neurotrophic or an apoptotic molecule? *Prog Brain Res* 2004; 146:101-10.

74. Nykjaer A, Lee R, Teng KK, Jansen P, Madsen P, Nielsen MS, Jacobsen C, Kliemannel M, Schwarz E, Willnow TE, Hempstead BL, Petersen CM. Sortilin is essential for proNGF-induced neuronal cell death. *Nature* 2004 Feb 26; 427(6977):843-8.
75. Hempstead BL. Dissecting the diverse actions of pro- and mature neurotrophins *Curr Alzheimer Res.* 2006 Feb; 3(1):19-24.
76. Corvaglia V, Cilli D, Scopa C, Brandi R, Arisi I, Malerba F, La Regina F, Scardigli R, Cattaneo A. ProNGF Is a Cell-Type-Specific Mitogen for Adult Hippocampal and for Induced Neural Stem Cells. *Stem Cells.* 2019 Sep;37(9):1223-1237.
77. Grutzendler, J., Kasthuri, N., & Gan, W. (2002). Long-term dendritic spine stability in the adult cortex. *420*(December).
<https://doi.org/10.1038/nature01276>.
78. Guttenplan, K. A., & Liddelow, S. A. (2019). Astrocytes and microglia: Models and tools. *Journal of Experimental Medicine*, 216(1), 71–83.
79. Ding, F., O'Donnell, J., Thrane, A. S., Zeppenfeld, D., Kang, H., Xie, L., ... Nedergaard, M. (2013). α 1-Adrenergic receptors mediate coordinated Ca^{2+} signaling of cortical astrocytes in awake,

- behaving mice. *Cell Calcium*, 54(6), 387–394.
80. De Simone, R., Ambrosini, E., Carnevale, D., Ajmone-Cat, M. A., & Minghetti, L. (2007). NGF promotes microglial migration through the activation of its high affinity receptor: Modulation by TGF- β . *Journal of Neuroimmunology*, 190(1–2), 53–60.
<https://doi.org/10.1016/j.jneuroim.2007.07.020>
81. Deemyad, T., Lüthi, J., & Spruston, N. (2018). Astrocytes integrate and drive action potential firing in inhibitory subnetworks. *Nature Communications*, 9(1).
<https://doi.org/10.1038/s41467-018-06338-3>
82. Deinhardt, K., Kim, T., Spellman, D. S., Mains, R. E., Eipper, B. A., Neubert, T. A., ... Hempstead, B. L. (2011). Neuronal growth cone retraction relies on proneurotrophin receptor signaling through rac. *Science Signaling*, 4(202), 1–9.
<https://doi.org/10.1126/scisignal.2002060>
83. Delekate, A., Fächtemeier, M., Schumacher, T., Ulbrich, C., Foddiss, M., & Petzold, G. C. (2014). Metabotropic P2Y1 receptor signalling mediates astrocytic hyperactivity in vivo in an Alzheimer's disease mouse model. *Nature Communications*, 5.

- <https://doi.org/10.1038/ncomms6422>
84. Denk, F., Bennett, D. L., & McMahon, S. B. (2017). Nerve Growth Factor and Pain Mechanisms. *Annual Review of Neuroscience*, *40*(1), 307–325. <https://doi.org/10.1146/annurev-neuro-072116-031121>
 85. Ding, F., O'Donnell, J., Thrane, A. S., Zeppenfeld, D., Kang, H., Xie, L., ... Nedergaard, M. (2013). α 1-Adrenergic receptors mediate coordinated Ca^{2+} signaling of cortical astrocytes in awake, behaving mice. *Cell Calcium*, *54*(6), 387–394. <https://doi.org/10.1016/j.ceca.2013.09.001>
 86. Dissing-Olesen, L., LeDue, J. M., Rungta, R. L., Hefendehl, J. K., Choi, H. B., & MacVicar, B. A. (2014). Activation of Neuronal NMDA Receptors Triggers Transient ATP-Mediated Microglial Process Outgrowth. *Journal of Neuroscience*, *34*(32), 10511–10527.
 87. Domeniconi, M., Hempstead, B. L., & Chao, M. V. (2007). Pro-NGF secreted by astrocytes promotes motor neuron cell death. *Molecular and Cellular Neuroscience*, *34*(2), 271–279. <https://doi.org/10.1016/j.mcn.2006.11.005>
 88. Eyjolfsson, H., Eriksdotter, M., Linderöth, B.,

- Lind, G., Juliusson, B., Kusk, P., ... Almqvist, P. (2016). Targeted delivery of nerve growth factor to the cholinergic basal forebrain of Alzheimer's disease patients: Application of a second-generation encapsulated cell biodelivery device. *Alzheimer's Research and Therapy*, 8(1), 1–11. <https://doi.org/10.1186/s13195-016-0195-9>
89. Eyo, U. B., Peng, J., Swiatkowski, P., Mukherjee, A., Bispo, A., & Wu, L.-J. (2014). Neuronal Hyperactivity Recruits Microglial Processes via Neuronal NMDA Receptors and Microglial P2Y12 Receptors after Status Epilepticus. *Journal of Neuroscience*, 34(32), 10528–10540. <https://doi.org/10.1523/JNEUROSCI.0416-14.2014>
90. Fahnstock, M., Michalski, B., Xu, B., & Coughlin, M. D. (2001). The precursor pro-nerve growth factor is the predominant form of nerve growth factor in brain and is increased in Alzheimer's disease. *Molecular and Cellular Neuroscience*, 18(2), 210–220. <https://doi.org/10.1006/mcne.2001.1016>
91. Fahnstock, M., Scott, S. A., Jetté, N., Weingartner, J. A., & Crutcher, K. A. (1996).

- Nerve growth factor mRNA and protein levels measured in the same tissue from normal and Alzheimer's disease parietal cortex. *Molecular Brain Research*, 42(1), 175–178.
[https://doi.org/10.1016/S0169-328X\(96\)00193-3](https://doi.org/10.1016/S0169-328X(96)00193-3)
92. Fahnstock, M., Yu, G., Michalski, B., Mathew, S., Colquhoun, A., Ross, G. M., & Coughlin, M. D. (2004). The nerve growth factor precursor proNGF exhibits neurotrophic activity but is less active than mature nerve growth factor. *Journal of Neurochemistry*, 89(3), 581–592
93. Friedman, W. J., Thakur, S., Seidman, L., & Rabson, A. B. (1996). Regulation of nerve growth factor mRNA by interleukin-1 in rat hippocampal astrocytes is mediated by NF κ B. *Journal of Biological Chemistry*, 271(49), 31115–31120.
<https://doi.org/10.1074/jbc.271.49.31115>
94. Galatro, T. F., Holtman, I. R., Lerario, A. M., Vainchtein, I. D., Brouwer, N., Sola, P. R., ... Eggen, B. J. L. (2017). Transcriptomic analysis of purified human cortical microglia reveals age-associated changes. *Nature Neuroscience*, 20(8), 1162–1171. <https://doi.org/10.1038/nn.4597>
95. Garaci, E., Caroleo, M. C., Aloe, L., Aquaro, S.,

- Piacentini, M., Costa, N., ... Levi-Montalcini, R. (1999). Nerve growth factor is an autocrine factor essential for the survival of macrophages infected with HIV. *Proceedings of the National Academy of Sciences of the United States of America*, *96*(24), 14013–14018. <https://doi.org/10.1073/pnas.96.24.14013>
96. García-Mauriño, J. E., Boya, J., López-Muñoz, F., & Calvo, J. L. (1992). Immunohistochemical localization of nerve growth factor in the rat pineal gland. *Brain Research*, *585*(1–2), 255–259. [https://doi.org/10.1016/0006-8993\(92\)91214-Y](https://doi.org/10.1016/0006-8993(92)91214-Y)
97. Gautier, E. L., Shay, T., Miller, J., Greter, M., Jakubzick, C., Ivanov, S., ... Randolph, G. J. (2012). Gene-expression profiles and transcriptional regulatory pathways that underlie the identity and diversity of mouse tissue macrophages. *Nature Immunology*, *13*(11), 1118–1128. <https://doi.org/10.1038/ni.2419>
98. Genoud, C., Quairiaux, C., Steiner, P., Hirling, H., Welker, E., & Knott, G. W. (2006). Plasticity of astrocytic coverage and glutamate transporter expression in adult mouse cortex. *PLoS Biology*, *4*(11), 2057–2064. <https://doi.org/10.1371/journal.pbio.0040343>

99. Ghézali, G., Dallérac, G., & Rouach, N. (2016). Perisynaptic astroglial processes: dynamic processors of neuronal information. *Brain Structure and Function*, 221(5), 2427–2442.
<https://doi.org/10.1007/s00429-015-1070-3>
100. Ginhoux, F., Greter, M., Leboeuf, M., Nandi, S., See, P., Gokhan, S., ... Merad, M. (2010). Fate mapping analysis reveals that adult microglia derive from primitive macrophages. *Science*, 330(6005), 841–845.
<https://doi.org/10.1126/science.1194637>
101. Ginhoux, F., & Prinz, M. (2015). Origin of Microglia: Current Concepts and Past Controversies. *Cold Spring Harbor Perspectives in Biology*, 7(8), a020537.
<https://doi.org/10.1101/cshperspect.a020537>
102. Gobbo, F., Marchetti, L., Jacob, A., Pinto, B., Binini, N., Pecoraro Bisogni, F., ... Cattaneo, A. (2017). Activity-dependent expression of Channelrhodopsin at neuronal synapses. *Nature Communications*, 8(1).
<https://doi.org/10.1038/s41467-017-01699-7>
103. Gómez-Gonzalo, M., Martín-Fernandez, M., Martínez-Murillo, R., Mederos, S., Hernández-

- Vivanco, A., Jamison, S., ... Araque, A. (2017). Neuron-astrocyte signaling is preserved in the aging brain. *Glia*, *65*(4), 569–580.
<https://doi.org/10.1002/glia.23112>
104. Gordon, G. R. J., Mulligan, S. J., & MacVicar, B. A. (2007). Astrocyte control of the cerebrovasculature. *Glia*, *55*(12), 1214–1221.
<https://doi.org/10.1002/glia.20543>
105. Goss, J. R., O'Malley, M. E., Zou, L., Styren, S. D., Kochanek, P. M., & DeKosky, S. T. (1998). Astrocytes Are the Major Source of Nerve Growth Factor Upregulation Following Traumatic Brain Injury in the Rat. *Experimental Neurology*, *149*(2), 301–309.
106. Gritton, H. J., Howe, W. M., Mallory, C. S., Hetrick, V. L., Berke, J. D., & Sarter, M. (2016). Cortical cholinergic signaling controls the detection of cues. *Proceedings of the National Academy of Sciences*, *113*(8), E1089–E1097.
<https://doi.org/10.1073/pnas.1516134113>
107. Grutzendler, J., Kasthuri, N., & Gan, W. (2002). *Long-term dendritic spine stability in the adult cortex*. *420*(December).
<https://doi.org/https://doi.org/10.1038/nature0>

1276

108. Guerra-Gomes, S., Sousa, N., Pinto, L., & Oliveira, J. F. (2018). Functional roles of astrocyte calcium elevations: From synapses to behavior. *Frontiers in Cellular Neuroscience*, *11*(January), 1–7. <https://doi.org/10.3389/fncel.2017.00427>
109. Guo, L., Bertola, D. R., Takanohashi, A., Saito, A., Segawa, Y., Yokota, T., ... Ikegawa, S. (2019). Bi-allelic CSF1R Mutations Cause Skeletal Dysplasia of Dysosteosclerosis-Pyle Disease Spectrum and Degenerative Encephalopathy with Brain Malformation. *The American Journal of Human Genetics*, *104*(5), 925–935. <https://doi.org/10.1016/j.ajhg.2019.03.004>
110. Guttenplan, K. A., & Liddelow, S. A. (2019). Astrocytes and microglia: Models and tools. *Journal of Experimental Medicine*, *216*(1), 71–83.
111. Haass, C., & Selkoe, D. J. (2007). Soluble protein oligomers in neurodegeneration: Lessons from the Alzheimer's amyloid β -peptide. *Nature Reviews Molecular Cell Biology*, *8*(2), 101–112. <https://doi.org/10.1038/nrm2101>
112. Hammond, T. R., Dufort, C., Dissing-Olesen, L., Giera, S., Young, A., Wysoker, A., ... Stevens, B.

- (2019). Single-Cell RNA Sequencing of Microglia throughout the Mouse Lifespan and in the Injured Brain Reveals Complex Cell-State Changes. *Immunity*, *0*(1), 1–19.
<https://doi.org/10.1016/J.IMMUNI.2018.11.004>
113. Hampel, H., Mesulam, M.-M., Cuello, A. C., Farlow, M. R., Giacobini, E., Grossberg, G. T., ... Khachaturian, Z. S. (2018). The cholinergic system in the pathophysiology and treatment of Alzheimer's disease. *Brain*, *141*(7), 1917–1933.
<https://doi.org/10.1093/brain/awy132>
114. Hanamsagar, R., Alter, M. D., Block, C. S., Sullivan, H., Bolton, J. L., & Bilbo, S. D. (2017). Generation of a microglial developmental index in mice and in humans reveals a sex difference in maturation and immune reactivity. *Glia*, *65*(9), 1504–1520. <https://doi.org/10.1002/glia.23176>
115. Meli G, Visintin M, Cannistraci I, Cattaneo A. Direct in vivo intracellular selection of conformation-sensitive antibody domains targeting Alzheimer's amyloid- β oligomers. *J Mol Biol* 2009 Apr 3;387(3):584-606. doi: 10.1016/j.jmb.2009.01.061. Epub 2009 Feb 4.
116. Meli G, Lecci A, Manca A, Krako N, Albertini V,

Benussi L, Ghidoni R, Cattaneo A.
Conformational targeting of intracellular A β
oligomers demonstrates their pathological
oligomerization inside the endoplasmic reticulum.
Nat Commun. 2014 May 27; 5:3867. doi:
10.1038/ncomms4867.



SCUOLA
NORMALE
SUPERIORE



*Il Laboratorio di Biologia della Scuola Normale Superiore
Consiglio Nazionale delle Ricerche, Pisa
13 ottobre 2011*

REFERENCES - NMC - SNS